Electromagnetic and thermal modelling for prognosis of distribution transformer

SVEINUNG ATTESTOG

SUPERVISOR

Hyunh van Khang

University of Agder, 2018
Faculty of Technology and Science
Department of Engineering

Abstract

In this thesis numerical modelling of electromagnetics and thermodynamic of a distribution transformer was studied. The model is based on two 5 MVA three phase distribution transformers located in Uleberg (Norway) owned by Agder Energi. The results include magnetic flux density in the core, current density, heat loss density and temperature distribution in the transformer. The maximum temperature of the transformer operating at full load with cooling fans turned on and ambient temperature 20 $°C$, reached the expected value based on temperature measurements from the transformers in Uleberg provided by Agder Energi. The results of the transformer operating at these condition were as a reference for the other simulations. The transformer model was simulated at different ambient temperatures and when the cooling fans were turned off. The effect of heat transfer by radiation and uniform current density were also investigated. The results of temperature of different operating condition were used to prognose the ageing rate of the transformer's paper insulation.

The measurement data provided by Agder Energi was processed in Excel, and the numerical modelling was executed in Comsol Multyphysics$^{®}$.
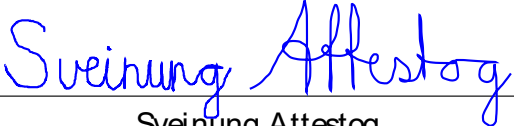
Preface

This Master thesis was the final task in the engineering course in Renewable Energy at University of Agder. The thesis contains the results from a numerical model based on two distribution power transformer located in Uleberg owned by Agder Energi. The main objective was to make the numerical model and investigate the temperature increase during different operation conditions and use this result to prognose the ageing rate of paper insulation.

The work is mainly performed independently at the University of Agder campus Grimstad with guidance from supervisor Huynh van Khang. Information about the transformers in Uleberg was provided by the contact persons at Agder Energi, Edgar Ommundsen and Katrine Smith.

I would like to thank my supervisor Hyunh Van Khang and my contacts at Agder Energi, Edgar Ommundsen and Katrine Smith, who provided me with guidance, informations and measurement data of the distribution transformers in Uleberg. I would also like to thank Johan Olav Brakestad for helping me with the installation of Comsol Multiphysics$^{®}$ on my personal computer and Birgit Attestog for reading my thesis and correcting any spelling errors.

University of Agder, Grimstad, Wednesday 30$^{\text{th}}$ May, 2018

Sveinung Attestog

Individual declaration

The individual student or group of students are responsible for the use of legal tools, guidelines for using these and rules on source usage. The statement will make the students aware of their responsibilities and the consequences of cheating. Missing statement does not release students from their responsibility.

1.	I hereby declare that my thesis is my own work and that I/We have not used any other sources or have received any other help than mentioned in the thesis.	☑
2.	I further declare that this thesis: - not been used for another exam at another department/university/university college in Norway or abroad; - does not refer to the work of others without it being stated; - does not refer to own previous work without it being stated; - have all the references given in the literature list; - is not a copy, duplicate or copy of another's work or manuscript.	☑
3.	I am aware that violation of the above is regarded as cheating and may result in cancellation of exams and exclusion from universities and colleges in Norway, see Universitets- og høgskoleloven §§4-7 og 4-8 og Forskrift om eksamen §§ 31.	☑
4.	I am aware that all submitted theses may be checked for plagiarism.	☑
5.	I am aware that the University of Agder will deal with all cases where there is suspicion of cheating according to the university's guidelines for dealing with cases of cheating.	☑
6.	I have incorporated the rules and guidelines in the use of sources and references on the library's web pages.	☑

III

Publishing Agreement

Authorization for electronic publishing of the thesis. Author(s) have copyrights of the thesis. This means, among other things, the exclusive right to make the work available to the general public (Åndsverkloven. §2). All thesis that fulfill the criteria will be registered and published in Brage Aura and on UiA's web pages with the author's approval. Thesis that are not public or are confidential will not be published.	
I hereby give the University of Agder a free right to make the task available for electronic publishing:	Yes ☑
Is the thesis confidential? (confidential agreement must be completed)	No ☑
- If yes: Can the thesis be published when the confidentiality period is over?	
Is the task except for public disclosure? (contains confidential information. see Offl. §13/Fvl. §13)	No ☑

Contents

List of Figures

List of Tables

Notations

Table 1: List of parameters - Part 1

Parameters	Unit	Description
$\mathbf{A}$	$\frac{V \cdot s}{m}$	Magnetic vector potential
A_{Arr}	s^{-1}	Pre-exponential factor
A_{coil}	m^2	Cross-sectinal area of winding
A_{core}	m^2	Cross-sectional area of the core
A_i	m^2	Surface area of body i
A_L	h	Constant used in the lifetime equations
a	$-$	Turn ratio
$\mathbf{B}$	T	Flux density
B	K	Exponent used in the equations of lifetime and F_{aa}
B_{aa}	K	Fitting parameter in general equation of acceleration ageing factor
B_L	K	Fitting parameter in lifetime equation
B_{max}	T	Peak value of magnetic flux density
C	F	Capacitance
C_p	$\frac{J}{kg \cdot K}$	Specific heat capacity
c	NA	Constant in general equation of a straight line
$\mathbf{D}$	$\frac{C}{m^3}$	Electric field flux
d_a	MD	Damping coefficient
$\mathbf{E}$	$\frac{V}{m}$	Electric field strength
E_a	$\frac{J}{mol}$	Activation energy
e_a	MD	Mass coefficient
e_{coil}	V	Phase voltage of the coils
e_{LP}	V	Induced voltage by leakage flux in primary
e_{LS}	V	Induced voltage by leakage flux in secondary
$\mathbf{F}$	$\frac{N}{m^3}$	External force
F_{aa}	$-$	Acceleration ageing factor
$F_{aa:B}$	$-$	Acceleration ageing factor for insulation class B
$F_{aa:F}$	$-$	Acceleration ageing factor for insulation class F
$F_{aa:H}$	$-$	Acceleration ageing factor for insulation class H
F_{ij}	$-$	View factor between the bodies i and j
F_s	NA	Source term
f	Hz	Frequency of the current
Gr	$-$	Grashof number
g	$\frac{m}{s^2}$	Gravitational acceleration
$\mathbf{H}$	$\frac{A}{m}$	Magnetic field intensity (Vector)
H	$\frac{A}{m}$	Magnetic field intensity (Scalar)
I	$-$	Identity matrix
I	A	Current
I_{cir}	A	Current in the electric circuit connected to the transformer model

Table 2: List of parameters - Part 2

Parameters	Unit	Description
I_L	A	Load current
i_p	A	Primary current
i_s	A	Secondary current
$\mathbf{J}$	$\frac{A}{m^2}$	Current density (Vector)
$\mathbf{J}_e$	$\frac{A}{m^2}$	Current density in the windings
J	$\frac{A}{m^2}$	Current density (Scalar)
J_R	$\frac{W}{m^2}$	Radiative flux leaving a body
$J_{R:i}$	$\frac{W}{m^2}$	Radiative flux leaving body i
$J_{R:j}$	$\frac{W}{m^2}$	Radiative flux leaving body j
k	$\frac{W}{m \cdot K}$	Thermal conductivity
k_e	$\frac{J \cdot s}{T^2}$	Eddy current loss constant
k_h	$\frac{J}{T^{1.6} m^3}$	Hysteresis loss constant
k_{rate}	s^{-1}	Rate of reaction in Arrhenius' equation
L	m	Characteristic length
$Lifetime_B$	$hours$	Lifetime of paper-insulation with thermal class B
$Lifetime_F$	$hours$	Lifetime of paper-insulation with thermal class F
$Lifetime_H$	$hours$	Lifetime of paper-insulation with thermal class H
L_{Loss}	$-$	Loss of lifetime
L_p	H	Leakage inductance of primary windings
L_{Rest}	$hours$	Remaining of lifetime of paper-insulation
L_s	H	Leakage inductance of secondary windings
m	MD	Slope in a general equation of a straight line
N	$-$	Number of turns
N_p	$-$	Number of turns in primary windings
N_s	$-$	Number of turns in primary windings
$\mathbf{n}$	$-$	Normal vector
n	$-$	Number or exponent
P_{Cu}	W	Total resistive loss
P_e	W	Total eddy current loss
P_d	W	Total dielectric loss
P_H	W	Total hysteresis loss
P_{out}	MW	Output load
p	Pa	Pressure
p_a	Pa	Absolute pressure
p_{hydro}	Pa	hydrostatic pressure
p_o	Pa	Relative pressure
Q	$\frac{W}{m^3}$	Heat generated in a material
Q_0	$\frac{W}{m^3}$	Heat source in material
Q_{ij}	W	Power transmitted between bodies i and j
Q_{Ted}	$\frac{W}{m^3}$	Thermoelastic damping

Table 3: List of parameters - Part 3

Parameters	Unit	Description
Q_{vd}	$\frac{W}{m^3}$	Viscous dissipation
$Q_{Windings}$	$\frac{W}{m^3}$	Heat loss density in the windings
R	$\frac{J}{mol \cdot K}$	Universal gas constant
R_C	Ω	Resistance representing core losses in transformer
R_e	Ω	Electric resistance
$R_{eq:P}$	Ω	Equivalent resistance in windings with respect to primary side
R_{load}	Ω	Resistance representing the transformer load
R_P	Ω	Resistance in primary winding
R_S	Ω	Resistance in secondary winding
Re	$-$	Reynold number
Ri	$-$	Richardson number
RTT	$-$	Relative temperature tolerance
$\Re$	H^{-1}	Magnetic reluctance
$\mathbf{r}$	m	Position in the model geometry
$\mathbf{r}_{ref}$	m	Reference position in the model geometry
S	VA	Apparent power
T	K or $°C$	Temperature
T_1	K or $°C$	Temperature at operating condition 1
T_2	K or $°C$	Temperature at operating condition 2
T_{am}	K or $°C$	Ambient temperature
T_{HS}	K or $°C$	Hotspot temperature
T_i	K	Temperature in body i
T_j	K	Temperature in body j
T_{ref}	K or $°C$	Reference temperature
T_{max}	K or $°C$	Maximum temperature
T_{ss}	K or $°C$	Steady state temperature
$\mathbf{u}$	$\frac{m}{s}$	Velocity
U_0	$\frac{m}{s}$	Inlet velocity
V	V	Voltage
$V1$	V	Voltage source of phase 1 in the three phase circuit
$V2$	V	Voltage source of phase 2 in the three phase circuit
$V3$	V	Voltage source of phase 3 in the three phase circuit
V_{core}	m^2	Volume of the core
V_L	V	Line voltage
V_p	V	Primary voltage
V_{RMS}	V	Phase voltage in RMS value
V_s	V	Secondary voltage
$X_{eq:P}$	Ω	Equivalent reactance in windings with respect to primary side
X_M	Ω	Magnetizing reactance
X_P	Ω	Reactance in primary winding

Table 4: List of parameters - Part 4

Parameters	Unit	Description
X_S	Ω	Reactance in secondary winding
α	NA	Absorption coefficient
α_p	$\frac{m^3}{K}$	Thermal expansion
α_T	$\frac{\Omega \cdot m}{K}$	Temperature coefficient
β	$\frac{m}{K}$	Thermal expansion used in Richardson number
β_f	$-$	Fudge factor
γ	NA	Source term
ΔH	$\frac{J}{kg}$	Sensible enthalpy
ΔT	K or $°C$	Temperature difference
δ	m	Skin depth
$\tan(\delta)$	$-$	Dissipation factor
ε	$-$	Emissivity
ε_r	$-$	Relative permittivity
μ	$Pa \cdot s$	Dynamic viscosity
μ_0	$\frac{H}{m}$	Permeability in vacuum
μ_r	$-$	Relative permeability
ν	$\frac{m^2}{s}$	Kinematic viscosity
ρ	$\frac{kg}{m^3}$	Density
ρ_e	$\Omega \cdot m$	Electric resistivity
ρ_{e0}	$\Omega \cdot m$	Reference resistivity
σ	$\frac{W}{m^2 K^4}$	Stefan-Boltzmann constant
σ_e	$\frac{S}{m}$	Electric conductive
σ_{sofeFe}	$\frac{S}{m}$	Electric conductive of the iron core
ϕ	Wb	Magnetic flux
ϕ_{LP}	Wb	Flux leakage from primary
ϕ_{LS}	Wb	Flux leakage from secondary
$\cos(\phi)$	$-$	Power factor

The units is of some of the parameters is makred with NA. This is because they are in general equations where the unit may change depending on what the equation is describing. The parameters written in bold font represent vectors and matrices and the parameters written with italic are scalars. Several parameters describing geometry is not mention in these tables. They are listed in Table 8 and the reference position in the geometry used in (60) are listed in Table 10.

1 Introduction

The role of the transformer in a power system is to step up the voltage for transmission over long distances and step it back down again for safe usage in industry and private homes. The most common transformers types are oil-filled transformers and dry-type transformers. Dry-type transformers are used in areas where the risk of fire hazard needs to be low. As the name implies, the dry-type transformer is not cooled by oil, but air flowing through ducts in the transformer windings. The dry-type transformer gets higher temperature rise and temperature is one of the most important parameters in prognosis the lifetime of the transformer. Some of the earliest works on temperature rise in a transformer were done in 1944 by Stewart and Whitman [1]. In later years it has become easier to make models of transformers with the use of finite element method, because of the advancement in computers.

Estimating the lifetime of the transformers is useful information for maintenance purposes. The replacement strategy can then be set into action and un-expected downtime of the network can be reduced. Several different methods are used to do the remaining life analysis. In oil-filled transformers, samples of the oil are extracted for dissolved gas analysis (DGA) and measurement of furan concentration. [2] Other examples of determining the state of a transformer include the degree of polymerization of paper insulation, partial discharge, displacement of windings, transfer function of the transformer and many more [2]. The strain on a transformer are subdivided into three different categorise: thermal, mechanical and electrical. Thermal stress occur due to overload, local overheating, flux leakage and malfunction of the cooling system. Electrical stress is caused by over voltage from the system in steady state or transient response when a transformer is connected and begins to supply power to the grid. Mechanical stress between conductors and windings is due to short circuit and inrush-current. Overall the system is too complexed for determining an exact time at which the transformer should be replaced, but it is possible to estimate the probability of failure during its lifetime. [2]
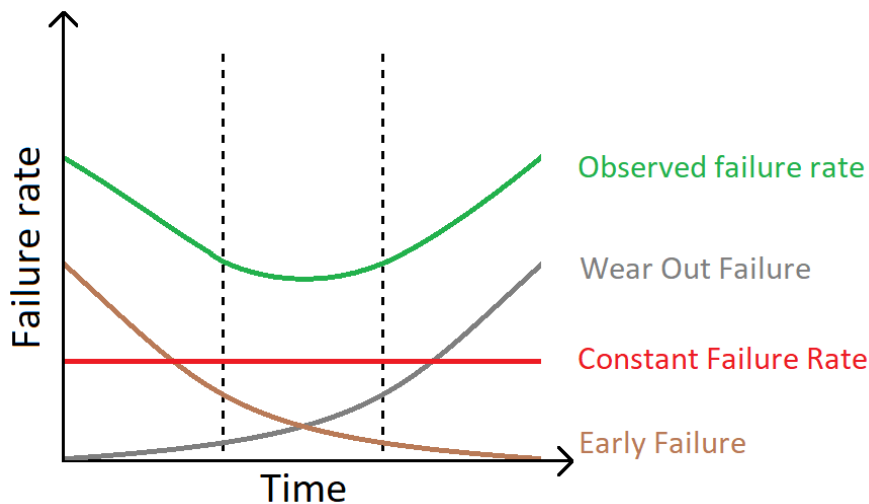
Figure 1: Transformer failure rate pattern

Figure 1 shows a sketch of how the failure rate of a transformer changes over time. It may fail in an early year due to imperfect manufacturing, handling or control processing. Eventually, the failure rate will be reduce to a certain level and stay constant until the end of life. Then the failure rate increases due to ageing. [2]

There are two types of dry-type transformer, cast resin transformer and vacuum pressure impregnated transformer [3]. Cast resin dry-type transformer is used in areas with high moister content. Because the windings are encapsulated with epoxy resin, it makes the transformer non-hygroscopic. This type of transformers is available in the ratings between 25 kVA and 12500 kVA. The insulation material of the windings of the vacuum pressure impregnated transformer is made of minimum flammable material and is void free impregnated. This type of transformer is available in the range between 5 kVA and 30 MVA [3]. The life expectancy of a dry-type transformer is mainly due to the breakdown of winding insulation. The most important parameter for determining the lifetime is temperature and the relation is often decried with Arrhenius' equation. This will be described in the background theory.

The aim of the project is to model the electromagnetics and the thermodynamics of a dry-type distribution transformer with numerical modelling. The model is based on two 5 MVA winding-encapsulated dry-type distribution transformers located in Uleberg owned by Agder Energi. Both the transformers have the voltage rating 6600 V/23000 V and aluminium windings. Comsol Multiphysics® was used to make the transformer models. The simulation instigated the effect of cooling air conditions, both ambient temperature and lack of forced convection (Cooling fans turned off). How much warmer would the transformer be if the cooling fans were not operating during nominal operation and what is the effect of ambient temperature on the maximum temperature? The importance of including radiation in the simulation and uniform heat loss density in the windings were investigated. What would the error be if radiation or skin- and proximity-effect in the windings were ignored? The last objective of the simulation was to use the temperature results to prognose the rate of ageing in the windings under different operating condition.

2 Method

The approach in this project is first to collect information about electromagnetic and thermal modelling of transformers. Modelling of dry-type transformer done in previous projects are reviewed in Section 3. A simulation model was made in COMSOL Multiphysics$^{®}$. This program can do finite element analysis (FEA) and can combine different physic models. The aim is to make a model of a dry-type transformer were electromagnetics, electric circuits, heat transfer and fluid dynamics are coupled. Primarily the default settings of physics, material properties and solver were used, but some adjustments of the equations were made. For example the electromagnetic heat loss (Joule Heating) in the windings in the model were set to zero and replaced by heat sources with self-derived equations. The dimensions of the transformer based on documents from Agder Energi. Hourly measurements from the last six years of voltage, current, power and temperature were also provided. [4]. These data were processed in Excel.

3 Literature review

The earliest works related to temperature rise in dry-type transformers were done in 1944. It was an experimental study done by Stewart and Whitman [1]. Today more and more work on the subject involves numerical modelling with finite element analysis.

Arjona, Hernandez, Escarela-Perez and Melgoza modelled a dry-type transformer in Comsol, but they used constant heat sources in transformer core, primary and secondary windings. [5] It was an axisymmetric FEA-model of one leg of a three-phase transformer. The main focus of the model was on the heat transfer and fluid dynamics. It takes into account both surface to surface radiation between objects and surface to ambient radiation. The model does not include electromagnetics and the heat loss is uniform. The article compares the temperature rise when the transformer is operating at no load and full load. [5]

Lee, Abdullah, Jofriet and Patel modelled a 2000 kVA dry-type transformer with foil-type windings in primary and disk-type winding in secondary [6, 7]. The model was a 2D FEA-model in Comsol with one leg of the transformer. The number of turns in the high-voltage and low-voltage windings were 460 and 16, respectively. The model included conduction, natural convection and radiation. The current density plot in [6] included skin-and proximity-effect in the foil-type windings and the maximum temperature reached 154 $°C$. The high-voltage side had disk type, but the number of turns were larger and 3 and 4 turns were lumped together. The current density was more uniform. The maximum temperature was 137 $°C$ when the transformer operated at full load. [7].

Ning and Ding did a 3D-model of a dry-type transformer [8, 9]. The geometry of the model was imported from SOLIWORKS and is much more detailed than the geometry used in this thesis. The model solves the model as a thermodynamics problem. It used several equation for heat loss based on transformer loading condition and empirical constants [8, 9]. The model simplifies convection with a constant convection coefficient. The results in reference [8] include plots of the temperature rise along the hight of the windings. The value of ambient temperature is not mentioned. It peaked around 70 $°C$ and 80 $°C$.

It is common to simplify the thermal model of a three-phase transformer with a single-phase model, because of the symmetry in the geometry. This was done in reference [6], [7] and [5], but there is one result a thermal model single-phase transformer (with one legged core) will never get. In a three-phase model the temperature rise of the windings in the middle phase is greater than the other. This is the case for an e-core transformer. A larger part of the outer surface of these windings face the surrounding. More heat can be transferred from the windings to the surroundings through radiation. The windings on the middle leg face more thermal resistance. [8]

The advantage is FEA accuracy and details in the results, but it is computational heavy. An empirical model is easier to solve, thus better suited for monitoring and control system. Soltanbayev, Sarmukhanov, Kazymow, Otelgen and Bagheri presented an algorithm for an automated ageing evaluation of dry-type transformers [10]. The model includes parameters which have been fitted with statistics, but they may change depending on the transformer design [10]. In this model the ratio between the increase of maximum temperature and ambient temperature equals to 1.

4 Background theory

Section 6 will give a more detailed description of equation systems describing the physics of the numerical models. First some basic principles about the transformer with turn ratio, equivalent circuit, magnetic material, power losses, skin-effect, proximity-effect and insulation classes. Then the section will describe briefly the different types of heat transfer and Arrhenius' equation and its relation to ageing of the paper insulation of the transformer.

4.1 Turn ratio and number of turns

One of the simplest designs of a single phase transformer is shown in Figure 2. The primary windings are wound around one leg of the transformer with N_p number of turns and the secondary windings are wound around the second leg of the transformer with N_s number of turns.
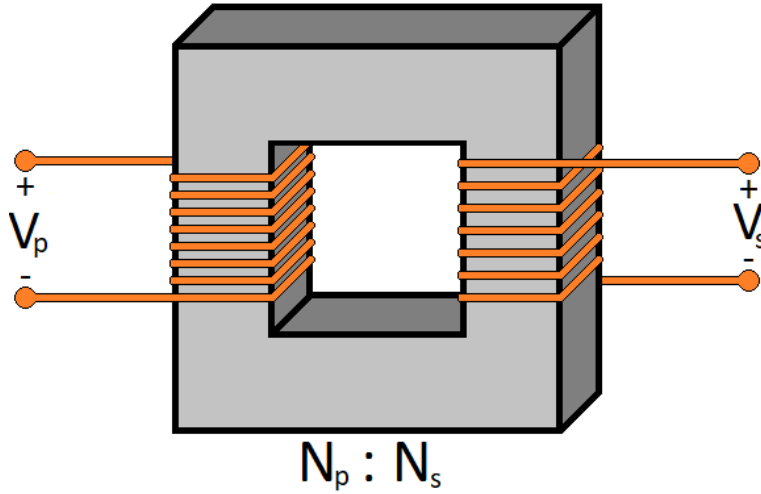
Figure 2: Sketch of a single-phase transformer

In an ideal transformer the ratio between primary voltage V_p and secondary voltage V_s are equal to the turn ratio a between the primary and secondary windings.

$$a = \frac{V_p}{V_s} = \frac{N_p}{N_s} \tag{1}$$

This is the case where both the primary windings and the secondary windings have a star or delta connection. If the transformer has a star-delta connection or opposite it is necessary to consider phase or line voltage. Both the primary and secondary voltage need to be line or phase in (1)

The number of turns in the windings of the transformer depends on the voltage rating, geometry of the transformer, current frequency and maximum flux density in the transformer core. It can be estimated by the following equation.

$$N = \frac{\sqrt{2}V_{RMS}}{2\pi B_{max} A_{core} f} \tag{2}$$

where V_{RMS} is the RMS value of the voltage across the windings, B_{max} is the peak value of magnetic flux density in the transformer core, A_{core} is the cross-sectional area of the transformer core and f is the frequency of the current. (2) is derived from Faraday's law and the derivation can be found in Appendix A. It is an approximation and assumes that is no flux leakage and all the magnetic flux induced by the coil is conducted through the transformer core.

4.2 Equivalent circuit

Figure 3 shows the circuit of a real transformer. R_p and R_s represents the resistive loss in the primary and secondary windings. X_p and X_s represents the leakage flux in the primary and secondary windings. The windings induce magnetic flux, but not all is conducted through the transformer core. Some of it "leaks" out of the transformer and passes through air. The reluctance of air is much larger than the core. The leakage flux in the windings is proportional to the current in the windings [11].

$$\phi_{Lp} = \frac{N_p}{\Re} i_p \tag{3}$$

$$\phi_{Ls} = \frac{N_s}{\Re} i_s \tag{4}$$

where $\Re$ is the reluctance of the path of the leakage flux.
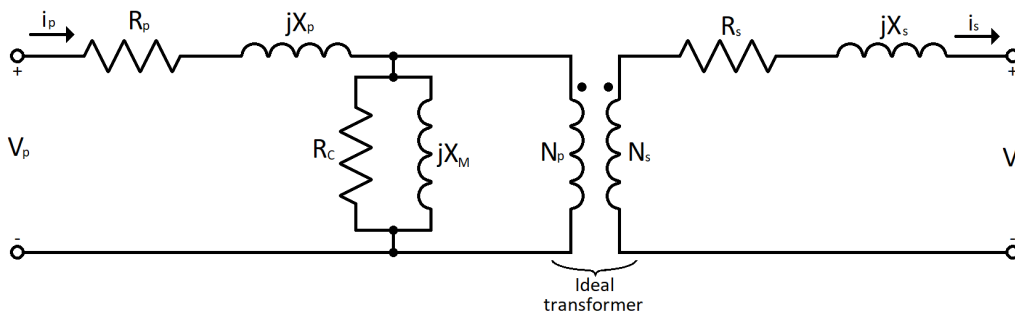
Figure 3: Equivalent circuit of a real transformer

The voltage induced by the leakage flux can be expressed as

$$e_{Lp} = L_p \frac{di_p}{dt} \tag{5}$$

$$e_{Ls} = L_s \frac{di_s}{dt} \tag{6}$$

where $L_p = \frac{N_p^2}{\Re}$ is the leakage inductance of the primary winding and $L_s = \frac{N_s^2}{\Re}$ is the leakage flux of the secondary winding. The reactance of the primary and secondary windings is represented by $X_p = 2\pi f L_p$ and $X_s = 2\pi f L_s$ respectively [11].

The power losses in the transformer core are represented by be the resistor R_C. The two main core losses are the hysteresis loss and eddy current loss. They are explained in more detail later in the thesis. The excitation of the transformer core is represented by the reactance X_M

6

The equivalent circuit in Figure 3 is often simplified to the circuit in Figure 4. The current through the excitation branch (the current through R_C and X_M) is much smaller compared to the load current. It is about 2-3 % of load current [11, p. 89]. Since this is the case, the resistance and reactance are lumped together.
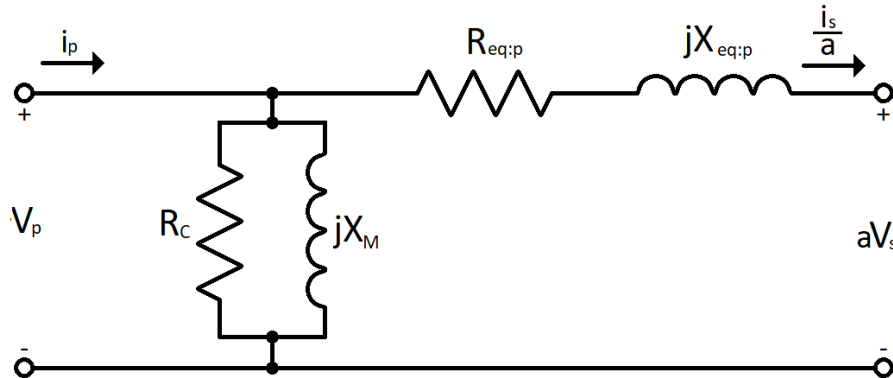
Figure 4: Approximate equivalent circuit

The approximate equivalent circuit in Figure 4 is in respect to the primary side of the transformer. The resistance $R_{eq:p}$ is equal to $R_p + R_s a^2$ and $X_{eq:p}$ is equal to $X_p + X_s a^2$.

4.3   Magnetic materials

The relation between the flux density B and flux intensity H is

$$B = \mu_r \mu_0 H \tag{7}$$

where μ_r is relative permeability and μ_0 is permeability in free space, which is equal to $4\pi \cdot 10^{-7} \frac{H}{m}$. When μ_r is constant, the magnetic material is linear. Most magnetic materials have a linear region but eventually it is saturated for magnetic flux.

When a core made of magnetic material is induced by an alternating current, the flux is lagging behind. Every time the value of current is equal to 0 A, there is some flux left in the core. This is due that the atoms of the material will resist the change in direction of the magnetic field. The resistance generates some heat and it is called hysteresis loss.

4.4   Power losses

The efficiency of a distribution transformer is typical around 98 % [12]. The majority of power loss in an AC-machine is subdivided into resistive losses, core losses and mechanical losses [11]. Resistive loss is often called copper loss, because copper is a common conductor material. It will be called resistive loss in this thesis, because the windings are made of aluminium. The core loss is divided into hysteresis loss and eddy current loss [13]. The main load loss is the resistive loss. It can be calculated with the equation

$$P_{Cu} = R_e I^2 \tag{8}$$

where R_e is the resistance of the windings and I is the current through the windings. There is some resistive loss during no load condition. The transformer draws some current when it gets a voltage applied on the primary side and the secondary side is open circuit. It is called no-load current and is typically 1 % to 2 % of the full load [13].

The core losses are also called no-load losses, because they are present when voltage is applied and the transformer is connected in open circuit. They are close to be independent of the load. Hysteresis is a no-load loss that occur in the core of the transformer. The alternating current of the transform alternates the direction of the magnetic field of core, but there is a time lag. Plotting the magnetic flux density (B) versus magnetic flux intensity (H) gives the hysteresis curve. The hysteresis loss is proposition to the area enclosed by the hysteresis curve. The total hysteresis loss (P_h) can be calculated with the empirical equation [13]

$$P_h = k_h B_{max}^{1.6} f V_{core} \tag{9}$$

where k_h is a constant depending on the characteristics of the material of the transformer core, B_{max} is the peak value of the flux density, f is frequency of the supply current and V_{core} is the volume of the transformer core. Hysteresis loss is included in the numerical model with the use a permeability with a complex value. This is described in more detail in Section 6

Eddy current loss is the second main power loss in the core. Applying voltage at the windings will induce a current in the core. This current is called eddy current. It is minimized by laminating the iron core. Eddy current loss (P_e) can be estimated by the empirical equation [13]

$$P_e = k_e B_{max}^2 f^2 \tag{10}$$

where k_e is a constant depending on material properties and lamination of the core. Eddy current loss can cause about 50 % of the power loss in the iron core [13]. It can possibly account for for 61.5 % of the no load loss. [14] This thesis will approximate the eddy current loss to be 50 % of the core loss. There are some eddy current in the conductor too, but these losses are negligible. [13] Figure 5a and Figure 5b illustrate the effect of lamination of the core. The laminated material has a high resistance in one direction, but not in the others.

(a)   (b)
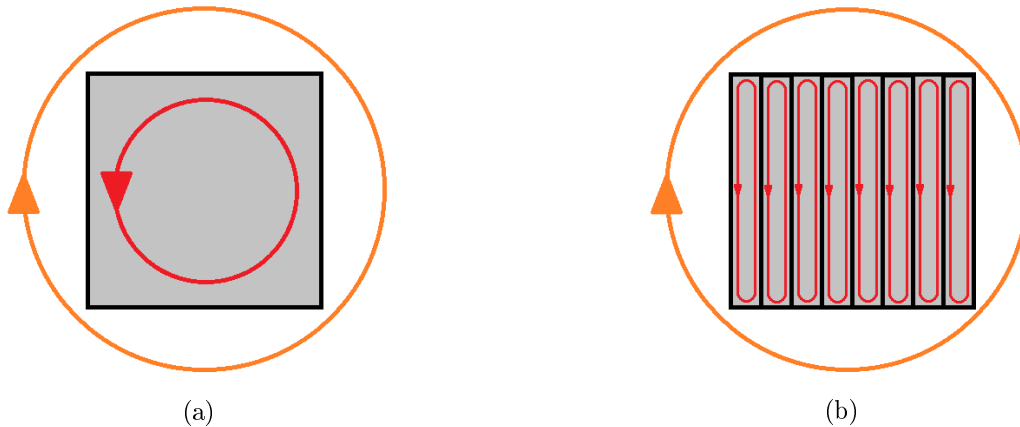
Figure 5: Eddy Current in a magnetic material (a) and laminated magnetic material (b)

Figure 5a shows the eddy current (red curve) in a magnetic material induced by a coil current (orange curve). The magnetic material is not laminated and the electric conductivity is isotropic. Figure 5b shows the same coil current induction eddy current in a laminated core. The eddy current is smaller. Lamination makes the iron core anisotropic. The electric conductivity is small in the direction across the lamination but it has the same conductivity in the other two directions.

Other smaller power losses in the transformer are dielectric loss and stray loss. These losses are not included in simulation models in this thesis. Dielectric losses occur in the insulation of the transformer. The insulation isolates the conductors from each other and cause a kind of capacitor known as a stray capacitor. Dielectric loss (P_d)can be calculated with the equation [13]

$$P_d = 2\pi f C V_{RMS}^2 \tan(\delta) \tag{11}$$

where C is the capacitance in F, U_{RMS} is the RMS value of the operating voltage and $\tan(\delta)$ is the dissipation factor. This factor is extremely temperature dependent. P_d is a small percentage of the losses in the transformer, but is the most dangerous one. $\tan(\delta)$ is strongly dependent on temperature. Increasing temperature may increase $\tan(\delta)$ and P_d. In turn this will increase the temperature until thermal breakdown [13].

Stray losses is the remaining power loss in the transformer which do not fall into any of the previous mention categories. [11] Stray losses may account for 5 % of the total. [13]

4.5   Skin-effect and proximity-effect

The current distribution in the cross-section of a conductor is uniform if the current is DC. In the case of AC the H-field induced by the alternating current is inducing an eddy current. This eddy current cancels out the current in the center and reinforces it in the "skin" of the conductor. Figure 6 illustrates this phenomena [15]
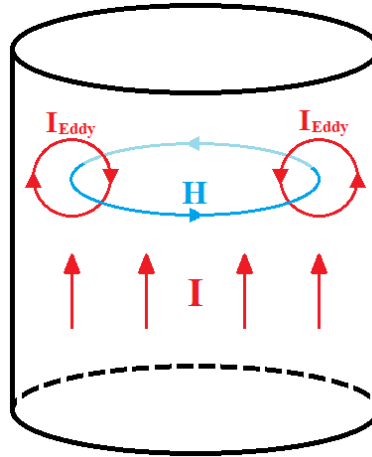
Figure 6: Sketch of Skin-effect

The skin depth δ for lower frequencies can be calculated with equation [15].

$$\delta = \sqrt{\frac{1}{\pi \mu_0 \mu_r \sigma_e f}} \tag{12}$$

where μ_0 and μ_r are permeability in vacuum and relative permeability in free space, respectively. f is the frequency of the current and σ_e is the electric conductivity of the conductor. For example the skin depth of copper and aluminium for an alternating current with frequency 50 Hz is 9.2 mm and 11.6 mm, respectively.

The proximity-effect describes the phenomena when a flux is induced in one conductor by a nearby conductor. This flux induces an eddy current and increases the apparent resistance of the conductor. [16]

4.6   Insulation classes

The insulation used for generators, motors and transformers are divided into insulation classes (also called thermal classification). The classes are defined by their maximum operating temperature. The most common insulation classes are B, F and H. The maximum ambient temperature is 40 °C.
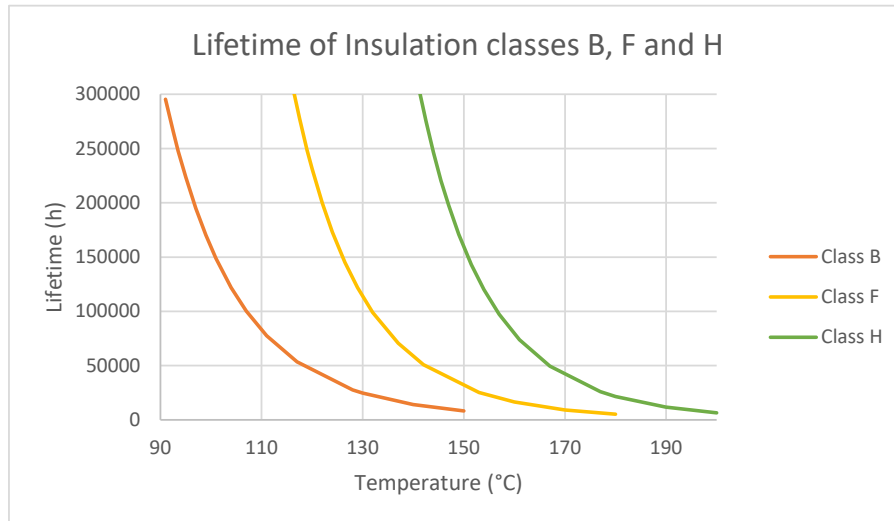
Figure 7: Mean insulation lifetime versus winding temperature

Figure 7 shows a typical plot of the mean lifetime versus operating temperature for insulation classes B, F and H from text book *Electric Machinery Fundamentals* (page 183) written by S. J. Chapman. [11] The lifetime decreases with increasing temperature. The plots shown are in the range between 0 and 300000 operating hours (34 years). An old rule of thumb states that 10 °C increase in operating temperature cuts the lifetime to the half [17]. The graphs in Figure 7 will be used to derive equations for the accelerated ageing factors. The derivations can be found in Appendix B and they are discussed in the results in Section 7.2.5. ABB often design transformers with a lifetime of 25 years. [18]

4.7   Heat transfer

Heat transfer is divided into three categorise: conduction, convection and radiation. Conduction is the transport of energy through a medium due to temperature difference. It is governed by Fourier's law. [19, p. 69]

$$\mathbf{q} = -k\nabla\mathbf{T} \tag{13}$$

Convection is the transfer of heat from a solid material to a fluid. Convective heat transfer involves heat diffusion and heat transfer due to bulk fluid flow. There are two types of convection: free and forced. Free convection occurs when fluid flow is induced by buoyancy forces resulted by density variation in the fluid. These variations occur, because density is dependent on temperature. Forced convection occurs when the fluid flow is caused by an outside source. Richardson number (Ri) is used to determine which type of convection is dominant [20].

$$Ri = \frac{Gr}{Re^2} \tag{14}$$

where Gr is Grashof number.

$$Gr = \frac{g\beta\Delta T L^3}{\nu^2} \tag{15}$$

where g is the gravitational constant, β is the thermal expansion, ΔT is the difference between the surface temperature and bulk temperature, L is the characteristic length and ν is the kinematic viscosity. Reynold's number (Re) is defined as

$$Re = \frac{uL}{\nu} \tag{16}$$

where u is the velocity of the fluid flow. Inserting (15) and (16) in (14) gives the expression

$$Ri = \frac{g\beta\Delta T L}{u^2} \tag{17}$$

Free convection is dominant when $Ri >> 1$. Equation (17) states that free convection is dominant with fluids with low velocity, larger temperature differences and characteristic length. Forced convection is dominant when $Ri << 1$. This is the case with large fluid velocities and low temperature differences. Both free and forced convections need to be considered when $0.1 < Ri < 10$. [20]

The last type of heat transfer is radiation. An object with temperature emits radiation and the total power it emits from the object is

$$P_{Radiation} = \epsilon\sigma\left(T^4 - T_{am}^4\right) \tag{18}$$

where ϵ is emissivity, σ is Stefan-Boltsmann constant, T is temperature and T_{am} is ambient temperature.

4.8   Arrhenius' equation

10 °C increase of operating temperature cuts the lifetime to the half is a common rule of thumb for estimating the lifetime of transformer insulation [17]. The rule originated from Arrhenius' equation. It represents reaction rates dependency on temperature. It was proposed by the Swedish scientist Svante August Arrhenius in 1889. The equation can be written in the following manner [21].

$$k_{rate} = A_{Arr} e^{-\frac{E_a}{RT}} \tag{19}$$

where k_{rate} is the rate constant, E_a is the activation energy, R is the universal gas constant, T is the absolute temperature (K) and A_{Arr} is the pre-exponential factor. The molecules in a material is not complicity fixed and collide with each other. The result of this is that paper insulation will deteriorate. The amount of collisions is represented by the constant A_{Arr}, but the unit may change due to the order of the reaction. The Unit is s^{-1} if it is a first order reaction. In this case the pre-exponential factor A_{Arr} is often called frequency factor. k_{rate} is the number of collisions that resulted in reaction per section, A_{Arr} is the number of collisions leading to a reaction per second and the term $e^{-\frac{E_a}{RT}}$ represents the probability that any given collision results in a reaction. Taking the natural logarithm of Arrhenius equation yields.

$$ln(k_{rate}) = -\frac{E_a}{R}\left(\frac{1}{T}\right) + ln(A_{Arr}) \tag{20}$$

this equation has the same shape as a straight line.

$$y = mx + c \tag{21}$$

where m is slope and c is a constant. The parameters E_a and A_{Arr} can be estimated by plotting $ln(k)$ versus $\frac{1}{T}$, which is called the Arrhenius' plot. The slope m and constant c are estimated by linear regression and the parameters E_a and A_{Arr} is estimated by the following equations.

$$E_a = -Rm \tag{22}$$

$$A_{Arr} = e^c \tag{23}$$

E_a and A_{Arr} may change due to temperature. The equations

$$k_{rate} = A_{Arr} T^n e^{-\frac{E_a}{RT}} \tag{24}$$

and

$$k_{rate} = A_{Arr} e^{-\left(\frac{E_a}{RT}\right)^{\beta_f}} \tag{25}$$

are two examples of correction of Arrhenius' equation. The exponent n in (24) is one way of taking the temperature dependency of constant A_{Arr} into consideration. The typical value of n is between -1 and 1. β_f in (25) is a empirical correction or fudge factor. [21] The acceleration ageing factor is the

13

ratio of the reaction rate at temperature T_2 and reference temperature T_1. It can be used instead of the 10 $°C$ rule of thumb.

$$F_{aa} = e^{\frac{E_a}{R}\left(\frac{1}{T_1} - \frac{1}{T_2}\right)} \tag{26}$$

F_{aa} for paper insulation with temperature rating 110 $°C$ is [22]

$$F_{aa} = e^{\left(\frac{15000}{383} - \frac{15000}{T_{HS}+273}\right)} \tag{27}$$

where T_{HS} is the hot-spot temperature (HST)in the windings. The lifetime is dependent on several parameters. The system is complexed, but temperature is one of the most important parameters [17]. This thesis will for simplification reasons, use F_{aa} as an estimate of the ageing rate of the transformer insulation.

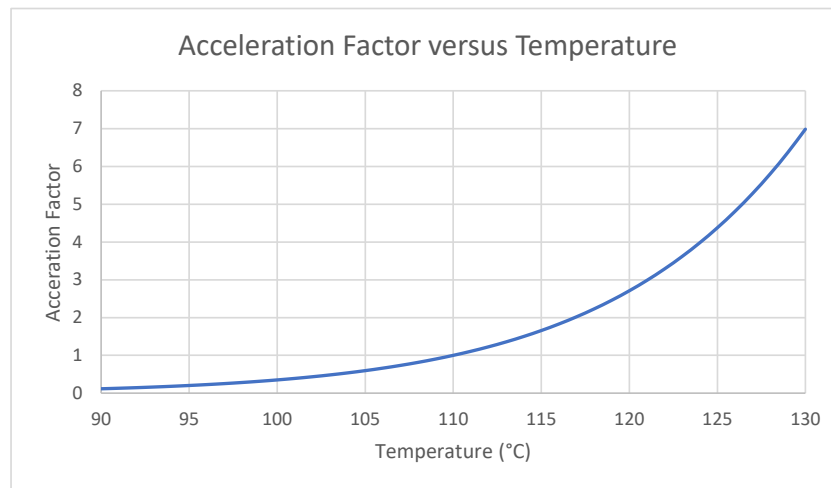Figure 8: Acceleration Factor versus Temperature

Figure 8 shows the plotted curve of equation 27. When HST is 110 $°C$, F_{aa} is equal to 1. This means that the insulation is ageing with one hour per hour of operation. When HST is equal to 120 $°C$, F_{aa} is equal to 2.7. This means that one hour of operation with HST equal to 120 $°C$ is equivalent to 2.7 hours of operation with HST equal to 110 $°C$.

5   Dry-type distribution transformers - Uleberg

The transformers studied in this thesis are two 5 *MVA* encapsulated-winding dry-type transformer (T1 and T2). The transformers are located in Uleberg. Uleberg is situated in the municipality of "Evje og Hornnes" in Norway. Key-parameters of the transformers are given in Table 5. [4]

Table 5: Parameters - Uleberg Transformers

Parameter	Value	Unit
Rated Apparent Power	5000	*kVA*
Primary line voltage0	6600	*V*
Secondary line voltage	23000	*V*
Primary line current	437.4	*A*
Secondary line current	125.5	*A*
Voltage ratio	3.48	−
Primary resistive loss	10	*kW*
Secondary resistive loss	6.1	*kW*
Core losses	5.4	*kW*
Frequency	50	*Hz*

In the documents from Agder Energi, the high voltage side is refereed to as the primary side and the low voltage side is the secondary. The electric power is generated by the generators at Uleberg Power Station and supplied to the low voltage side of the transformers. Then the line voltage is stepped up to 23 *kV*. In this thesis, the primary side is refereed to the low-voltage side and the secondary is the high-voltage side. The connection of the transformer is Ynd11. [4] The transformer model in this thesis has star connection on both sides of the transformer. The simulation model in Comsol struggled with delta connection.

These transformers were selected for this study, because they had hourly measurements of voltage, current, temperature, active and reactive power have been collected by Agder Energi in the period between 2th April 2012 and 26th January 2018. The data was processed in Excel.

Table 6: Measurements of the transformers T1 and T2 in Uleberg

Parameter	T1	T2	Unit
Line Voltage (Low-voltage side)	6.68	6.69	*kV*
Power Factor ($\cos(\phi)$)	0.99	0.99	−
Operation during measurement period	86.2	72.5	%

Table 6 shows the average line voltage on the low-voltage side of the transformer power factor and how much of the measurement period the transformers have been operating. The transformer was defined to be operating when the apparent power was larger than 0.01 MVA. The line voltage had a standard deviation of approximate 60 *V*. The power factor is close to unity for both transformers, thus the load can be represented by a resistor.

The temperature measurements are located on the low voltage windings. Figure 9a and 9b shows the plot of temperature and line current on the low voltage side. The measurement is indicated by the blue points. [4]

(a) (b)
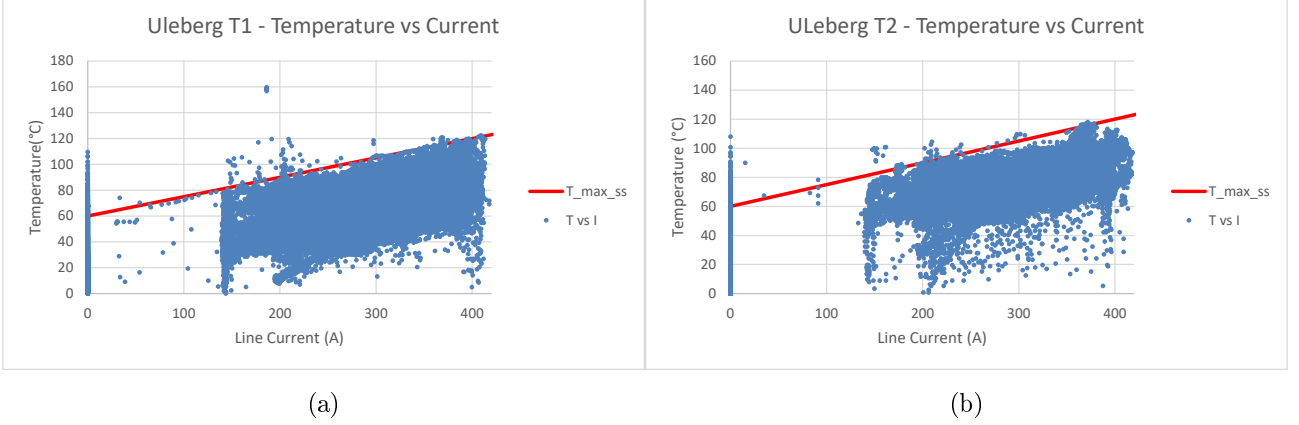
Figure 9: Temperature versus Current for Transformer T1 (a) and T2 (b) in Uleberg

The temperature of the transformers increase, when they start to operate. This is of course due to heat loss in core and windings. The temperature also changes, depending on the loading of the transformer and ambient temperature. The red lines in Figure 9a and Figure 9b indicate a maximum limit of temperature measured in the windings. Under normal operating conditions the temperature does not exceed this limit.

$$T_{ss} = 0.15I_L + 60 \tag{28}$$

where T_{ss} is the steady state temperature in $°C$, I_L is the line current. The equation is a rough estimate by observing the plots in Figure 9a and Figure 9b. The slope and constant are adjusted by trial and error. The resistive loss of electric current is RI^2. Therefore a second order polynomial would probably be better, but the plots in the figures show that a straight line is a good approximation in the current range 150 A to 400 A. The maximum temperature will probably be lower during the winter due to lower ambient temperature. The dataset consists of hourly measurements for almost 6 years (over 52000 measurements). (28) will be used for validating purposes in the simulation. If the estimated temperature exceeds the relation in (28) or is too small the model may be incorrect.

The terminal voltage of the transformers are almost fixed and power factor can be assumed to be unity, thus the active power and load current are proportional. The plots of temperature versus active power would look similar, but the x-axis has a different scale and unit.The relation between T_{ss} and active power (output load) P_{out} can be described by this equation

$$T_{ss} = \frac{40}{3}P_{out} + 60 \tag{29}$$

The active power P_out is in MW. The equation is a rough estimation after studying the measurements.

6 Numerical modelling

This section will describe the simulation models in COMSOL Multiphysics®, material properties and the equations system that describes the different boundary conditions and domain conditions. Two models were used in this master thesis. The first one is a three-phase E-core transformer model that modelled electromagnetics with multiple single-turn coils. This model included skin- and proximity effect in the windings, which gave a non-uniform current density. The second model was a single-phase transformer with an one-legged core. Electromagnetics and thermodynamics were coupled in this model. The model was simplified with multi-turn coil approximation. This coil gives uniform current density and heat loss distribution in the windings, but the heat losses in the windings were replaced by self derived equations.

6.1 Description of boundary and domain conditions

Comsol Multiphysics® has several in-built physic interfaces. The different physicals systems can be described general with the following general differential equation [23]

$$e_a \frac{\partial^2 u}{\partial t^2} + d_a \frac{\partial u}{\partial t} + \nabla \cdot (-c_d \nabla u - \alpha u + \gamma) + \beta \cdot \nabla u = F_s \tag{30}$$

where e_a is the mass coefficient, d_a is the damping or mass coefficient, c_d is diffusion coefficient, α is the absorption coefficient and γ and F_s is the source terms. The different coefficient can have different meaning and unit for different types of physics. u is the dependable parameter. It can be temperature in heat transfer, electric potential in electric current and magnetic vector potential in magnetics. ∇ is the mathematical operator gradient. The gradient of a function $F(x, y, z)$ with x-, y- and z-coordinate F_1, F_2 and F_3 is [24]

$$\nabla F(x, y, z) = \left[\frac{\partial F_1}{\partial x}, \frac{\partial F_2}{\partial y}, \frac{\partial F_3}{\partial z} \right] \tag{31}$$

The symbol $\nabla \cdot$ is divergence and the divergence of a function $F(x, y, z)$ is [24]

$$\nabla \cdot F(x, y, z) = \frac{\partial F_1}{\partial x} + \frac{\partial F_2}{\partial y} + \frac{\partial F_3}{\partial z} \tag{32}$$

The gradient of a vector is a vector, but the divergence of a vector is a scalar. The symbol $\nabla \times$ is the curl and the curl of function $F(x, y, z)$ is [24]

$$\nabla F(x, y, z) = \left[\frac{\partial F_3}{\partial y} - \frac{\partial F_2}{\partial z}, \frac{\partial F_1}{\partial z} - \frac{\partial F_3}{\partial x}, \frac{\partial F_2}{\partial x} - \frac{\partial F_1}{\partial y} \right] \tag{33}$$

The type of shape function in the numerical model can be selected in the settings *Discretization*. The option available is linear, quadratic and cubic. By default the magnetic vector potential is solved with quadratic shape function while temperature and surface radiation use linear. The default settings are used.

6.1.1 Magnetic fields

The governing equations for the magnetic field interface are [23]

$$\nabla \times \mathbf{H} = \mathbf{J} \tag{34}$$

$$\mathbf{B} = \nabla \times \mathbf{A} \tag{35}$$

$$\mathbf{J} = \sigma_e \mathbf{E} + j\omega \mathbf{D} + \sigma_e v \times \mathbf{B} + \mathbf{J}_e \tag{36}$$

$$\mathbf{E} = -j\omega \mathbf{A} \tag{37}$$

where $\mathbf{H}$ is magnetic field intensity $\frac{A}{m}$, $\mathbf{J}$ is current density $(\frac{A}{m^2})$, but $\mathbf{J}_e$ is the current density in the coils. $\mathbf{B}$ is the magnetic flux density (T), (σ_e) is electric conductivity $(\frac{S}{m})$, $\mathbf{E}$ is electric field field strength $(\frac{V}{m})$, $\mathbf{D}$ is electric flux $(\frac{C}{m^3})$ and $\mathbf{A}$ is magnetic vector potential $(\frac{Vs}{m})$. The outer edges got the boundary condition *Magnetic Insulation*. It is described with the equation [23]

$$\mathbf{n} \times \mathbf{A} = 0 \tag{38}$$

The air domain is made large but not infinite. The size is still sufficient for this model. A smaller space may have the problem with magnetic flux being reflected by the outer edges and this may disturb the results. The two remaining boundary condition used in the magnetic field interface are *Ampere's Law* and *Coil*. The are described by four governing equations, (34), (35), (36) and (37). In *Ampere's Law* (37) can be simplified to [23]

$$\mathbf{J} = \sigma_e \mathbf{E} + j\omega \mathbf{D} \tag{39}$$

and current density in the *Coil* domains are defined with (37). J_e is defined as [23]

$$\mathbf{J}_e = \frac{N I_{cir}}{A_{coil}} e_{coil} \tag{40}$$

when homogeneous multi-turn coil approximation is applied. N is number of turns in the winding, I_{cir} is current determined by the electric circuit connected to the terminals of the transformer, A_{coil} is the cross-sectional area of each winding and e_{coil} is the voltage across the windings.

6.1.2   Electric circuits

The voltage across the transformer windings is applied by a external circuit in the model. It is defined by the electrical current interface in Comsol. [23] It used the the following three electrical components:

- Voltage Source
- Resistance
- External I Vs U

and was connected with the arrangement shown in Figure 10.
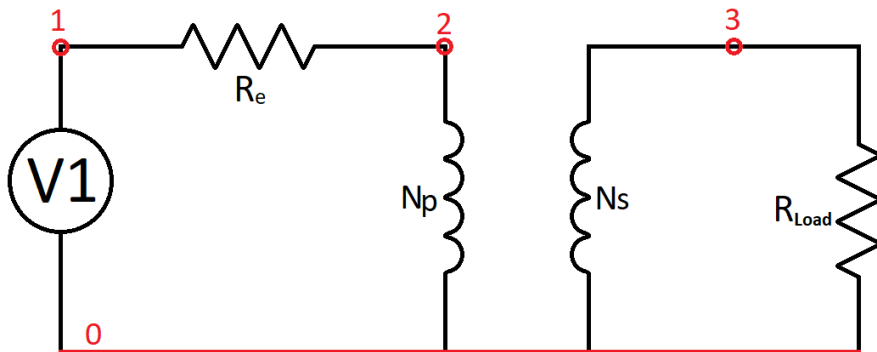
Figure 10: Sketch of Transformer Circuit

The voltage source is an AC-source with amplitude 5388.9 V $\left(\sqrt{\frac{2}{3}} \cdot 6600 \ V\right)$ and frequency 50 Hz. The resistance R_e is a dummy resistance and is included because Comsol did not allow to connect the voltage source directly to the *External I vs U* component. Resistance R_e was given a small value (1 $m\Omega$). In a three phase transformer with star connection on both primary and secondary side, $R_{load} = \frac{V_L^2}{S}$. The output line voltage is 23 kV (V_L) and the rated apparent power 5 MVA (S) gives R_{Load} a value of 105. 8 Ω.

The nodes of the different components of the electric circuit are labelled and the nodes with the same label are connected. The nodes of the electric components are indicated in Figure 10 are labelled 0, 1, 2 and 3. In the three phase circuit, there are three sets of this nodes. They need to be sorted between the phases with addition to the labelling named in this section. For example all nodes belongs to phase 1 is label with additional 1. The nodes of phase 1 will than be called. 10, 11, 12 and 13. A similar pattern is done for phase 2 and 3.

6.1.3 Heat transfer

The governing equation of heat transfer in steady state condition can be written like this [23]

$$\rho C_p \mathbf{u} \cdot \nabla T - \nabla \cdot \mathbf{q} = Q \tag{41}$$

where ρ is the density in $\frac{kg}{m^3}$, C_p is the heat capacity in $\frac{J}{kg \cdot K}$ and u is the velocity field of the material. $\mathbf{q}$ is the heat flux vector defined as [23]

$$\mathbf{q} = -k\nabla T \tag{42}$$

where k is the thermal conductivity in $\frac{W}{m \cdot K}$. Q in (41) is the heat generated in the material. In other words, a heat source. Comsol has heat transfer interfaces for both solid and fluids. The main difference between these two domain is the heat source Q. In solid domain it is defined as [23]

$$Q = Q_0 + Q_{ted} \tag{43}$$

where Q_0 is defined by a *Heat Source* domain. The heat generated in the core is computed in the magnetic-field interface, but the heat loss density in the windings is defined by *Heat Source* domains. Q_{ted} is thermoelastic damping. This parameter may be significant with small structures vibration at high frequencies. This model do not look into vibrations, thus this term is negligible. In fluids, Q is defined as [23]

$$Q = Q_0 + Q_p + Q_{vd} \tag{44}$$

where Q_p is the pressure work. This calculates the heat generated in fluids due to adiabatic compression as well as some themoacoustic effects. It is computed by using relative pressure and is generally small for low Mach number flows. Q_{vd} is the viscous dissipation. This parameters accounts from the transformation of kinetic energy into internal energy due to viscous stresses. This is expected in fluid regions with large velocity gradients or with high turbulence levels. Both Q_p and Q_{vd} is negligible in the thermal model of this thesis.

When making the model, the outer edges have the boundary condition *Thermal Insulation* by default. They are replaced by the boundary conditions *Inflow* and *Outflow*. If the outer edged are perfectly thermal insulated the temperature will keep increasing to infinity. The equations describing the *Inflow* boundary condition are [23]

$$-\mathbf{n} \cdot \mathbf{q} = \rho \Delta H \mathbf{u} \cdot \mathbf{n} \tag{45}$$

where $\mathbf{n}$ is normal vector and ΔH is sensible enthalpy and is defined as [23]

$$\Delta H = \int_{T_{ustr}}^{T} C_p dT + \int_{p_{ustr}}^{p_A} \frac{1}{\rho}\left(1 - \alpha_p T\right) dp \tag{46}$$

The upstream temperature is set as ambient temperature (T_{am}) and upstream pressure is set as 1 atm. α_p is the coefficient of thermal expansion and is defined as [23]

$$\alpha_p = \frac{1}{\rho}\left(\frac{\partial p_A}{\partial t}\right)_p \tag{47}$$

Outflow boundary condition is described by the expression [23]

$$-\mathbf{n}\cdot\mathbf{q} = 0 \tag{48}$$

The last boundary condition from the heat transfer interface is *Diffuse Surface*. This boundary conditions takes into account radiative heat flux between the surfaces of the transformer and ambient. Heat flux from a body i to a body j can be written like this [25]

$$Q_{ij} = F_{ij}\left(J_{R:i} - J_{R:j}\right) \tag{49}$$

where Q_{ij} is the power transmitted (W) from body i to j through radiation. F_{ij} is the view factor and is only dependent on the geometry of the radiating bodies and can be seen as the fraction of radiation from the surface of body i that is intercepted by body j. A_i is the surface area of body i $J_{R:i}$ and $J_{R:j}$ is the total radiative flux leaving surfaces body i and body j, respectively. The radiative flux J can be defined as [25]

$$J_R = \sigma\varepsilon T^4 \tag{50}$$

where σ is Stefan-Boltzmann constant $(5.67\cdot 10^{-}8\ \frac{W}{m^2 K^4})$, ε is the emissivity. Assuming the emissivity is the same for the surfaces of the bodies i and j and they have the temperature T_i and T_j, respectively the total power transmitted from between the to surfaces through radiation is [25]

$$Q_{ij} = A_i F_{ij}\varepsilon\sigma\left(T_i^4 - T_j^4\right) \tag{51}$$

Most of the default settings of the *Diffuse Surface* boundary condition was used and it was applied to all surfaces of the transformer model. Ambient temperature was change from 20 $°C$ (default) to T. This makes Comsol find the ambient temperature view by the surfaces of the transformer. ε was set equal to 0.8 for all surfaces. This was done in numerical model in reference [5]. T stands for temperature and is the dependent variable of heat transfer in Comsol.

6.1.4   Laminar flow

Laminar flow is used to model the movement of fluids (air) around the transformer. The interface is only applied to the air-domain, because it is the only domain that is a fluid. The governing equations for laminar flow is [23]

$$\rho \left(\mathbf{u} \cdot \nabla \right) \mathbf{u} = \nabla \cdot \left(-p\mathbf{I} + \mu \left(\nabla \mathbf{u} + \left(\nabla \mathbf{u} \right)^{T} \right) - \frac{2}{3} \mu \left(\nabla \cdot \mathbf{u} \right) \mathbf{I} \right) + \mathbf{F} + \rho \mathbf{g} \tag{52}$$

and is called Navier-Stokes equation [26]. The term which includes time derivative is not included, because the model is solved for steady state. $\mathbf{u}$ is velocity ($\frac{m}{s}$), ρ is density ($\frac{kg}{m^3}$), p is pressure (Pa), $\mathbf{I}$ is a identity matrix, μ is dynamic viscosity ($Pa \cdot s$), $\mathbf{F}$ is external forces applied to the fluid ($\frac{N}{m^3}$) and $\mathbf{g}$ is the gravitational acceleration (9.81 $\frac{m}{s^2}$). Note that the T in (52) do not stand for temperature, but the matrix transformation *transpose*. The next governing equation is the continuity equation. [23]

$$\nabla \cdot \left(\rho \mathbf{u} \right) = 0 \tag{53}$$

(52) represents the conservation of momentum, while (53) is the conservation os mass. Inertial, pressure, viscous and external forces are included in (52) [26]. The outer edges have the default boundary condition *Wall*. This also includes the surfaces of the transformer, because the laminar flow physics is only applied to the air domain. The *Wall* boundary condition is described with equation. [23]

$$\mathbf{u} = 0 \tag{54}$$

The velocity is 0 $\frac{m}{s}$ at the walls. No fluid is entering or leaving the air domain through the edges defined as walls. The boundary condition on the bottom edge is replace by the boundary condition *Inlet*. The air enters the model from the bottom with a uniform velocity. This represents the cooling fans of the transformer. *Inlet* is described by the equations [23]

$$\mathbf{u} = -U_0 \mathbf{n} \tag{55}$$

$\mathbf{n}$ is a normal vector and U_0 is inlet velocity. The air exits the model through the top, which got the boundary condition *Outlet*, which is described by the equation [23].

$$\left(-p\mathbf{I} + \mu \left(\nabla \mathbf{u} + \left(\nabla \mathbf{u} \right)^{T} \right) - \frac{2}{3} \mu \left(\nabla \cdot \mathbf{u} \right) \mathbf{I} \right) \mathbf{n} = - \left(p_0 + p_{hydro} \right) \mathbf{n} \tag{56}$$

The equation is based on the equilibrium of forces like Naiver-Stokes equations. The term on the left side of the equations represents the inertia force and a similar term can be found in (52). The term on the right side represents the pressure force. p_0 is relative pressure because the reference pressure p_{ref} is set as 1 *atm*. It it was 0 *atm*, p_0 would be the absolute pressure. p_0 is equal to 0 *Pa*. p_{hydro} the pressure due ot the weight of the liquid in the control volume, which is pulled down by gravity [23].

$$p_{hydro} = \rho_{ref} g \cdot \left(\mathbf{r} - \mathbf{r}_{ref} \right) \tag{57}$$

were **r** is the position in the geometry and **r**$_{ref}$ the reference position. it is defined at origin in the geometry (Spacial coordinate [0,0])

6.2   Material properties

Table 7: Material properties

Property	Symbol	Aluminium	Soft Iron	Air	Unit
Relative permittivity	ε_r	1	1	1	$-$
Heat capacity	C_p	900	444	Figure 12a	$\frac{J}{kgK}$
Heat capacity ratio	γ	Not needed	Not needed	1.4	$-$
Thermal Conductivity	k	238	74	Figure 12b	$\frac{W}{mK}$
Density	ρ	2700	7870	Figure 13a	$\frac{kg}{m^3}$
Relative permeability	μ_r	1	1100+25j	1	$-$
Electric conductivity	σ_e	Linear resistivity	Anisotropic	1	$\frac{S}{m}$
Dynamic viscosity	μ	Not needed	Not needed	Figure 13b	$Pa \cdot s$

Most of the material properties listed in Table 7 have the default values from the material library in Comsol. The electric conductivity is the inverse of electric resistivity. Temperature dependence of aluminium's resistivity is included in the thermal model and is described by the linear resistivity model (ρ_e) [23].

$$\rho_e(T) = \rho_{e0} \left(1 + \alpha_T \left(T - T_{ref}\right)\right) \tag{58}$$

where ρ_{e0} is reference resistivity at reference temperature T_{ref} and α_T is temperature coefficient. ρ_{e0} is $2.65 \cdot 10^{-8}$ Ωm for aluminium at reference temperature 20 $°C$ and α_T is 0.0039. [27].

The electric conductivity is isotropic by default with the value of $1.12 \cdot 10^7$ $\frac{S}{m}$. Experience with simulation revealed large value of eddy current in the core. It induced a magnetic field that cancelled out the magnetic field induced by the current in the windings. Eddy current in transformer core is usually minimized by laminating the core. The lamination of transformer core is represented by an anisotropic electric conductivity.

$$\sigma_{SoftFe} = \begin{bmatrix} 1.12 \cdot 10^7 & 0 & 0 \\ 0 & 1.12 \cdot 10^7 & 0 \\ 0 & 0 & 1 \end{bmatrix} \frac{S}{m}$$

The core conducts in x- and y-direction, but not in the z-direction. This mimics the laminated core and reduces the eddy current. The conductivity in the z-direction was adjusted to 1 $\frac{S}{m}$, because this gave the required value eddy current loss in the core. The improvement of the magnetic flux density with anisotropic core versus isotropic core is included in the results.

The second material property of the core that was changed, was permeability. Magnetic materials are usually non-linear, but have a region where they are approximately linear.
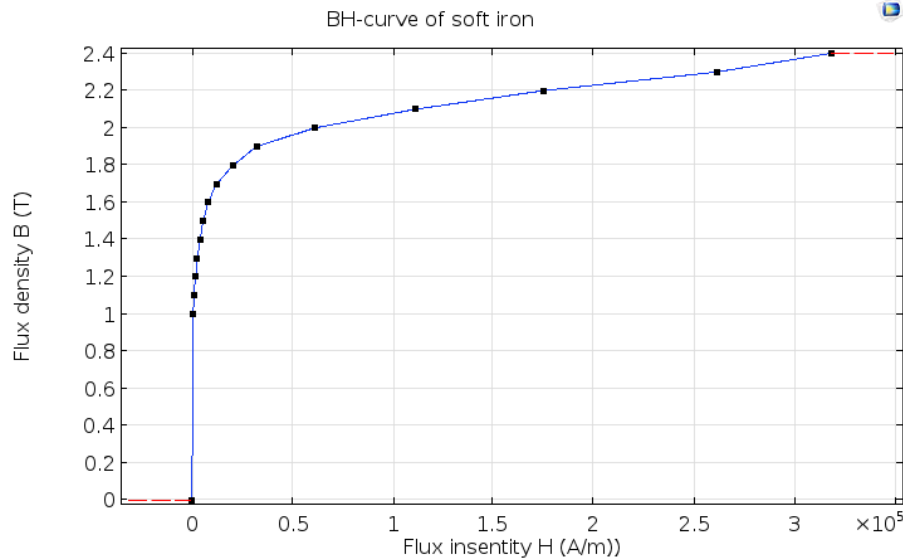
Figure 11: BH-curve of Soft Iron - Comsol

Figure 11 shows the BH-curve of soft iron from the material library in Comsol [23]. The x-axis is magnetic field strength (H) in $\frac{A}{m}$ and y-axis is magnetic flux density (B) in T. Below 1.4 T is close to linear. The transformer typically operates in the linear region. The linear relative permeability is set as 1100. The imaginary part of μ_r for soft iron in Table 7 is for modelling hysteresis loss. This is possible by using the frequency domain study in Comsol. Heat capacity, thermal conductivity and density are values of pure iron from respectively references [28], [29] and [30].

All the properties of air are the default value from material library in Comsol, except for σ. It was change from 0 $\frac{S}{m}$ and 1 $\frac{S}{m}$. This change makes the model more numerically stable according to Comsol support. Air has four temperature dependent parameters: heat capacity, thermal conductivity, density and dynamic viscosity [23].
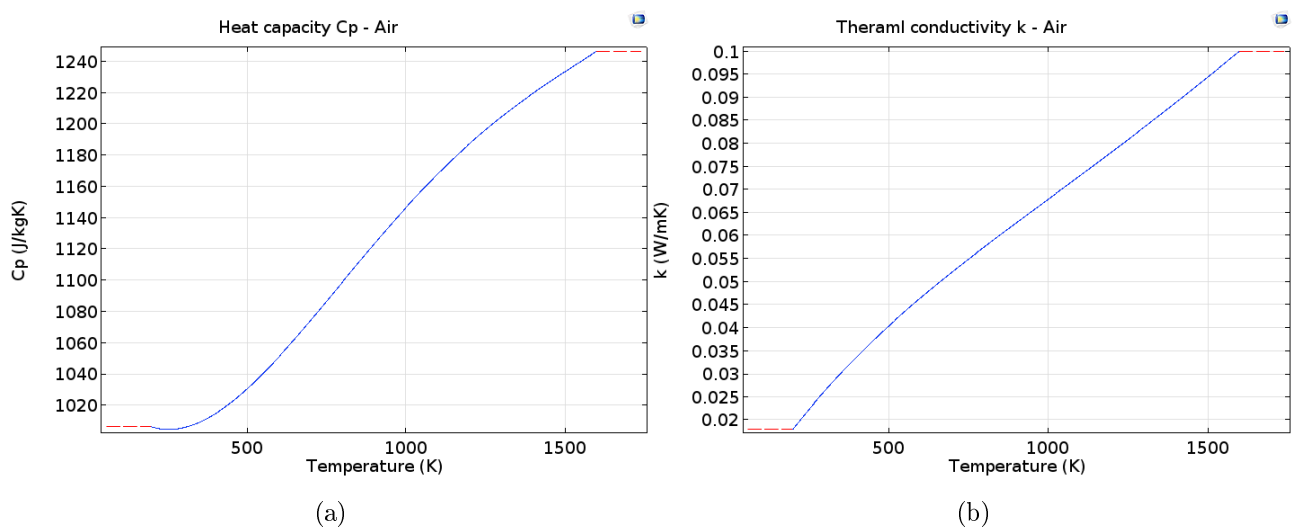

(a)

(b)

Figure 12: Air properties - Heat capacity (a) and thermal conductivity (b)

Figure 12a and Figure 12b show heat capacity and thermal conductivity of air between the temperature range 200 K to 1600 K. They are described with datasets in Comsol's material library and linear interpolation between the points in the dataset.
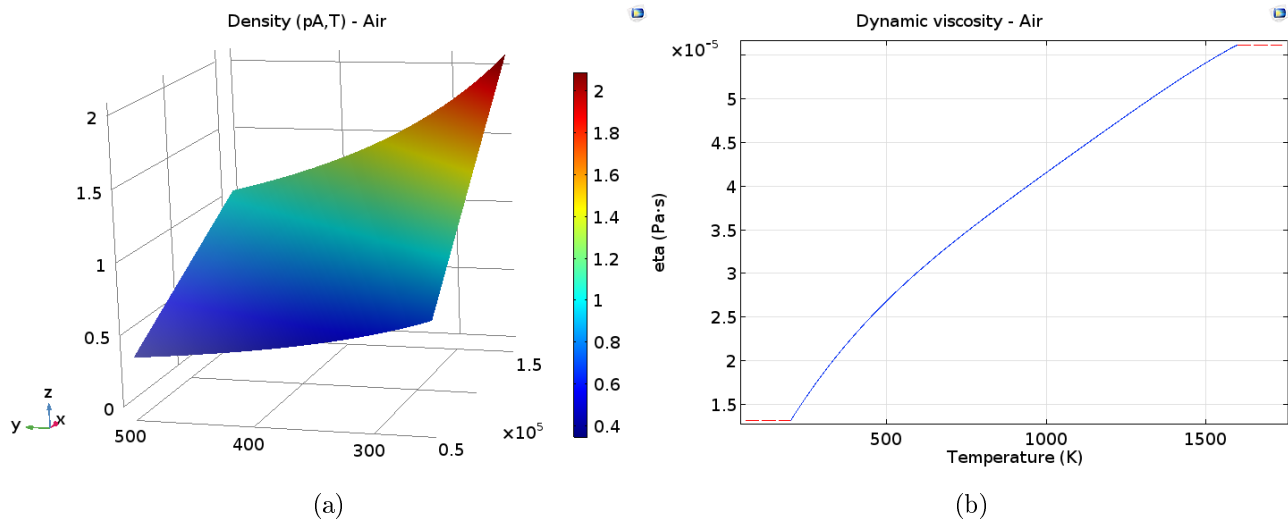

(a)

(b)

Figure 13: Air properties - Density (a) and dynamic viscosity (b)

Figure 13a and Figure 13b show density and dynamic viscosity of air in between 200 °C and 1600 °C, respective [23]. Density is described with continuous function defined by the ideal gas law. It is dependent on both absolute pressure (x-axis) and temperature (y-axis). The definition range of absolute pressure in Figure 13a is 50000 Pa to 150000 Pa and the temperature range is 250 K to 500 K. The orientation of the axis is indicated by the small coordinate system down to the left in Figure 13a. The colour legend shows that the density vary between 0.4 $\frac{kg}{m^3}$ to 2 $\frac{kg}{m^3}$ in the given ranges of pressure and temperature. Dynamic viscosity in Figure 13b is described by a dataset and interpolation in the temperature range from 200 K to 1600 K

Heat capacity ratio and dynamic viscosity of aluminium and soft iron is not included in the model. The expected temperature rise in the model is less than 200 °C. Both iron and aluminium are solid at that temperature. These parameters are necessary in modelling laminar flow. Only the fluid domains is modelled for laminar flow.

6.3   Three-phase transformer model

The whole geometry of the three-phase model is shown in Figure 14a. The outer edges of the geometry of the model are magnetic insulated. The large air domain is a simple way to mimic infinitely large free space. Figure 14b shows the model zoomed in at the windings.
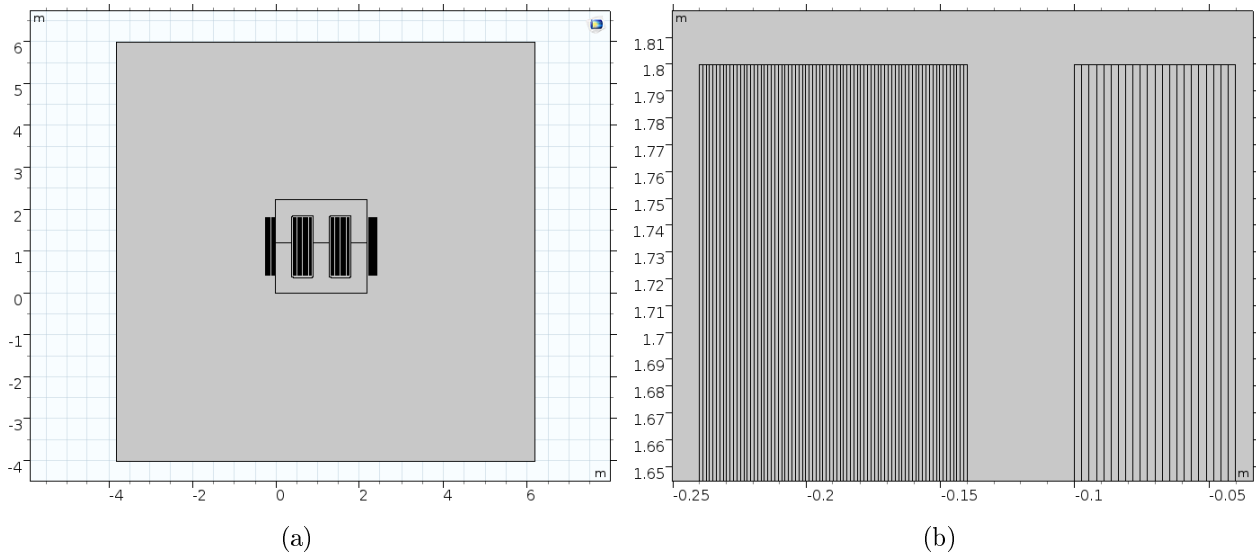

(a)   (b)

Figure 14: Three-phase model - Whole geometry (a) and zoomed in at windings (b)

Table 8: Geometry parameters of transformer models

Parameter	Value	Description
x_leg	380 mm	Thickness of transformer legs
x_gap1	20 mm	Air gap between the core and primary winding
x_gap2	20 mm	Air gap between primary and secondary winding
x_coil_p	60 mm	Total thickness of primary winding
x_coil_s	90 mm	Total thickness of secondary winding
y_cyl	1370 mm	Height of windings
y_gap	50 mm	Air gap between the windings and core in the y-direction
N_p	44	Number of turns in primary winding
N_s	156	Number of turns in secondary winding

The geometry is defined by the parameters in Table 8. The total height of the transformer in the model is 2.13 m and the windings are a few millimetres thick. The model is made easier to compute by rearranging the windings. Originally the windings are thin layers that reach from top to bottom. They are instead cut in half horizontally in the middle. The number of turns is the same, but the foil windings are twice as thick. The length of the cross-section to each winding is cut in half. The current density will be unchanged, because the thickness of the winding is smaller than the skin depth of aluminium (11.6 mm). The results in Section 7.1.2 verify this and show why further splitting of the foil-type winding is not possible.

The model is subdivided into 1205 domains. 1200 of them are the windings. Figure 15 shows a zoomed in view of Figure 14a and different groups of domains are labelled. 1 is the air domain surrounding the transformer core and windings. 2 is the transformer core. The domain groups 3, 5 and 7 belong to the three-phases of the primary windings and 4, 6 and 8 are the three-phases of the secondary windings.
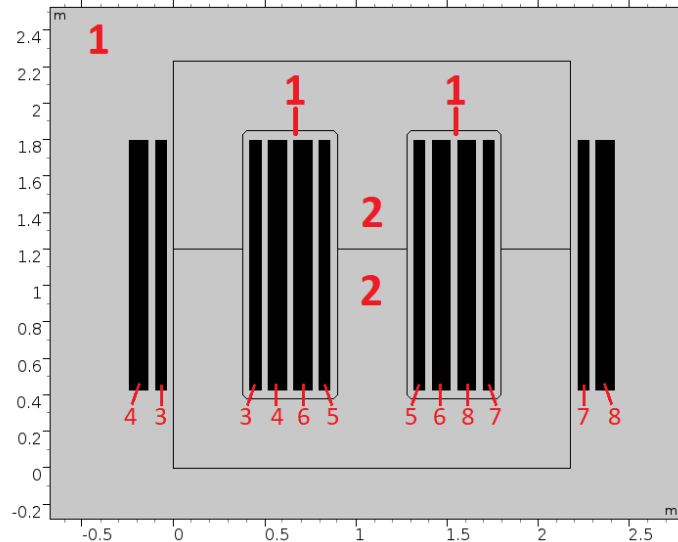

Figure 15: Zoomed in view of three-phase model with general domains

The air domains are described by the *Ampere's law* domain condition with linear relative permeability and no hysteresis loss. The core domains are described by another *Ampere's law* domain condition. The core is linear and includes hysteresis loss. The windings are described by *Coil* domains. There are 6 *Coil* domains in total (3 phases in primary and 3 phases in secondary) and the domains in each of the coils are connected in series. Each phase surrounds one leg of the transformer. The current direction for half of the *Coil* domains are in plane, but the rest is out of plane. Figure 16a and Figure 16b show the *Coil* domains with current direction out of plane coloured in blue in the primary and secondary windings, respectively.
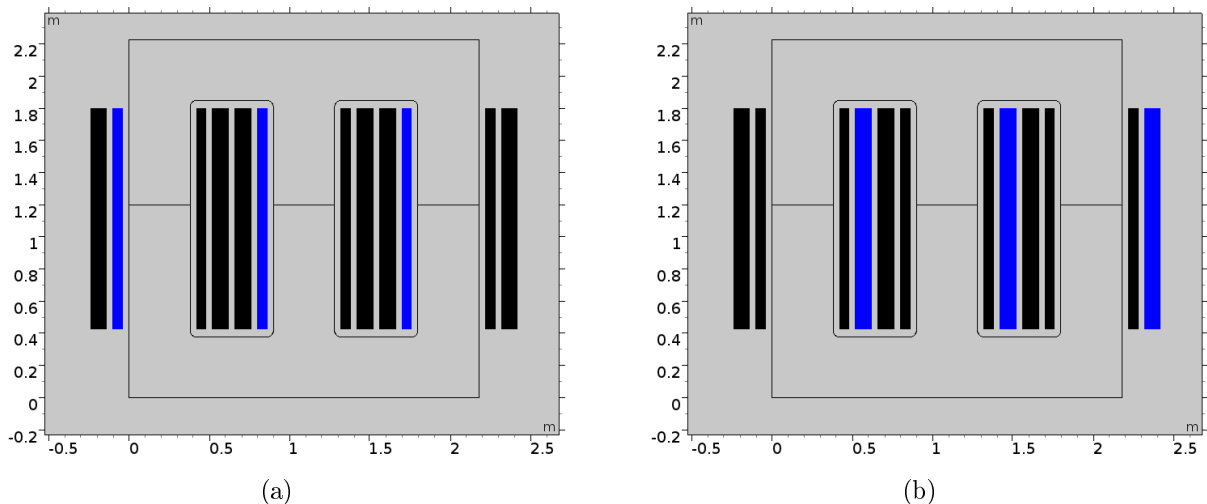

(a)

(b)

Figure 16: Current direction out of plane in primary (a) and secondary windings (b)

6.4   Single-phase transformer model

Figure 17a shows the whole geometry of the single-phase transformer model. The geometry is defined by the parameters in Table 8. Figure 17b shows show a zoomed in view of the transformer with each domain labelled with a number. The different domains are: air (1), iron core (2), primary windings (3) and secondary windings (4).
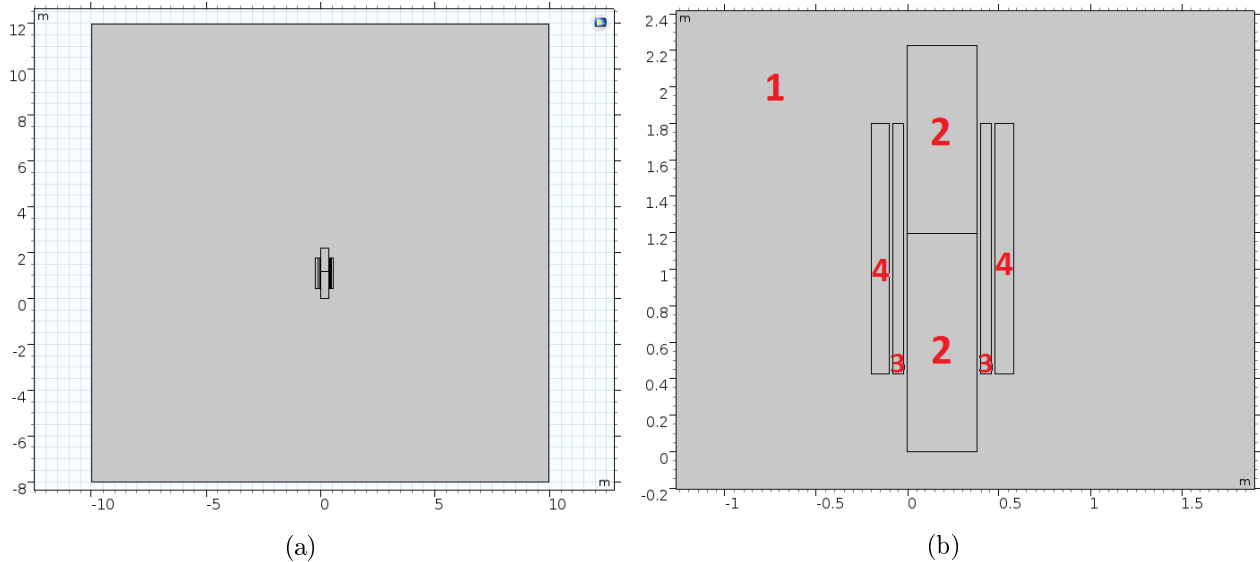

Figure 17: Single-phase model - Whole geometry (a) and zoomed in view of transformer (b)

The electromagnetic conditions are similar to the three phase model. The air domain has *Ampere's law* domain condition with no hysteresis loss and the core domains have *Ampere's law* domain with hysteresis loss. The windings are defined by two *Coil* domains. The current direction for half of the windings in plane and the second half is out of plane. The amplitude of voltage and current in the single-phase model were similar to the three-phase model, except primary current. It was several times larger. This is probably due to change in transformer core and reluctance. This is not a problem, because the heat loss in the core was the same. It is determined by the voltage across the coil and the geometry of the windings. The heat losses in the windings are uniform due to multi-turn winding approximation, but they are replaced by *Heat source* domains in the heat transfer physic-interface. These sources are described by the product of linear resistivity and the function $J^2(x, y)$ (Current density squared).

$$Q_{Winding} = \frac{\rho_e(T)}{A_{coil}} J^2(x, y) \tag{59}$$

where $\rho_e(T)$ is defined by (58). $J^2(x, y)$ is current density squared in the windings as a function of x- and y-coordinates in the 2D-model. It is derived from plots of J^2 exported from the results of the electromagnetic study of the tree phase model. $J^2(x, y)$ is used instead of $(J(x, y))^2$, because $J^2(x, y)$ will probably have a smaller difference from the original plot of J^2. A_{coil} represents the cross-sectional area of the the windings. It will be used as an adjustment factor, because of the approximations of

current density. The average heat loss in the transformer was adjusted to fit the requirements in Table 9

Table 9: Average heat loss density criteria

Part of transformer	Heat Loss (kW)	Volume (m^3)	Average volumetric heat loss ($\frac{kW}{m^3}$)
Core	5.4	1.3	4.3
Primary windings	6.1	0.7	8.7
Secondary windings	10	1.3	7.6

The resistivity was fixed at the reference resistivity at 20 °C, because the total heat losses given in Table 9 are based on the resistance at 20 °C [4]. The volume is based on the geometry of the transformer model. The general equation for $J^2(x, y)$ is proposed in this thesis to be

$$J^2(x,y) = f(x) \left(e^{b(y-y_{ref1})} + e^{-b(y-y_{ref2})} \right) + g(x) \tag{60}$$

where b is a constant 110 and $f(x)$ is a function of x (it is the x-coordinate in the geometry) defined by the plot of J^2 on top and bottom of the windings. ($g(x)$) is defined by plots of J^2 across the middle of the windings. The equations for $f(x)$ and $g(x)$ can be found in Section 4.2.

The air surrounding the transformer has the *Fluid* domain and the rest of the domains (core and windings) are defined as *Solid*. The outer boundaries to the left and right of the model have *Temperature* boundary conditions. It is set to be ambient temperature. The bottom outer boundary got *Inflow* boundary condition and the top got *Outflow* boundary condition. All the surfaces of the transformer have the *Diffuse surface* boundary condition. This includes surface to surface radiation and heat transfer from the transformer to the surroundings by radiation. The emissivity ϵ is set to 0.8 on all surfaces.
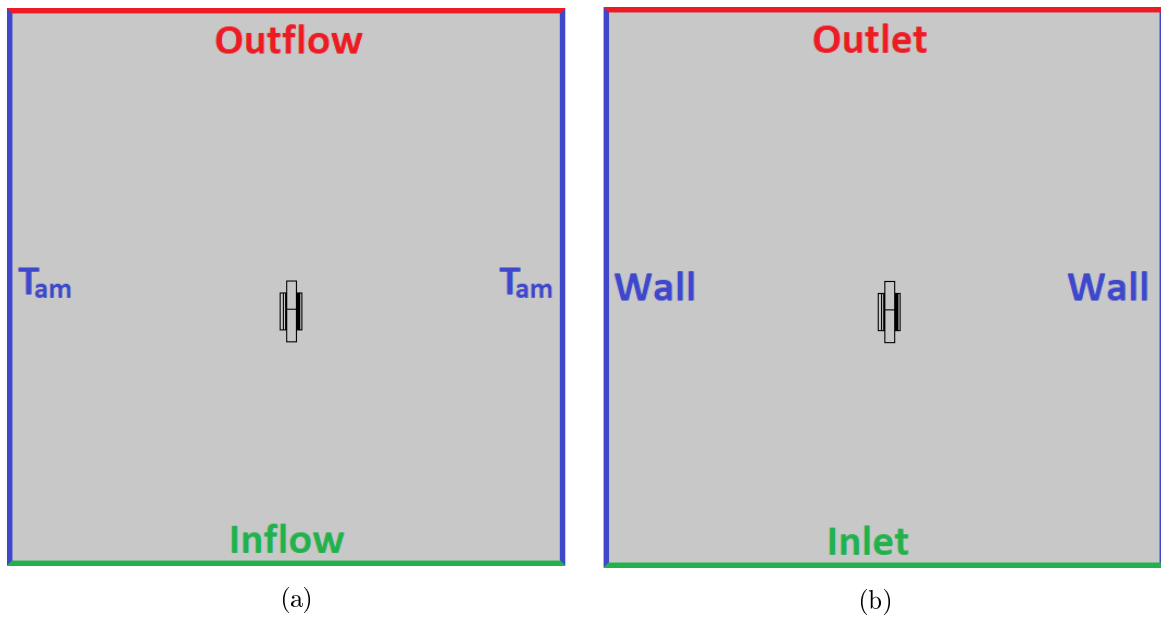

(a)   (b)

Figure 18: Outer surface boundary conditions - Heat transfer (a) and Laminar flow (b)

The outer boundaries of the model also have boundary conditions from laminar flow physics-interface. The left and right side got the *Wall* boundary condition. This means no flow is flowing in or out of those surfaces. The *Inlet* condition is applied to the bottom of the model. The inlet air enters at the bottom of the model with a uniform velocity across the boundary. The top outer edge had the *Outlet* condition. The air is flowing at the bottom and out of at the top of the model and these conditions will include forced convection. This is better illustrated in Figure 18a and Figure 18b. Free convection is modelled by including *Gravity* in the laminar flow interface. It is an external force that causes movement in the air due to variation in density.
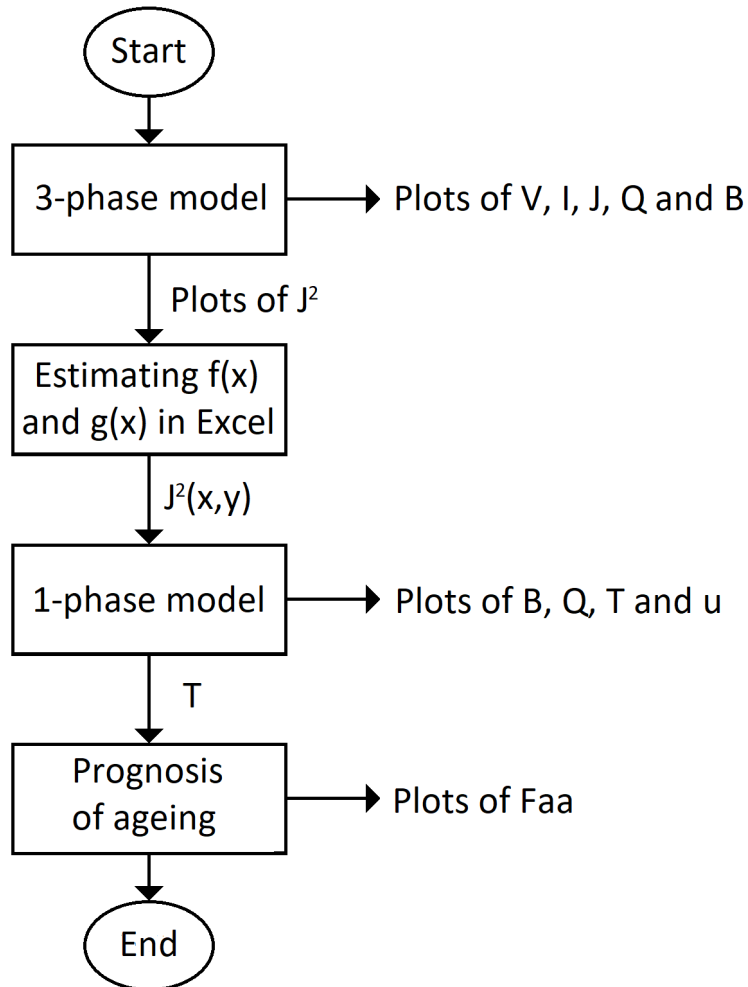
Figure 19: Flow shart of modelling procedure

Figure 19 shows the modelling procedure of the two models. First the three-phase model was used to model the electromagnetics of the transformer with skin- and proximity-effect included in the windings. Plots of J^2 were exported to Excel and used to derive the $J^2(x,y)$. It was used in the heat source equations in the single-phase model. The temperature results of the single-phase model were used to prognose the ageing rate of the paper insulation.

6.5   Simulation cases

The three phase transformer model with multiple single-turn windings was first modelled at full load. It is operating at full load when the load resistance is equal to 105.8 Ω. Then the plots of J^2 were exported to Excel and processed. These results give the function $J^2(x, y)$, which was used in the heat source functions in the windings. It replaced the uniform heat loss distribution from the multi-turn windings.

The single-phase transformer model was first modelled at full load with ambient temperature 20 $^\circ C$ and inlet velocity of air equal to 1.3 $\frac{m}{s}$. The results of this case study as used as a reference plot. The following case studies were done

- Comparing uniform to non-uniform current density in the windings

- Investigating the deviation in temperature when heat transfer by radiation is not included

- Modelling the transformer operating at full load with the ambient temperatures 10 $^\circ C$, 40 $^\circ C$ and 70 $^\circ C$

- Modelling the transformer with the cooling fans turned off (Inlet velocity 0 $\frac{m}{s}$)

The last results presented in this thesis are the prognosis of the rate of ageing at different operating conditions.

7 Results and Discussion

This section contains the simulation results from the numerical modelling in Comsol. First the results from the electromagnetic of the three-phase model is presented, then the results from the single-phase model. The last results presented is the study of acceleration ageing factor (F_{aa}) and the prognosis of rate of ageing of the transformer at the different operating conditions. The last part of this section evaluates the numerical models in this thesis and gives suggestion for improvement and future work.

7.1 Results from three-phase model

The voltage and current waveforms of the transformer are shown in Figure 21a, Figure 21b, Figure 20a and Figure 20b.

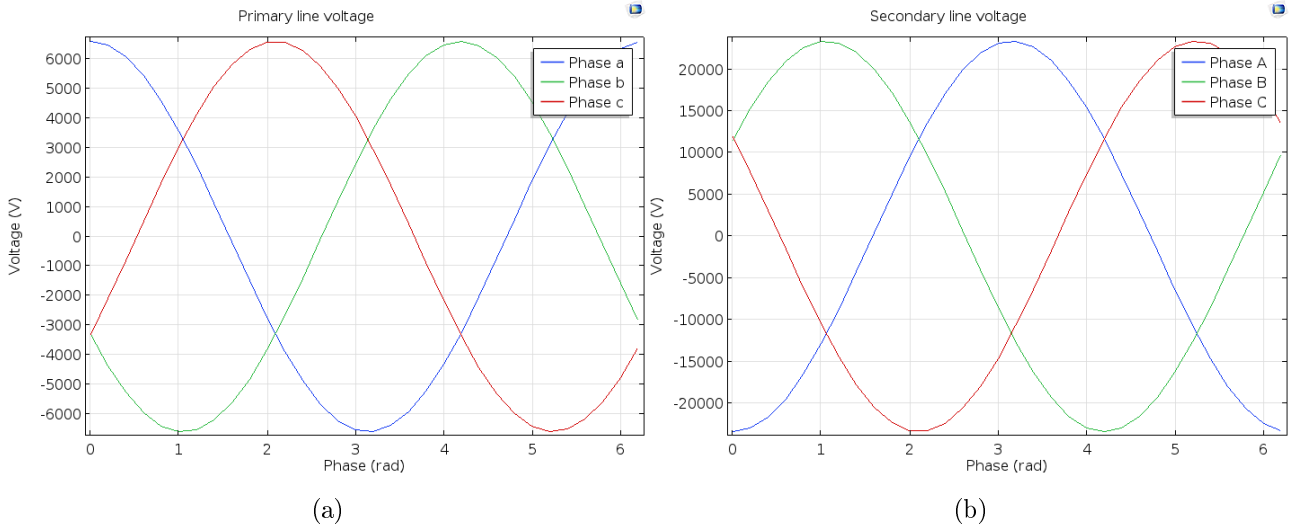(a)   (b)

Figure 20: Line voltage in primary (a) and secondary (b) windings

These plots show that the transformer is operating under balanced condition with expected amplitudes of both voltage and current. The transformer gets out of balance if the load resistance is small. If it is very small it is the same as short circuiting the terminals. Modelling experiences showed that too high number of turns in the windings made the secondary voltage smaller. The primary voltage is fixed, because it is connected to a voltage source (Infinity bus). Magnetic flux density in the core was reduced when the number of turns increased. Leakage inductance of a transformer is proportional to the number of turns squared. Understanding equivalent circuit of a real transformer in Figure 4 and the theory in Section 4.2 the impedance across the transformer is larger, thus the voltage drop is greater.
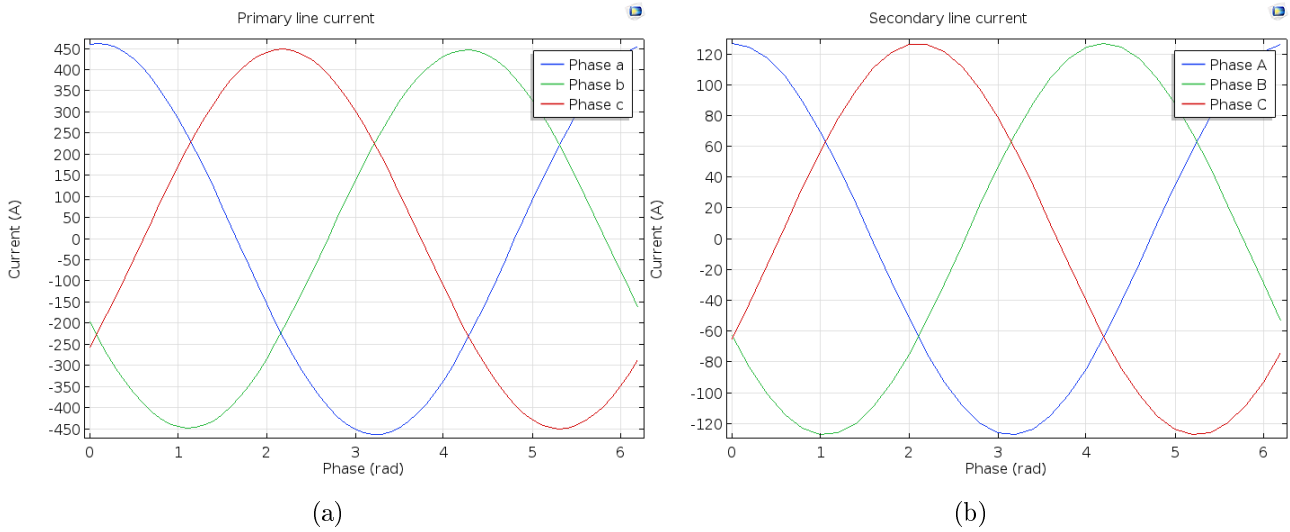
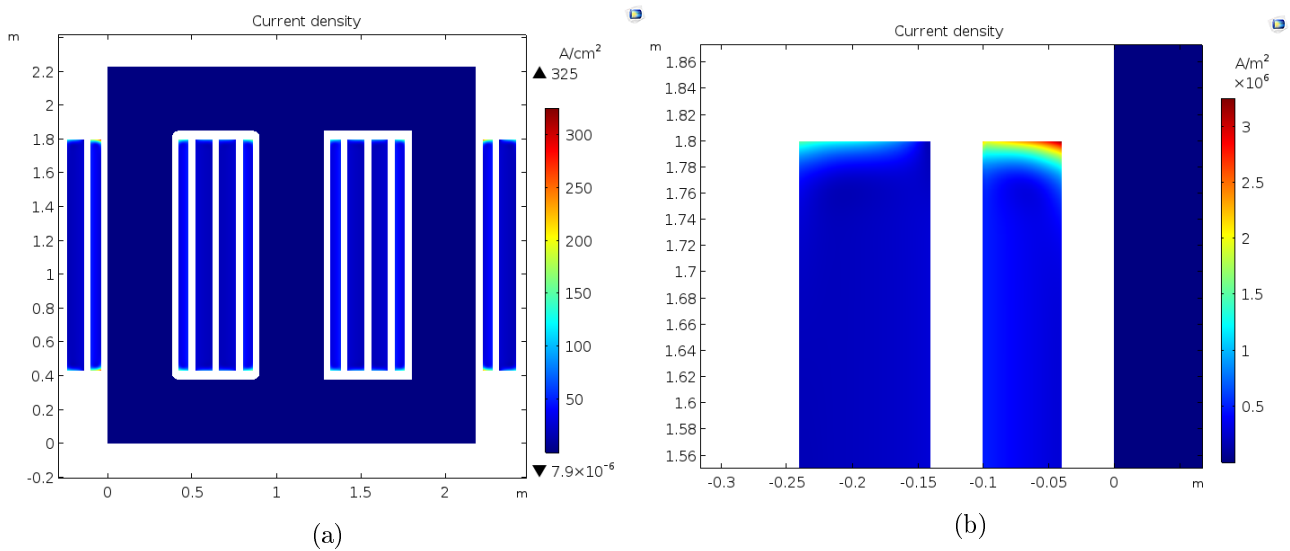Figure 21: Line current in primary (a) and secondary (b) windings

Figure 22: Current density of the transformer (a) and zoomed in at windings (b)

The current density peaks at the top and the bottom of primary windings. This is due to skin effect and proximity effect in the foil type windings. The colour range in the plot in Figure 22a and Figure 22b is from 0 $\frac{A}{m^2}$ to the maximum value of 325 $\frac{A}{cm^2}$ / $3.25 \cdot 10^6 \frac{A}{m^2}$. The edges of the domains of the three-phase model are removed, because they made it hard to see the plot. Figure 22b shows a zoomed in view of the plot at the top of the windings on the far left side of the transformer model. The current density in the transformer is much smaller than the maximum values at the ends of the windings.
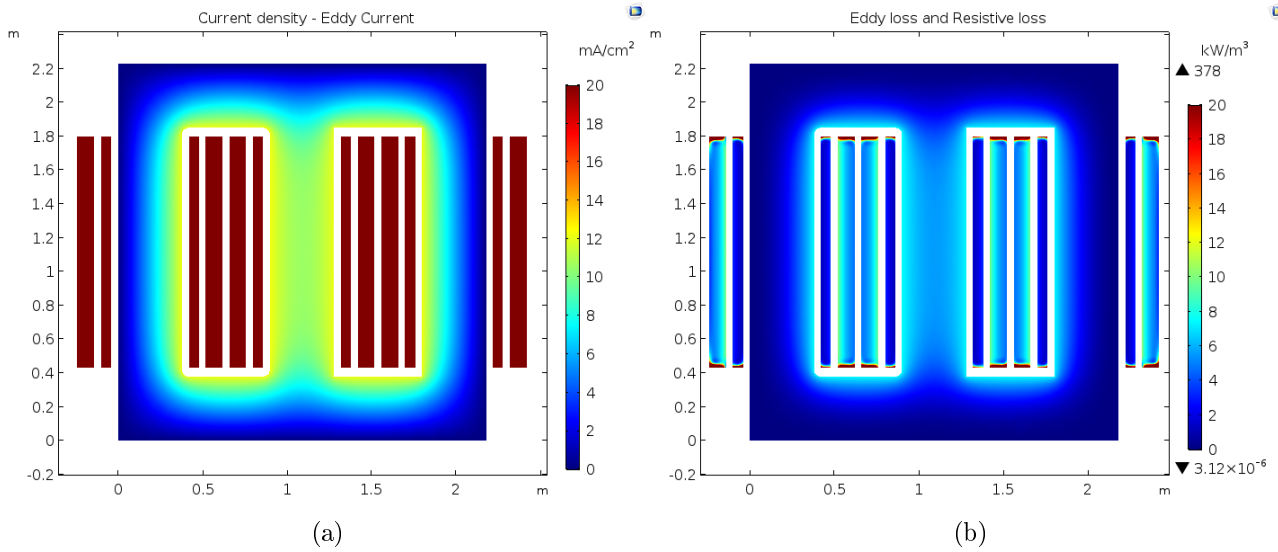
33

Figure 23: Eddy current (a) and Eddy current loss and resistive loss (b)

Reducing the maximum value of the current density in the colour range from $3.25 \cdot 10^6 \ \frac{A}{m^2}$ to 200 $\frac{A}{m^2}$ reveals the current density in the transformer core. This is the eddy current. Figure 23b shows a plot of both the eddy current loss density in the core and restive loss density in the windings. The range is from 0 to 20 $\frac{kW}{m^3}$. The greatest loss is in the primary windings, but the resistance is fixed. Thermodynamics are not included and the temperature is set fixed at 20 °C.
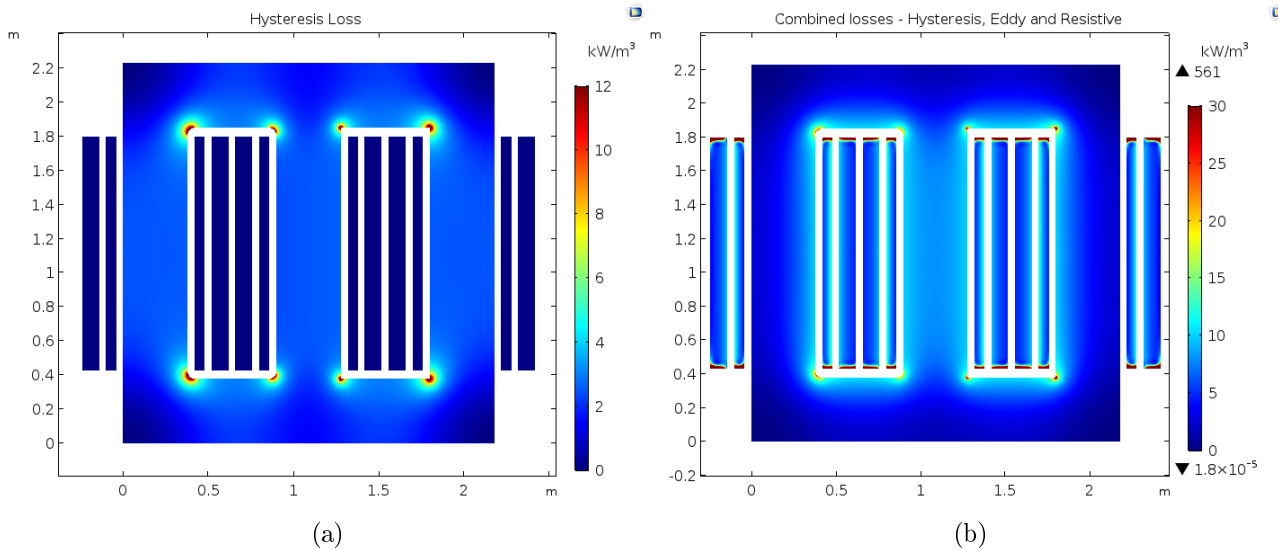

Figure 24: Hysteresis loss (a) and Total loss (b)

Figure 24a shows the hysteresis loss in the transformer. The hysteresis loss in the windings is 0 W in the windings, due to the set-up of the model. The core has a relative permeability of $\mu_r = 1100 + 25j$. Figure 24b shows the sum of hysteresis loss, eddy current loss and resistive loss. The colour range is set at 0 $\frac{kW}{m^3}$ to 30 $\frac{kW}{m^3}$. The maximum heat loss density is at the top and the bottom of the primary windings, which is significantly larger than the rest.

34

7.1.1 Flux density in the core

The very first problem that occurred when starting modelling the transformer, was that almost no magnetic flux was present in the core and the edges close to the windings had an unrealistic large flux density. The problem was caused by electric conductivity of the core, which was isotropic. Large eddy currents were induced in the core, which cancelled out the flux density. Normally the eddy current is reduced by laminating the core. The solution of the problem was to make the electric conductivity of the core anisotropic. This mimics the behaviour of a laminated core.
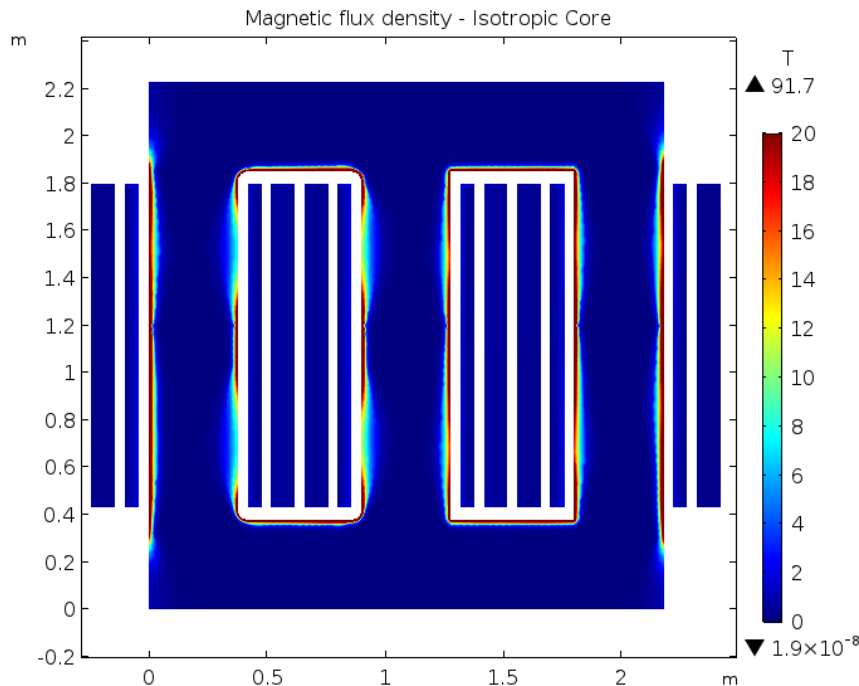

Figure 25: Flux density - Non-Laminated core

Figure 25 shows the flux density in three-phase transformer model with an isotropic core and linear permeability. The flux density reaches values over 91.7 T. Flux density in the majority of the core is close to 0 T.

Figure 26a and Figure 26b show the plots of flux density in the transformer with non-linear permeability and linear permeability. The average flux density is 1.1 T in both cases. The transformer usually operates when the core is unsaturated [11]. Linear permeability will make the model simpler, but the main reason to use linear permeability is to model the hysteresis loss. The *Ampere's law* domain in condition in Comsol has an option called Magnetic Losses, which use a complex permeability. This is only available for frequency domain studies.
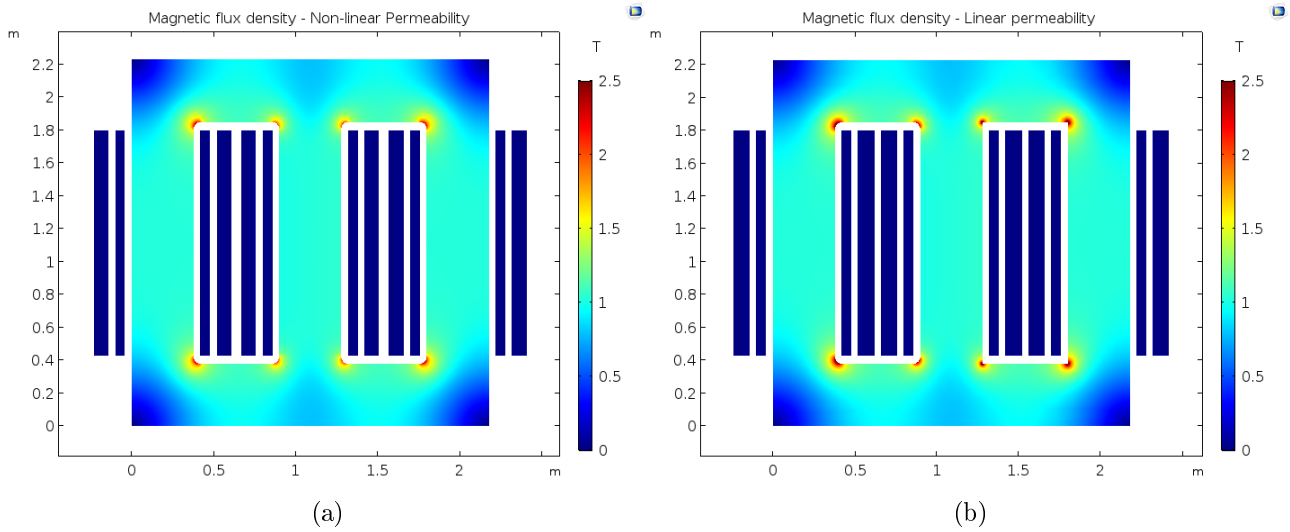
(a)

(b)

Figure 26: Flux density - Non-linear permeability (a) and linear permeability (b)

The difference in flux density with linear and non-linear core seems to be negligible. The difference is better illustrated in Figure 27.
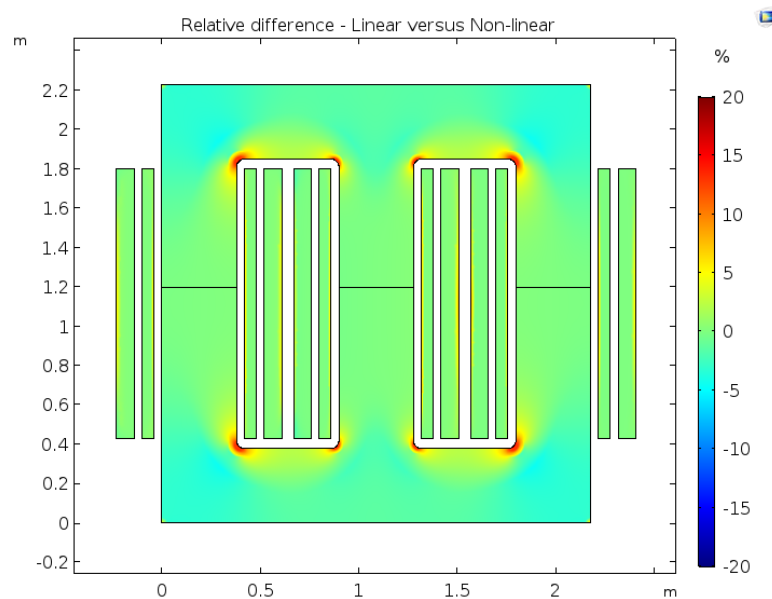

Figure 27: Flux density - Difference in linear and non-linear core

Figure 27 shows the relative difference between the flux density of non-linear core without hysteresis losses and linear core with hysteresis losses in %. The majority of the flux density in the transformer with linear core deviates less than 5 % from the non-linear core. The greatest difference is located in the corners where singularities occurred. The flux density is very high. This is over a small area and they will not occur in the thermal model with the single-phase transformer with one-legged core. The singularities occurs in a small area and the end results of temperature distribution will not significant. Therefore the linear core with hysteresis loss will be sufficient for further modelling.

36

7.1.2   Winding arrangement in coils

The *Coil* domain in Comsol can model single-turn windings and homogeneous multi-turn windings. The last type simplifies the model and allows it to be solved faster, but the current density is uniform. This is not the case due to skin- and proximity-effect. The model in reference [6] had multiple single-turn windings. The current density is greater in at the top and the bottom of the foil windings, but they have fewer turns.

The *Coil* domains account for 1200 domains in the three-phase model and each winding is a few millimetres thick. The minimum size of the mesh in the model is determined by this thickness. The mesh then needs to be finer and this increases the computation time of the model. It is suggested to rearrange the windings. Figure 28a shows the current density along the hight the windings with 60 foil windings with total thickness 6 *cm*. The hight of each winding is 137 *cm*. Figure 28b shows the current density along the hight of same cross-section, but the windings is cut in half horizontally. The hight of each winding is cut in half and the thickness is doubled. The number of turns are the same and the dimension of the total cross-section is the same. The current in the windings is 400 *A*
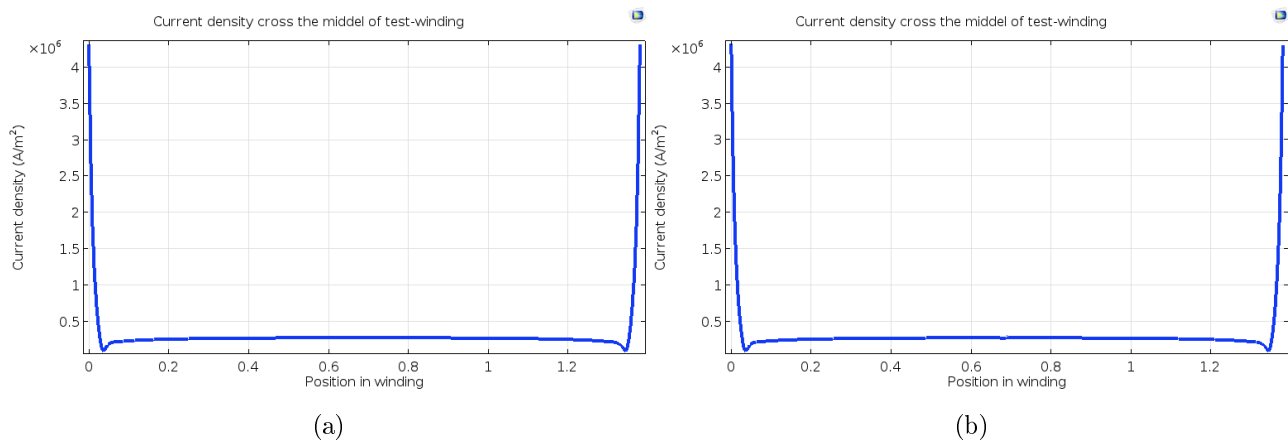

Figure 28: Current density along the hight of test-winding in 1 part (a) and 2 parts (b)

The horizontal axis in Figure 28a and Figure 28b is the hight of the windings. 0 *m* is the bottom and 1.37 m is the top. The rearrangement of the windings allowed thicker windings (the width doubled). This increased the minimum size of the mesh inside the windings and made the mesh courser and reduced the computation time. The number of turns is the same (60 turns). The difference between the plots in Figure 28a and Figure 28b is negligible. Figure 29 illustrates the rearrangement of the winding done in this simulations.

Figure 30a and Figure 30b show when the windings are divided into 3 and 30, respectively. The thickness is 3 and 30 times larger compared to the original windings. The dimension of the total cross section, number of windings and current are the same. Figure 30a shows clearly a peak at the border-region between the top, middle and bottom section. This is due to skin effect. Figure 30b illustrates how different the current density is in a bundle of wires instead of layers of foil windings in the same cross-section, current and number of turns.
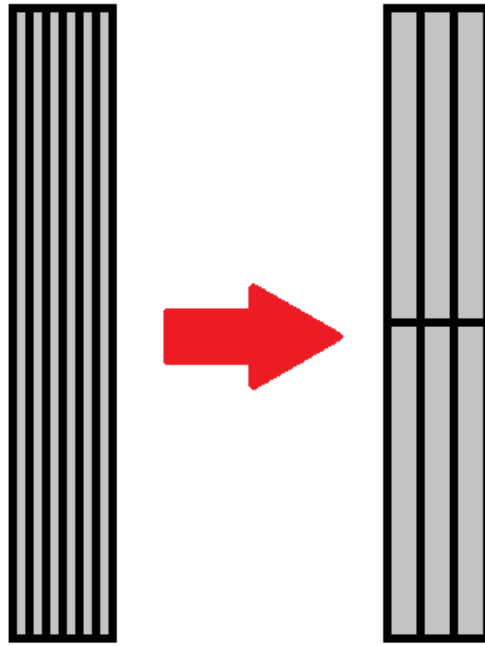
Figure 29: Wining rearrangement
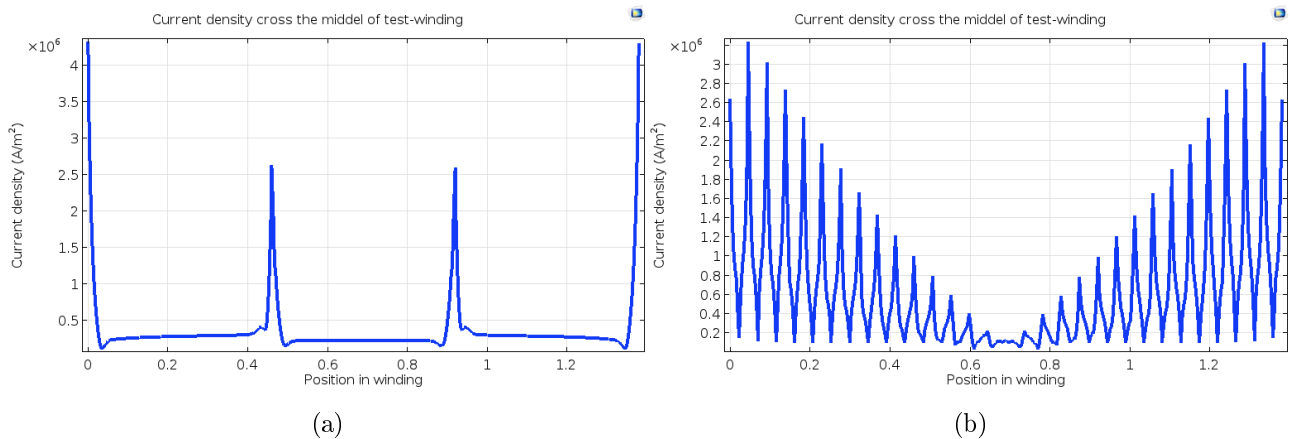
Figure 30: Current density along the hight of test-winding in 3 parts (a) and 30 parts (b)

The conclusion of these plots is that foil-type windings, which stretches from top to bottom of the cross-section of the coil, can be replaced by foil windings which are divided on the middle and twice as thick. Note that this is true because the skin depth of aluminium (11.6 mm) is much larger than the thickness of the windings ($\approx 1\ mm$).

7.1.3   Current density in coils

The three phase transformer model became too computational heavy with multiple single-turn windings. When the model only included electromagnetics, it used approximately 10 *min*. One attempt of coupling heat transfer and laminar flow was executed, but was too time consuming in the short period with work on this master thesis. The solver used over an hour to do 10 iterations and was no where close to converge to any solution. The single-phase transformer model was used instead to model the electromagnetics of the transformer coupled with thermodynamic and fluid dynamics. Single-phase transformer with one-legged core is common simplification, because of symmetry of the transformer [5–7,31]. The single-turn windings were replaced by multi-turn windings. The windings of one phase of the transformer can now be described with 4 domains in stead of 400. (1200 domains for all three phases). The current density and heat loss density are uniform across the windings, but the skin- and proximity-effect can still be included. Plots of J^2 were exported from Comsol to Excel.
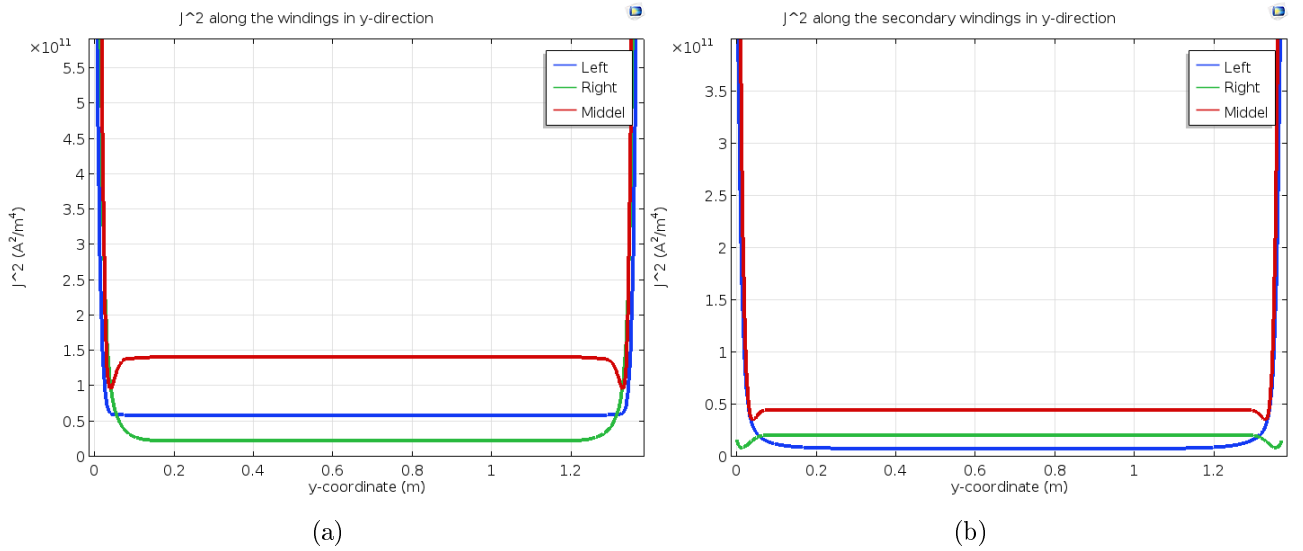

Figure 31: J^2 along the vertical of primary (a) and secondary windings (b)

Figure 31a and Figure 31b show line plots of the current density squared (J^2) along the hight of the primary windings and the secondary windings, respectively. It is suggested that the general equation

$$J^2(x,y) = (f(x) - g(x)) \left(e^{b\left(y - y_{ref1}\right)} + e^{-b\left(y - y_{ref2}\right)} \right) + g(x) \tag{60}$$

will describe J^2. $f(x)$ is an approximated function defined by the plot of J^2 at the top and bottom of the foil-type windings and $g(x)$ is defined by the plots of J^2 across the middle of the windings. The constant b were fitted for the plots of J^2 in Figure 31a and Figure 31b with the solver function in Excel. It was set as 110, which was an average value. (60) could benefit with an addition of a sinusoidal in the equation, to be able to fit the shape of J^2 in the windings more accurately (See the red curves in Figure 31a and Figure 31b). The different reference positions in (60) are described in Table 10

Table 10: Reference positions

Paramter	Equation	Value (cm)
x_{ref1}	-x_gap1 - x_coil_p - x_gap2 - x_coil_s	-23
x_{ref2}	-x_gap - x_coil_p	-10
x_{ref3}	x_leg + x_gap1	42
x_{ref4}	x_leg + x_gap1+x_coil_p+x_gap2	52
y_{ref1}	x_leg + y_gap + y_cyl	43
y_{ref2}	x_leg + y_gap	180

The position of the reference position in the coordinate system is indicated in Figure 32.
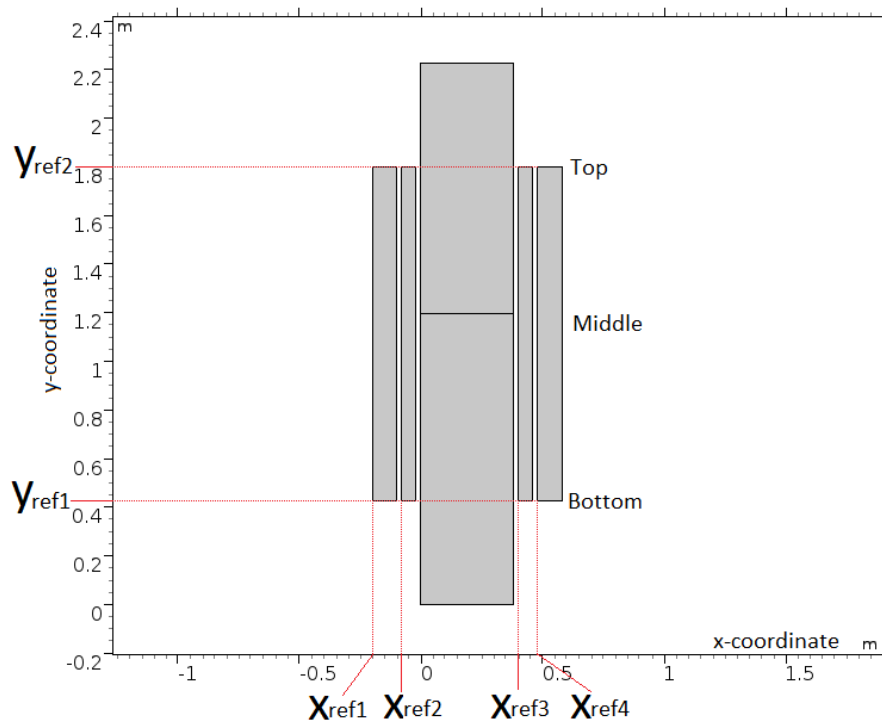

Figure 32: Reference positions

Note that the indication of *middle* in Figure 32 does not refer to the same middle in Figure 31a and Figure 31b. It indicates the middle across the windings parallel to the x-axis.
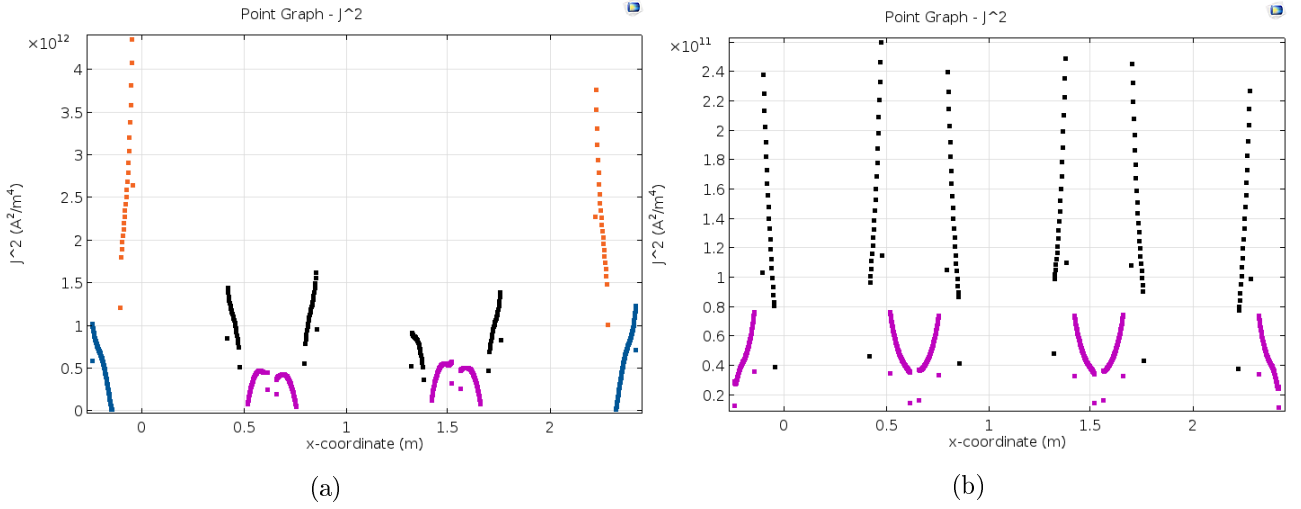
Figure 33: J^2 across the top (a) and the middle (b) of transformer windings

Figure 33a and Figure 33b show the point plot of J^2 across the top and middle of the windings, respectively. The points are sorted into different groups indicated by the colours. Black indicates J^2 in the primary windings and purple indicates the secondary windings, in Figure 33b. As expected the current is larger in the primary windings. It is the same in Figure 33a, but J^2 in the primary windings and the secondary windings on the far left and far right side of the transformer have a different shape and magnitude than the rest. Therefore they are sorted in from the rest in different groups. Orange indicates J^2 in the primary and blue indicates J^2 in the secondary windings. The plots in Figure 33a and Figure 33b were used to derive the equation form $f(x)$ and $g(x)$. The equation of $f(x)$ derived from the plots of J^2 on the far left and right side of the transformer (Indicated orange and blue) were used to describe J^2 on the left side of the single-phase transformer model. $f(x)$, defined by the remaining plots of J^2, was used on the right side. $g(x)$ was the same on both sides.

Table 11: $f(x)$ and $g(x)$ for the different windings

Cross-section	Function	Equation
Primary winding	$f(x)$	$5.76 \cdot 10^{14} \left(x - x_{ref1}\right)^2 + 5.56 \cdot 10^{12} \left(x - x_{ref1}\right) + 1.74 \cdot 10^{12}$
left side of core	$g(x)$	$3.17 \cdot 10^{13} \left(x - x_{ref1}\right)^2 - 4.56 \cdot 10^{12} \left(x - x_{ref1}\right) + 2.47 \cdot 10^{11}$
Primary winding	$f(x)$	$-1.08 \cdot 10^{13} \left(x - x_{ref2}\right) + 1.32 \cdot 10^{12}$
right side of core	$g(x)$	$3.17 \cdot 10^{13} \left(x - x_{ref2}\right)^2 + 7.56 \cdot 10^{11} \left(x - x_{ref2}\right) + 8.75 \cdot 10^{10}$
Secondary winding	$f(x)$	$-1.05 \cdot 10^{13} \left(x - x_{ref3}\right) + 5.34 \cdot 10^{10}$
left side of core	$g(x)$	$-3.25 \cdot 10^{12} \left(x - x_{ref3}\right)^2 + 7.15 \cdot 10^{10} \left(x - x_{ref3}\right) + 3.36 \cdot 10^{10}$
Secondary winding	$f(x)$	$6.93 \cdot 10^{14} \left(x - x_{ref4}\right)^3 - 1.86 \cdot 10^{14} \left(x - x_{ref4}\right)^2$
right side of core		$+1.56 \cdot 10^{13} \left(x - x_{ref4}\right) + 7.05 \cdot 10^{10}$
	$g(x)$	$3.29 \cdot 10^{12} \left(x - x_{ref4}\right)^2 - 7.29 \cdot 10^{11} \left(x - x_{ref4}\right) + 7.36 \cdot 10^{10}$

Table 11 contains all the equations of $f(x)$ and $g(x)$ used in the single phase model, derived from the exported plots of J^2. All the equations are unique with their reference position described in Table 10. The plots of the equations are given in Appendix C.

7.2   Results from single-phase model

The model with only electromagnetics included, used on average 10 *min* to solve the task. The single-turn windings were then replaced by homogeneous multi-turn coils. This would simplify the model and make it possible to solve with an acceptable computation time. The heat loss distribution in the core is approximately the same. Figure 34a shows the magnetic flux density in the core in the single-phase transformer model. The singularities occurring at the corners of the e-core transformer are gone. The colour range of the magnetic flux density is similar to Figure 26b. Figure 34b shows the hysteresis loss in the single-phase transformer model.

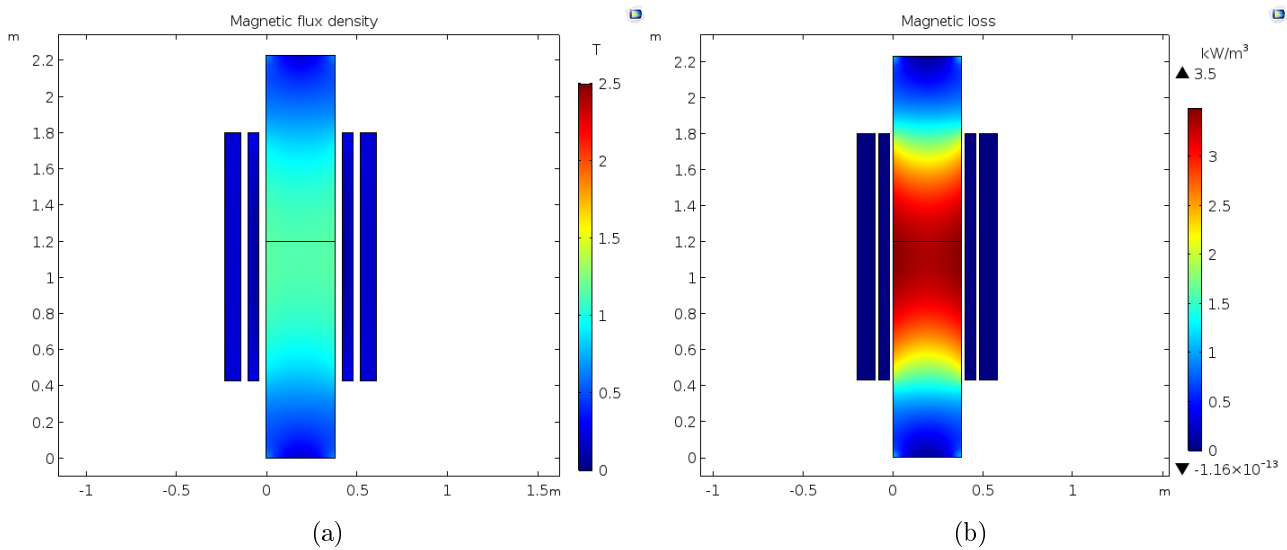(a)   (b)

Figure 34: Flux density (a) and hysteresis loss (b) in single-phase transformer model

The plots are similar to the three phase model (See Figure 26b and Figure 34b). Both models show that average value of hysteresis loss across the transformer leg is 3.5 $\frac{kW}{m^3}$ and average magnitude of magnetic flux density is 1.1 T. The main difference between the one phase and the three phase model is the loss distribution in the winding. The one-phase model with multi-turn coil has uniform heat loss density in the windings. Also the input current (primary current) is several times higher. This will not be a problem for the model since the loss distribution in the windings is replaced with temperature dependent resistivity and $J^2(x, y)$.

Figure 35 shows the heat loss density in the single-phase model. The resistivity is temperature dependent. The heat loss peaks at the top of the primary winding on the left side. This is due to the equations defining J^2 in the windings and the linear resistivity model. The maximum heat loss calculated in the model is 566 $\frac{kW}{m^3}$, but this is over a very small area. Most of the windings have a heat loss density less than 25 $\frac{kW}{m^3}$. The majority of the transformer core has a heat loss density less than 5 $\frac{kW}{m^3}$.
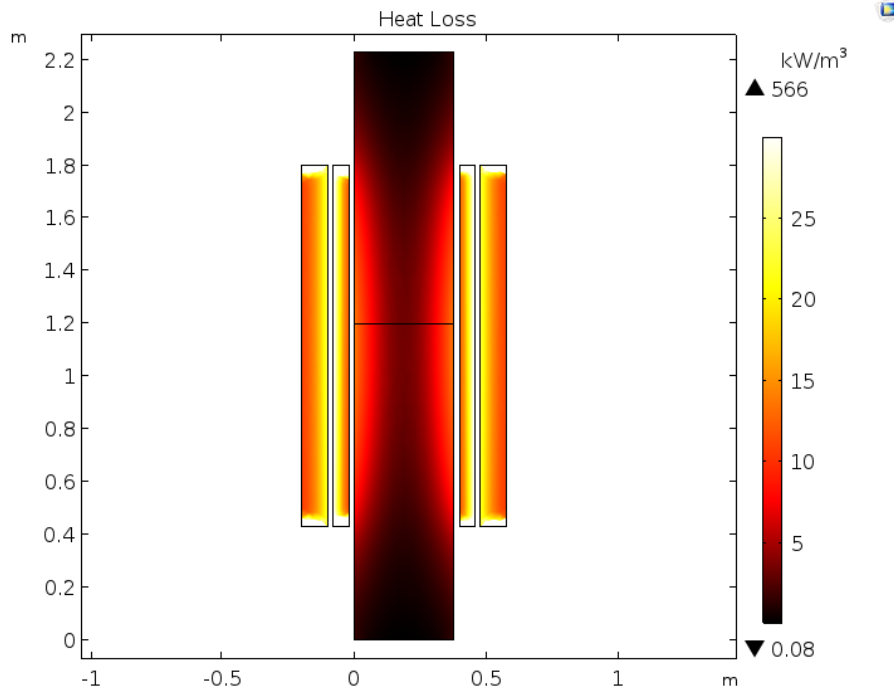
Figure 35: Heat loss density - Single-phase model

Figure 36a shows the temperature distribution in transformer model with fixed resistivity at 20 $°C$. The heat loss is adjusted to match the average heat loss density criteria given in Table 9. The hysteresis loss and eddy current loss are 2.03 $\frac{kW}{m^3}$ and 2.05 $\frac{kW}{m^3}$, respectively. The resistive losses in the primary and the secondary windings are 9.01 $\frac{kW}{m^3}$ and 7.16 $\frac{kW}{m^3}$.
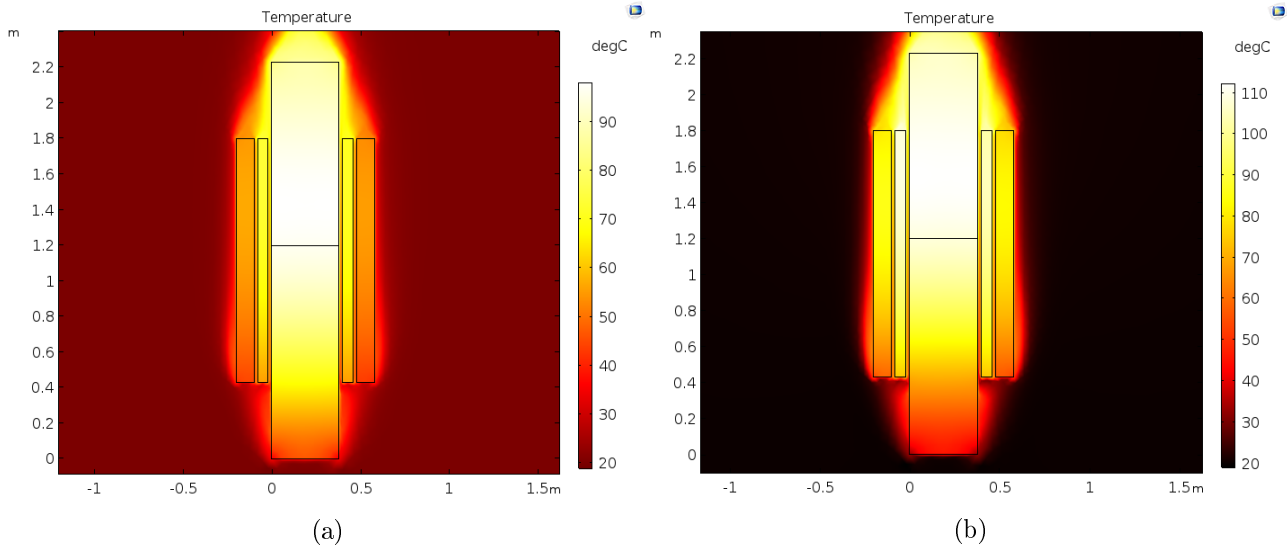

(a)   (b)

Figure 36: Temperature with constant (a) and temperature dependent resistivity (b)

43

The temperature peaks around 70 °C in the primary winding. This is to low according to the measurement plotted in Figure 9a and Figure 9b. The maximum temperature (T_{max}) should be minimum 100 °C. Temperature dependent resistivity will increase the losses in the windings. Figure 36b shows the temperature distribution when the resistance is temperature dependent. T_{max} peaks at 108.8 °C. The average heat loss in the windings increased to 22.5 $\frac{kW}{m^3}$ in the primary windings and 17.3 $\frac{kW}{m^3}$ in the secondary windings. The core losses stayed the same. Figure 37a shows a plot of the *relative resistivity* in the transformer winding. This is the resistivity of the windings divided by the reference resistivity of aluminium at temperature 20 °C. Overall the *relative resistivity* is 1.25, but peaks at 1.38. Figure 37b shows a plot of the temperature along hight of the primary windings and the secondary windings. The current density on the left side is slightly larger than on the right side. Therefore the temperature at the left side will be larger too.

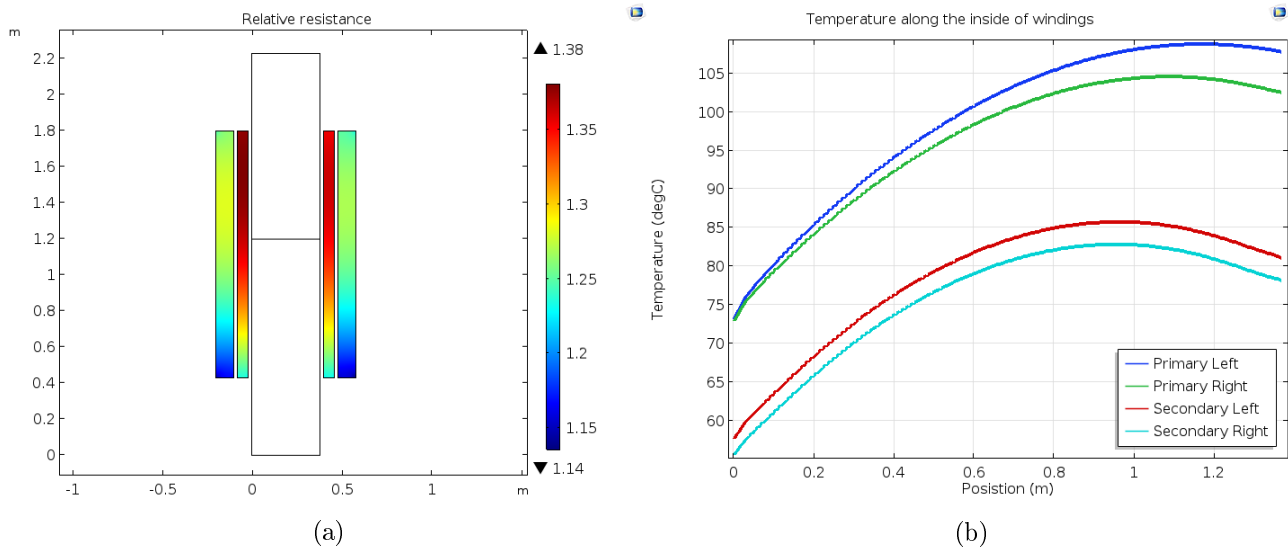(a)   (b)

Figure 37: Relative resistivity (a) and temperature along the windings(b)

The temperature peaks close to the top of the windings. The heat transfer due to convection is poorer at the top compared to the bottom and the resistivity is larger, due to higher temperature. The current density is also larger at the top and the bottom of the foil windings. The position of T_{max} will probably be lower if the heat loss in the windings were uniform. The potion of T_{max} in the model is approximately a fifth of the hight from the top of the windings. The temperature in the windings of real transformers is usually measured a third of the hight from the top of the windings. [4]

7.2.1   Uniform current density

This section shows the results of the single-phase model, when the current density is assumed to be uniform. The average heat loss across the windings is the same as the heat loss of non-uniform current density with constant resistivity of $2.65 \cdot 10^{-8}\ \Omega m$. Linear resistivity is included in the simulation.
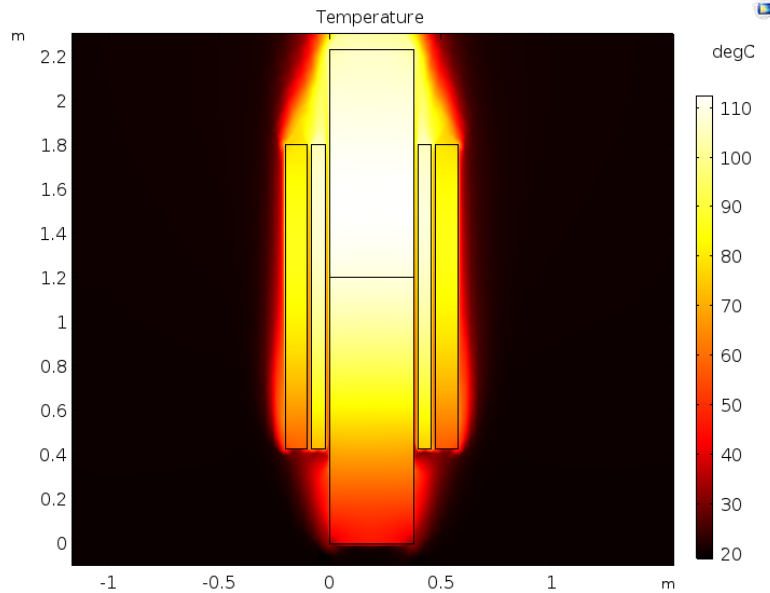

Figure 38: Temperature distribution - Uniform current density

The temperature plot in Figure 38 does not look much different form Figure 36b. The difference is highlighted in Figure 39
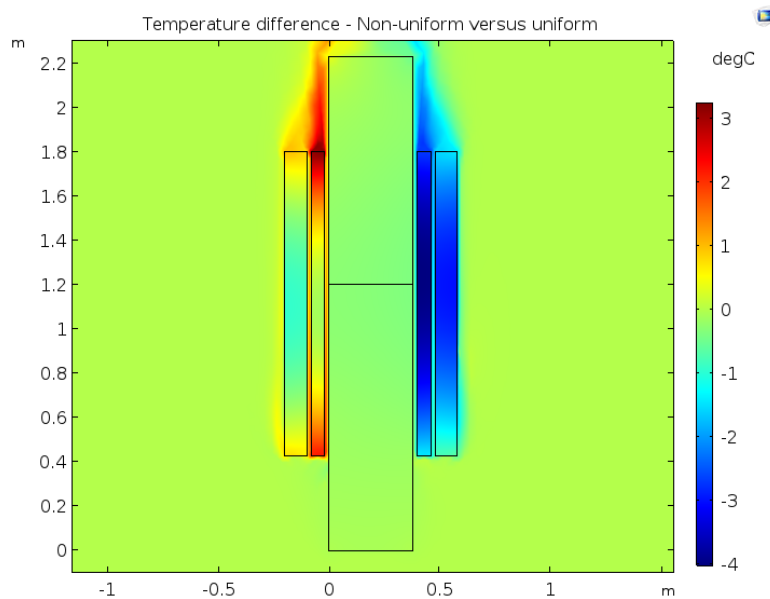

Figure 39: Temperature difference - Non-uniform versus uniform

One major reason for this is that the average heat loss is an average of windings on both the right and the left side. The average heat loss in the windings is larger on the left side than on the right. That is why the windings on the right are blue and the left are red. The left side is warmer than in the case of non-uniform current density at the top and bottom of the windings. A small area in the middle has the same temperature. The difference in temperature distribution is due to the different in heat loss density.
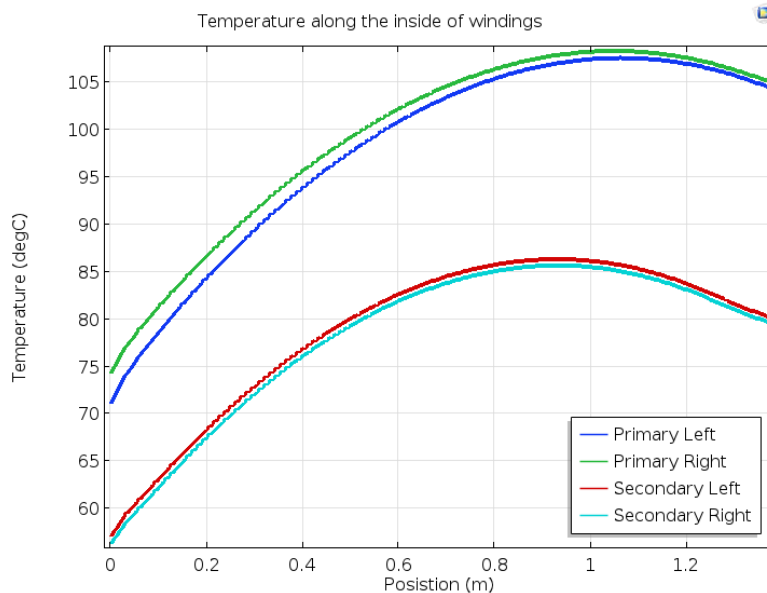

Figure 40: Temperature along the hight of the windings - Uniform current density

Figure 40 shows a plot of temperature along the hight of the primary and secondary winding with uniform current density. To determine the maximum temperature in stationary study, non-uniform and uniform current density do not show much difference. It is much more important to include temperature dependent resistivity. The position of T_{max} however will be off. Figure 40 shows that the T_{max} occur 32 cm from the top of the windings. Figure 37b shows T_{max} in the primary windings occur 27 cm. T_{max} occur closer to the top of the windings with non-uniform current density. The difference is small, but not negligible. The current density could be simplified to a uniform current density, but this depends on the application of the model and level of accuracy required.

7.2.2   Surface to surface radiation

Figure 41a shows the temperature distribution in the transformer at full load, ambient temperature 20 °C, temperature dependent resistivity and the inlet velocity of the cooling air is 1.3 $\frac{m}{s}$, but heat transfer by radiation is ignored.

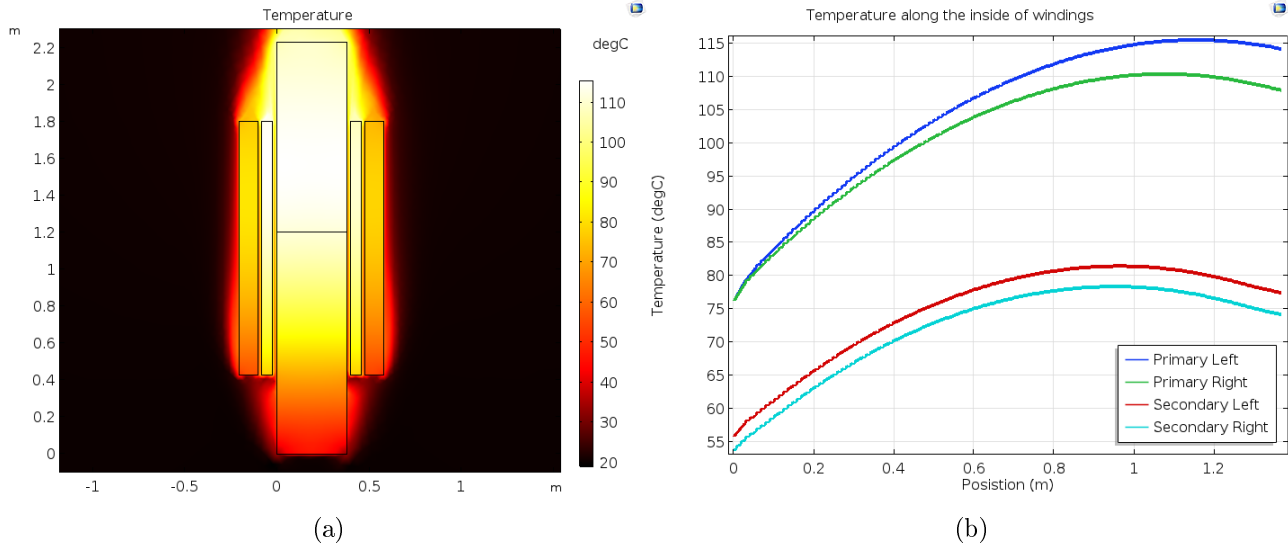(a)   (b)

Figure 41: Distribution (a) and line plot (b) of temperature - Radiation not included

Figure 37b shows the line plot of temperature alomng the hight of the windings when radiation is not included. T_{max} increased from 108.8 °C to to 115.5 °C in the primary windings. The secondary winding have the opposite trend. T_{max} in the secondary windings decreased from 85 °C to 80 °C (See Figure 37b and Figure 41b). When heat transfer by radiation is considered, more heat from the primary windings is transferred to the secondary windings. This makes it hotter. When it is not included, the heat only travels by conduction or convection. Radiation is not a dominant part of heat transfer in transformers due to relative low temperature, but it is still a significant part of it. It should be included in thermal models of transformers.

7.2.3   Different ambient temperature

The transformer is working at rated load, under different ambient temperatures. Agder Energi mention that they had an excitation transformer that works inside a mountain and may operate with an ambient temperatures of 70 $°C$. The distribution transformers in Uleberg are not the same size as this distribution transformer modelled in this thesis. The hypothesis is: The ratio between the increase of maximum temperature T_{max} and ambient temperature T_{am} is equal to 1. In other words, if T_{am} increases 10 $°C$, will T_{max} in the transformer increase 10 $°C$?

<center>(a)   (b)</center>
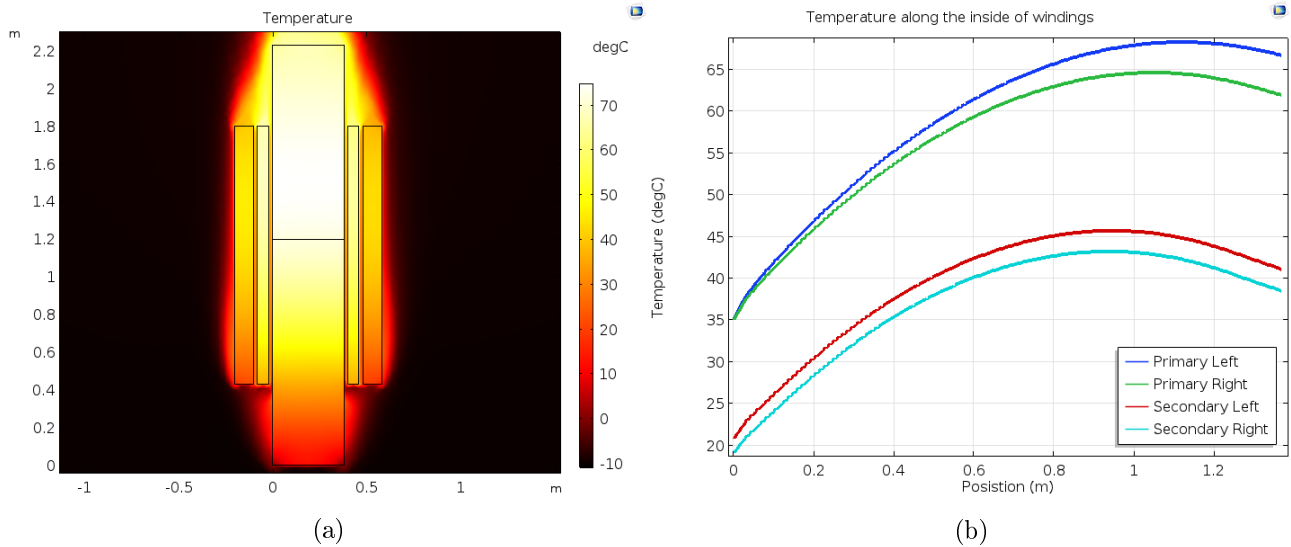
<center>Figure 42: Distribution (a) and line plot (b) of temperature - Ambient temperature -10 $°C$</center>

Figure 42a shows the temperature distribution in the transformer with ambient temperature -10 $°C$ and Figure 42b shows the temperature along the hight of the windings. The temperature in the windings on the left side of the core are higher than on the right. This is due to greater current density over the cross-section. The position of T_{max} in the primary windings is close to the top of the windings. T_{max} in the primary winding on the left side is 68.3 $°C$. Figure 43a and Figure 43b show similar plots, but ambient temperature is 40 $°C$.
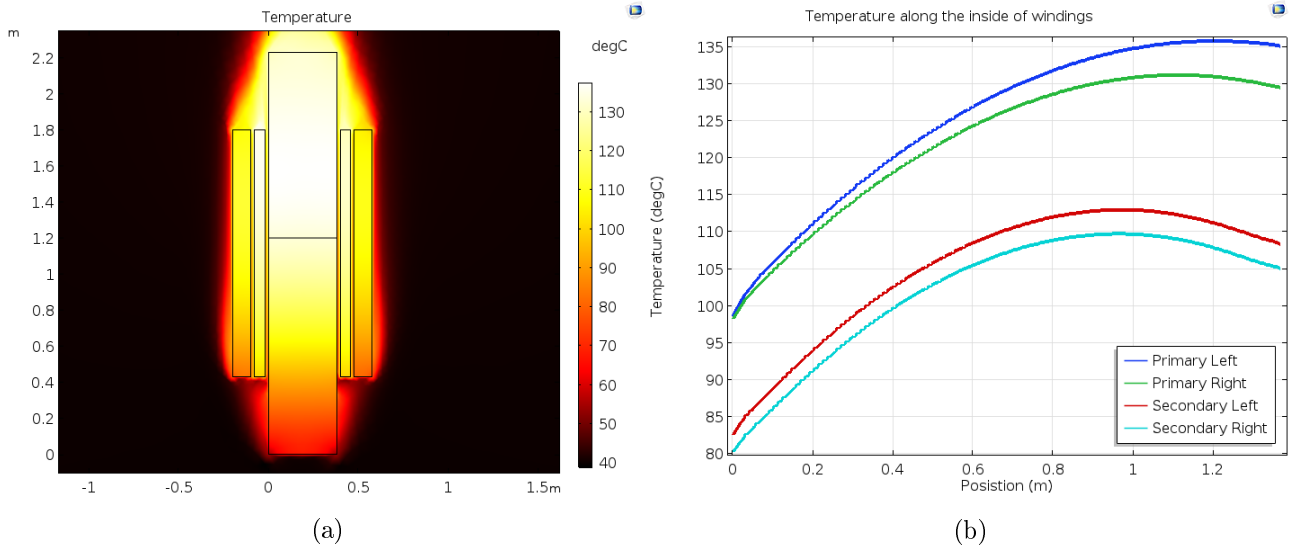
<center>48</center>

Figure 43: Distribution (a) and line plot (b) of temperature - Ambient temperature 40 °C

The curves in Figure 43b have similar shape as the graphs in Figure 42a and 36b with almost the same position of T_{max} in the different windings. The temperature overall has increased. T_{max} is 135.8 °C.
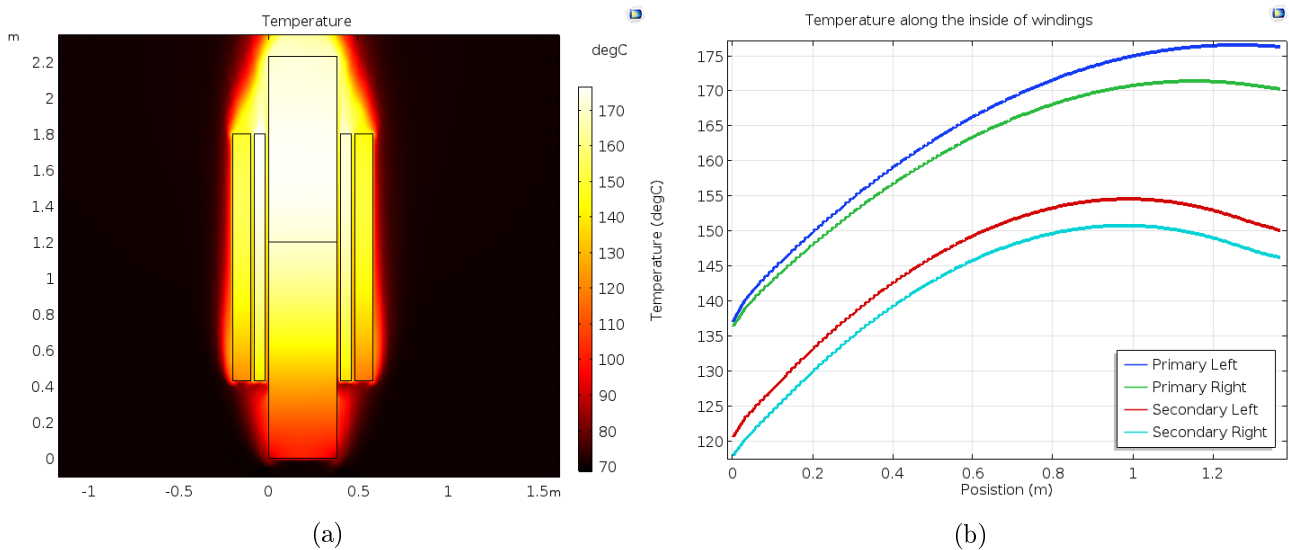
Figure 44: Distribution (a) and line plot (b) of temperature - Ambient temperature 70 °C

The third set of temperature plots in this section are Figure 52b and Figure 44b. The ambient temperature is now 70 °C. It shows similar results, but T_{max} is 176.6 °C.

Figure 45 shows the plot of T_{max} primary windings versus and T_{am}. It includes data point from -10 °C to 80 °C. The points lie on a straight line. The equation in the figure is the function of this trend-line of the dataset. It is derived with regression tool in Excel.
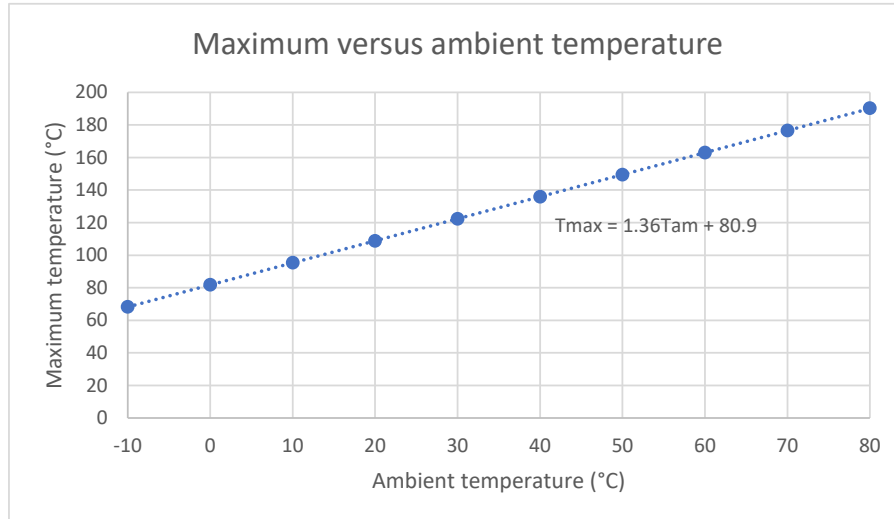
Figure 45: Maximum temperature in primary windings versus ambient temperature

The ratio between the increase of T_{max} and increase T_{am} is not 1, but 1.36. T_{max} increases with a higher rate than T_{am}, because of temperature dependent resistivity, which increases the load loss when the temperature in the windings increases.

7.2.4   Free and forced convection

This simulation case investigated the effect of the transformer's cooling fans. The fans blow air into the cooling ducts of the transformer and allow it to operate with larger loads. The temperature in the windings would of course increase, if the cooling fans were turned off, but by how much?
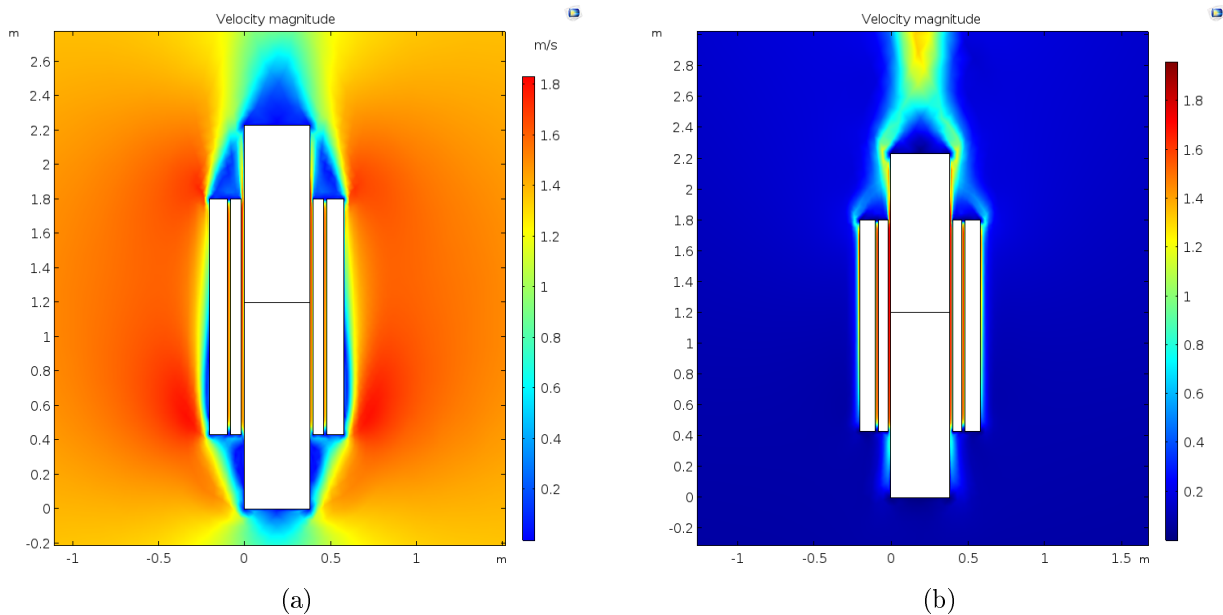
Figure 46: Velocity - Cooling fans turned on (a) and off (b)

Figure 46a and Figure 46b show the velocity of the air surrounding the transformer. The movement of air in Figure 46b is only due to free convection. The maximum temperature in the transformer increased to 126 °C, but the secondary windings had the largest increase.
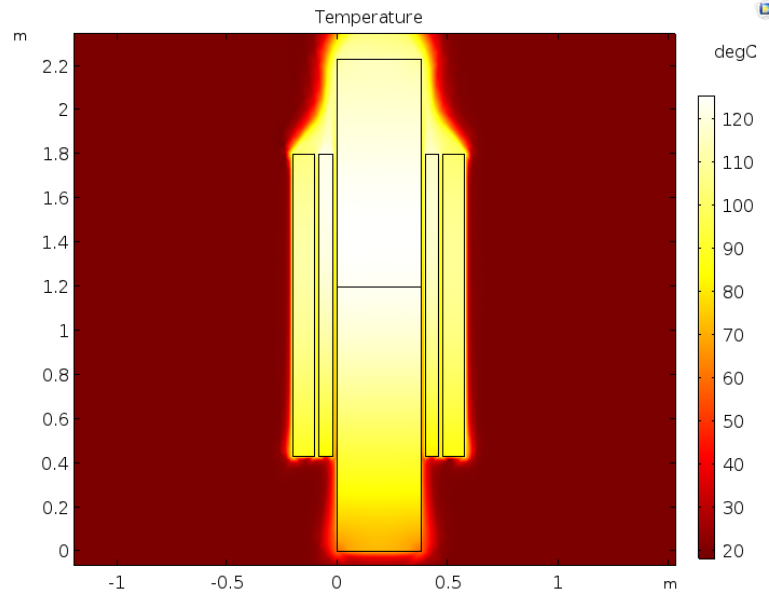
Figure 47: Temperature distribution - Cooling fans turned off

There is more movement of air surrounding the secondary windings when the cooling fans are on. The temperature along the hight of the secondary is always colder than the primary windings, when the fans are on. The bottom part of the secondary windings is warmer than the primary windings when the fans are turned off.

Figure 48: Temperature along the hight of windings - Cooling fans turned off

7.2.5 Acceleration ageing factor - F_{aa}

Equation (27) was mention in Section 4.8 and is an example of F_{aa} for an insulation class with reference temperature 11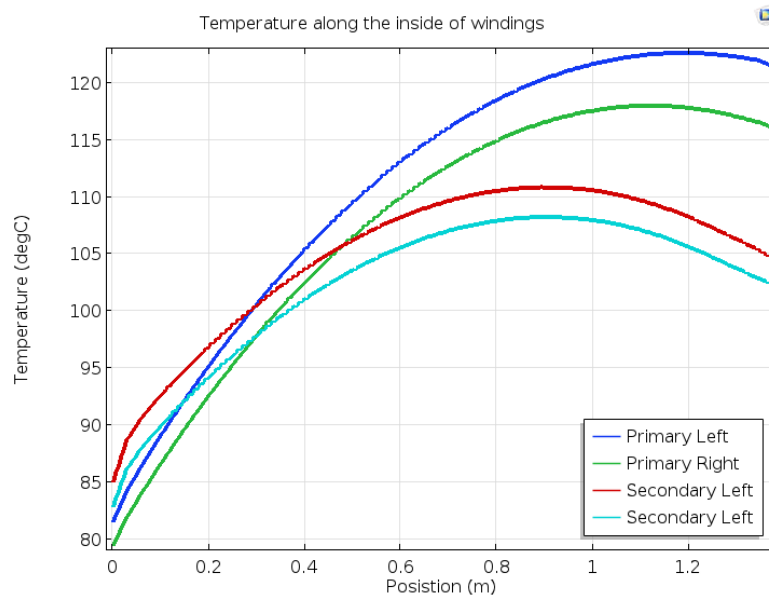0 $°C$. The textbook by S.J. Chapman [11] includes plots of the expected lifetime of different insulation classes A, B, F and H. The expressions for the lifetime (in hours) for insulation class B, F and H are

$$Lifetime_B = 2.124 \cdot 10^{-6} e^{\frac{9340}{T+273}} \tag{61}$$

$$Lifetime_F = 8.762 \cdot 10^{-8} e^{\frac{11240}{T+273}} \tag{62}$$

$$Lifetime_H = 1.122 \cdot 10^{-8} e^{\frac{12810}{T+273}} \tag{63}$$

The derivation can be found in Appendix B. Equations (61), (62) and (63) give an estimation of number of hours which the transformer can operate continuously at a certain reference temperature for the different insulation classes. The expected lifetime can be used in probability distribution functions. Appendix D describes the probability functions: Gamma, Weibull, Lognormal and GG3. The lifetime equations are assumed to be proportional to the inverse of F_{aa}. The equations derived for F_{aa} for insulation classes B, F and H are

$$F_{aa:B} = e^{\frac{9340}{403} - \frac{9340}{T+273}} \tag{64}$$

$$F_{aa:F} = e^{\frac{11240}{428} - \frac{11240}{T+273}} \tag{65}$$

$$F_{aa:H} = e^{\frac{12810}{453} - \frac{12810}{T+273}} \tag{66}$$

The derivation is shown in appendix B. The derivation resulted in some variation of the constant in the exponent of the equations. Table 12 shows different values of F_{aa} for insulation class B, H and F with the reference temperatures 130 $°C$, 155 $°C$ and 180 $°C$, respectively. Calculated values for F_{aa} from (27) is also included in Table 12 with reference temperature 110 $°C$.

Table 12: F_{aa} versus temperature difference from rated temperature

ΔT	B	F	H	Equation (27)
-10	0.55	0.53	0.53	0.35
-9	0.59	0.57	0.56	0.39
-8	0.63	0.61	0.60	0.43
-7	0.66	0.65	0.64	0.48
-6	0.70	0.69	0.68	0.54
-5	0.75	0.73	0.73	0.60
-4	0.79	0.78	0.78	0.66
-3	0.84	0.83	0.83	0.73
-2	0.89	0.88	0.88	0.81
-1	0.94	0.94	0.94	0.90
0	1.0	1.0	1.0	1.0
1	1.1	1.1	1.1	1.1
2	1.1	1.1	1.1	1.2
3	1.2	1.2	1.2	1.4
4	1.3	1.3	1.3	1.5
5	1.3	1.4	1.4	1.7
6	1.4	1.4	1.4	1.8
7	1.5	1.5	1.5	2.0
8	1.6	1.6	1.6	2.2
9	1.7	1.7	1.7	2.5
10	1.8	1.8	1.8	2.7

The difference between the self-derived equations of F_{aa} for insulation classes B, F and H are close to negligible, but they deviates from the equation (27). The insulation class of the transformer is F [4]. (27) is from standard IEEE Std C57.91 [22]. It will be used for prognosis of the rate of ageing of the paper insulation. The deviation between the equations derived in this thesis and (27) is small, but close to the reference temperature. Further derivation of F_{aa} in Appendix B resulted in these equations

$$RTT = \frac{\ln\left(\frac{1}{1-L_{Loss}}\right)}{\frac{B}{T_{ref}} - \ln\left(\frac{1}{1-L_{Loss}}\right)} \tag{67}$$

$$RTT = \frac{\ln\left(\frac{1}{1-L_{Loss}}\right)}{\ln\frac{L_{Life}(1-L_{Loss})}{A_L}} \tag{68}$$

RTT stands for relative temperature tolerance. B is the exponent of the equations of F_{aa} and A_L is the constant in the equations of expected lifetime, may depend on the insulation class. L_{Loss} is the *loss of life* from the expected lifetime. It is suggested that the relation between the L_{Loss} and F_{aa} is

$$F_{aa} = \frac{1}{1 - L_{Loss}} \tag{69}$$

Equation (67) is plotted in Figure 49. The range of L_{Loss} is between 0 % and 90 % (x-axis) and T_{ref} is between 60 °C and 200 °C (y-axis). The plots show that RTT is increases with rise of temperature and peaks at 7.5 %. The difference in RTT across the temperature range is negligible when L_{Loss} is small. This could mean that insulation design for higher temperatures can tolerate higher deviation from the design temperature. It could also indicate that the equation for F_{aa} is best suited for monitoring the transformer during stable operation and not to larger temperature difference from reference.
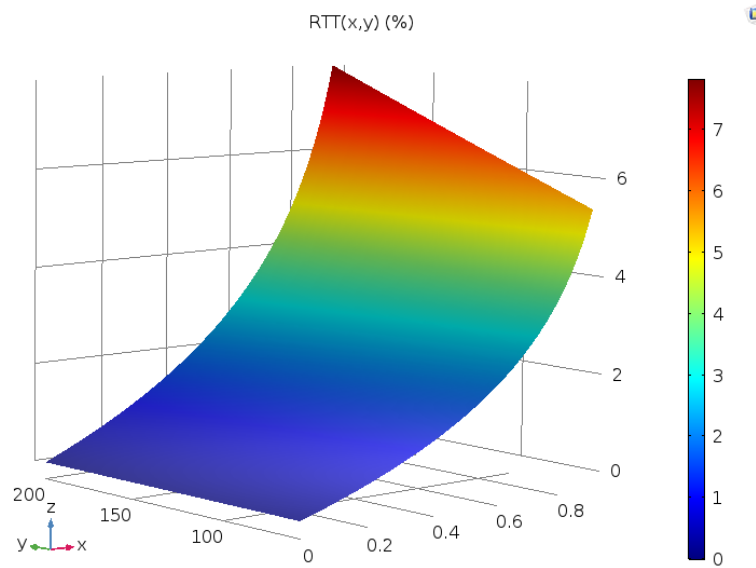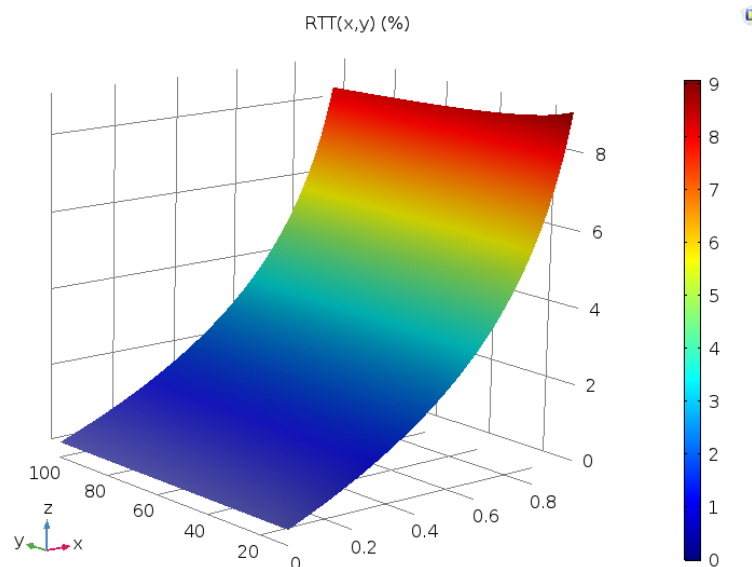

Figure 49: RTT verus L_{Loss} and T_{ref}

Figure 50: RTT verus L_{Loss} and L_{Life}

Figure 50 shows the plot of (68). The range of L_{Loss} is between 0 % and 90 % (x-axis) and the range of L_{Life} is between 10 and 100 years (y-axis). RTT is close to constant across the range of L_{Life}. Table 13 shows the average value of RTT for different values of L_{Loss}

Table 13: Average RTT versus L_{Loss}

L_{Loss} (%)	Average RTT (%)
0	0
10	0.4
20	0.8
30	1.2
40	1.8
50	2.4
60	3.2
70	4.3
80	5.8
90	8.6

The old rule of thumb related to insulation lifetime and temperature tells us that a temperature increase of 10 °C cuts the lifetime to the half. Table 13 shows when RTT is 2.5 %, when lifetime is cut to the half. ΔT for the reference temperatures 60 °C, 120 °C and 180 °C are 8.3 °C, 9.8 °C 11.3 °C, respectively. This correlates to the old rule of thumb.

7.2.6 Age prognosis by measurements

An attempt in this thesis was to prognose the age of the transformer in Uleberg by using the measurement data. It is suggested to use this equation

$$L_{Rest} = A_L e^{\frac{B}{T_{ref}}} - \sum_{i=1}^{n} F_{aa_i} \Delta t_i \tag{70}$$

The first term of (70) is a general form of expected lifetime equations: (61), (62) and (63). The second term is the accumulated ageing over n number of hours. Equation (70) was used for the temperature measurements from Agder Energi of the transformers in Uleberg. T_{ref} equal to 110 °C resulted in an estimated accumulated age of less than an hour in the total six year of measurements. The temperature is usually not 110 °C or higher. The load varies and sometimes the transformer was not operating at all. T_{ref} was adjusted to 80 °C, then the accumulated age began to match the chronological age. The expected lifetime estimated by (62) is then over half a millennium. If one of the transformers had failure today, it would probably not be because of gradual ageing of the paper insulation. This result may also indicate that (68) is better suited to prognose the remaining lifetime for transformers which are continuously operating close to full load.

7.2.7   Prognosis of ageing rate

The temperature results in Figure 36b, Figure 42a, Figure 43a, Figure 44a and Figure 47 were used to prognose the rate of ageing in the windings.
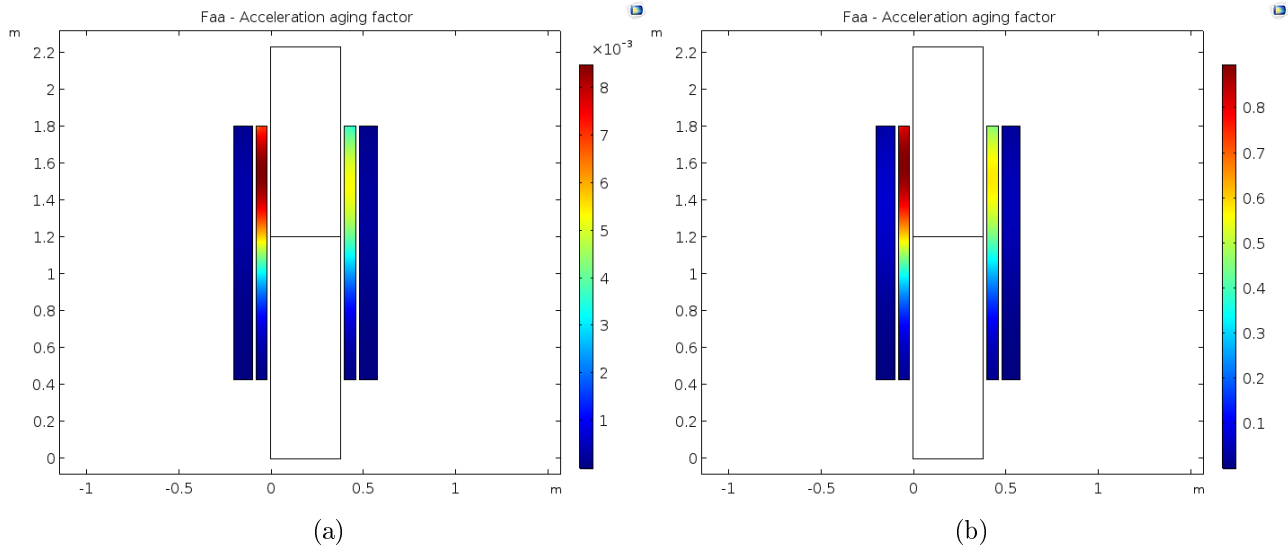

Figure 51: F_{aa} with ambient temperatures -10 °C (a) and 20 °C (b)

Figure 51a shows F_{aa} over the windings of the single-phase transformer model using equation (65) with reference temperature 110 °C. The highest temperature is located in the primary windings on the left side of the core. The paper insulation will also age fastest at that point as well. Since the ambient temperature is -10 °C the value of F_{aa} is very small. If the ambient temperature is 20 °C, which is typical for Uleberg in summer, maximum value of F_{aa} is just below 1. The paper insulation age most rapidly at the same area. (See Figure 51b)
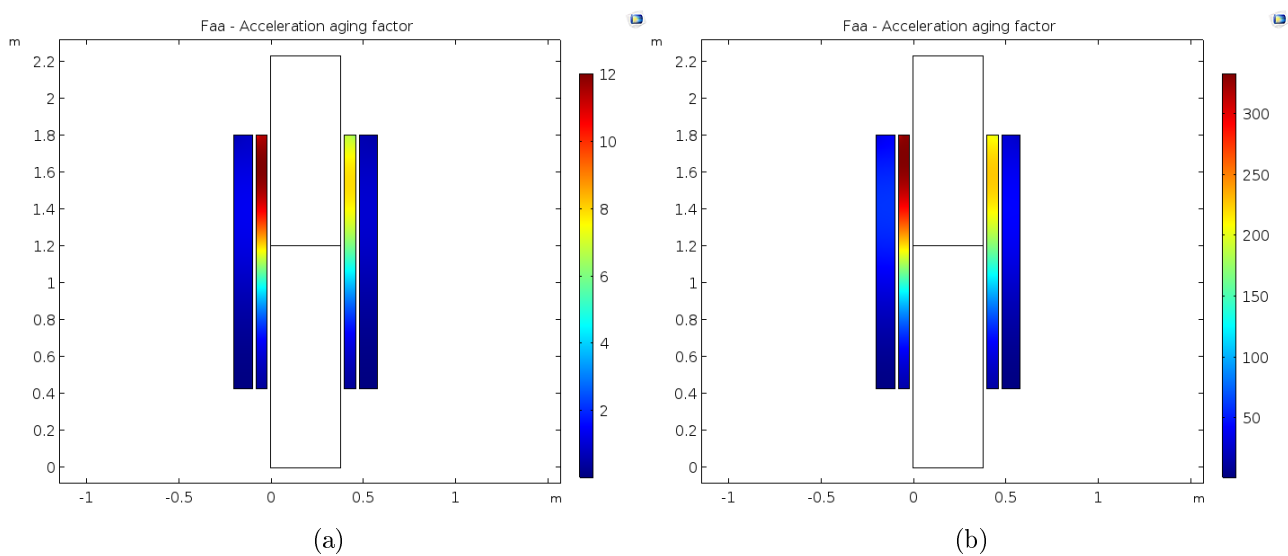

Figure 52: F_{aa} with ambient temperatures 40 °C (a) and 70 °C (b)

If T_{am} increases to 40 °C, the maximum value of F_{aa} is 6.5. It is equal to 4.5 in the primary windings of the right side of the transformer core. This is due to the difference in current density. According to Agder Energi, one of their excitation transformers operates with an ambient temperature of 70 °C. In this case, the maximum F_{aa} is larger than 300. The paper insulation is then ageing 300 times faster, compared to the case where it operated with ambient temperature 20 °C. The problem with the high ambient temperature should be solved. The distribution transformers in Uleberg would not last more than 0.5 % of expected lifetime, if any of them operated with the ambient temperature 70 °C. Figure 53 shows the plot of F_{aa} in the windings of the single-phase transformer model with the cooling fans turned off. Maximum F_{aa} is 3.5.
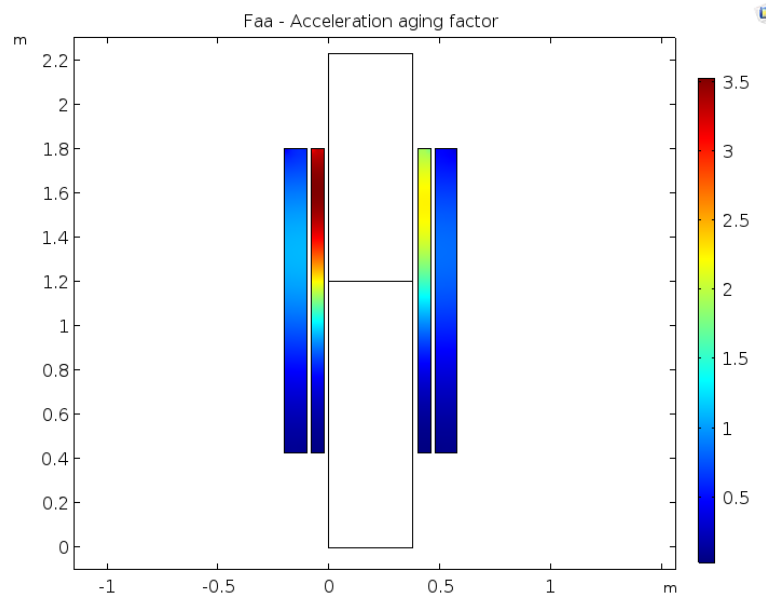

Figure 53: F_{aa} - Cooling fans turned off

7.3   Evaluation of the models

In this thesis a 5 MVA three-phase distribution transformer (based on two distribution transformers located in Uleberg) was modelled by combining a three-phase model and a single-phase model. The advantage of this was the reduction of computation time. The three-phase model used over an hour to do to 10 iterations and was not close to converged to any solution, when electromagnetics, thermodynamics and fluid dynamics were included. The simulations in this thesis combined numerical modelling and analytical derived heat sources. They were based on plots of J^2 exported from the results of the electromagnetic study of the three phase model with multiple single-turn windings and into Excel. This made it possible to include skin- and proximity-effect in the windings. Linear resistivity was also included in the equations of the heat loss in the windings. The single phase model with electromagnetics, thermodynamics and fluid dynamics coupled together used 1.5 min to converge to a solution. Other strong points of the numerical model are the inclusion of eddy current loss, hysteresis loss and both free and forced convection.

The weak point of the model is the geometry of the windings. Detailed information of the geometry of the interior of the windings were not available. The dimension sketch of the transformer from the documents provided by Agder Energi gave an overall dimension from an outside view of the transformer [4]. They did not give a detailed description of the windings and the cooling ducts. The distance from the transformer core to the outside of the surface of the high-voltage windings was roughly 20 *cm*. The geometry was more detailed in the 3D-transformer model in [8].

In the three-phase model the windings were rearranged to make it easier to solve. The difference of current density in the windings were negligible. This made it possible to do an electromagnetic study of the model with high number of turns. The number of turns in primary windings of the transformer modelled in [6] was 16 while this model had 44. The windings are also thicker with air-ducts between them. The three-phase model in this thesis used single-turn coils for the secondary windings, which had 156 turns. The model in [7] had 460 turn in secondary windings, but there were used multi-turn coils approximations.

7.4 Improvements and further work

This section mentions what can be improved in the transformer model and possible further work.

- Model fluid dynamics with turbulent flow. The model used laminar flow, but there may be some turbulence. This can affect the results.

- The density of air is based on the ideal gas law. Including properties which closer resemble the real gases may improve the accuracy of the model.

- The geometry is based on dimensions drawing of the real transformer located in Uleberg, but the details about the interior of the coils are almost unknown. The thickness of the windings and the air ducts between them were assumed. Only the distance from the core to the outer edges of the high-voltage windings were known from the dimension sketch of the transformer (≈ 20 *cm*).

- Studying the material properties of the insulation in detail, for example relative permittivity. In this thesis it has been assumed to be 1. It is related to dielectric loss. It is a small part of the total loss, but can be crucial for the estimation of local hotspots.

- Make a 3-dimensional model and compare the results from the 2D-model. Verify if a simplified 2D-model can give the same results as a full 3D-model.

- Study how temperature rises when a short circuit occur.

- The cooling fans of the transformer are represented by a uniform inlet flow at the bottom of the model. Due to the behaviour of fluids hitting a plate parallel to the flow, almost no air from the cooling fans entered the cooling ducts. This could be solved by location of the fans. If the air hit the transformer at an angle, more air would enter the cooling ducts and improve the cooling of the primary windings.

- The transformer in the current model is surrounded by a large air-domain. In other words, the transformer is standing in a large room high above the floor/ground. The next step in the modelling may include a more realistic set-up of the surrounding.

8 Conclusion

In this thesis electromagnetic and thermal modelling of dry-type distribution transformers have been studied. The electromagnetic study revealed the distribution of current in the transformer core and windings. The three-phase model used multiple single-turn coils to describe the windings. This made it possible to include skin- and proximity-effect in the windings, but became too computational heavy. It used 10 min to solve when only electromagnetics were included. Plots of the J^2 from the three-phase model were exported and used to derive equations for the heat sources in the windings of a single-phase model. The model was able to solve in 1.5 min with electromagnetics, thermodynamics and fluid dynamics coupled together in the model. T_{max} in the primary windings was 108.8 °C, when the transformer operated at full load, cooling fans turned on and ambient temperature 20 °C. This is close to the temperature measurement provided by Agder Energi. Depending on level of accuracy required from the model, a uniform current density may be sufficient to estimate T_{max}. The temperature distribution will be different and the largest deviation can be found on the top and bottom of the windings. Further study of the numerical model revealed the importance of heat transfer by radiation and temperature dependent resistivity. T_{max} in the primary was 6.7 °C warmer when radiation was ignored. The temperature rise was too small with fixed resistivity (Reference resistivity). The linear resistivity in the windings increased more than 25 % and almost 40 % in hottest areas of the primary windings.

In the thermal modelling, the effect of ambient temperature was investigated. One result of this study is that the increase in T_{max} and T_{am} are proportional and the ratio between them is 1.36. In other words, if the T_{am} increases with 10 °C, T_{max} increases with 13.6 °C. This is true in the temperature range -10 °C to 80 °C. This could be useful information for developing empirical models which have a small fraction of computational load than a finite element analysis.

The temperature in the primary windings increased to 126 °C when the cooling fans were turned off, but the secondary windings experienced the largest temperature increase and the bottom part was warmer than the primary windings.

The equation of F_{aa} is inspired by Arrhenius' equation. The equations for the lifetime and F_{aa} were derived for insulation class B, F and H. Rearranging the equations of F_{aa} revealed that the RTT for insulation class was approximately constant in the lifetime range between 10 to 80 year. An increase of continuous operating temperature of 2.5 % would cut the lifetime to the half. This is in proximity of 10 °C, which correlated with the old rule of thumb related to paper insulation. In the single-phase model F_{aa} with T_{ref} 110 °C was used to prognose the ageing rate of the paper insulation. At normal conditions the maximum F_{aa} was below 1. When cooling fans were turned off it increased to 3.5, which means that the insulation is ageing 3.5 times faster. If the ambient temperature is 70 °C, F_{aa} is over 300. In this case the transformer would not be in operation for very long. This is not a problem for the distribution transformer in Uleberg, but it is worrisome for the excitation transformer of Agder Energi, which according to them is operating with that ambient temperature inside the mountain.

References

[1] H. C. Stewart and L. C. Whitman, "Hot-spot temperatures in dry-type transformer windings," *Electrical Engineering*, vol. 63, no. 10, pp. 763–768, Oct 1944, [Online; accessed 2-February-2018].

[2] S. Chakravorti, D. Dey, and B. Chatterjee, *Recent Trends in the Condition Monitoring of Transformers.* Springer London, 2013, [Chapter 1][Online; accessed 1-January-2018].

[3] electrical4u.com, "Dry-Type Transformer," Online Article, 2018, [Online; accessed 5-April-2018]. [Online]. Available: https://www.electrical4u.com/dry-type-transformer/

[4] E. Ommundsen and K. Smith, "Documents from Agder Energi," [Accessed Spring 2018].

[5] M. A. Arjona, C. Hernandez, R. Escarela-Perez, and E. Melgoza, "Thermal analysis of a dry-type distribution power transformer using fea," in *2014 International Conference on Electrical Machines (ICEM)*, Sept 2014, pp. 2270–2274, [Online; accessed 29-January-2018].

[6] M. Lee, H. A. Abdullah, J. C. Jofriet, and D. Patel, "Temperature distribution in foil winding for ventilated dry-type power transformers," *Electric Power Systems Research*, vol. 80, no. 9, pp. 1065–1073, sep 2010, [Online; accessed 27-February-2018].

[7] ——, "Thermal modeling of disc-type winding for ventilated dry-type transformers," *Electric Power Systems Research*, vol. 80, no. 1, pp. 121–129, jan 2010, [Online; accessed 27-February-2018].

[8] X. Ding and W. Ning, "Analysis of the Dry-type Transformer Temperature Field Based on Fluid-solid Coupling," in *2012 Second International Conference on Instrumentation, Measurement, Computer, Communication and Control*, Dec 2012, pp. 520–523, [Online; accessed 12-February-2018].

[9] W. Ning and X. Ding, "Three-dimensional finite element analysis on fluid thermal field of dry-type transformer," in *2012 Second International Conference on Instrumentation, Measurement, Computer, Communication and Control*, Dec 2012, pp. 516–519, [Online; accessed 12-February-2018].

[10] I. Soltanbayev, R. Sarmukhanov, S. Kazymov, T. Otelgen, and M. Bagheri, "Automated dry-type transformer aging evaluation: A simulation study," in *2017 International Siberian Conference on Control and Communications (SIBCON)*, June 2017, pp. 1–6, [Online; accessed 12-February-2018].

[11] S. J. Chapman, *ELECTRIC MACHINERY FUNDAMENTALS*, 5th ed. McGraw Hill Higher Education, 2011, [page 184-186]. [Online]. Available: https://www.amazon.com/ELECTRIC-MACHINERY-FUNDAMENTALS-Chapman/dp/007108617X?SubscriptionId=0JYN1NVW651KCA56C102&tag=techkie-20&linkCode=xm2&camp=2025&creative=165953&creativeASIN=007108617X

[12] Wikipedia contributors, "Transformer," Wikipedia The Free Encyclopedia, 2018, [Online; accessed 12-March-2018]. [Online]. Available: https://en.wikipedia.org/w/index.php?title=Transformer&oldid=830027078

[13] Top Electrical Engineers, "11 Secrets about Losses in Transformer you don't know before," Online article, Aug. 2017, [Online; accessed 12-March-2018]. [Online]. Available: http://www.top-ee.com/losses-in-transformer/

[14] J. C. Olivares-Galvan, R. Escarela-Perez, E. Campero-Littlewood, F. de Leon, and C. A. Cruz, "Separation of core losses in distribution transformers using experimental methods," *Canadian Journal of Electrical and Computer Engineering*, vol. 35, no. 1, pp. 33–39, Winter 2010. [Online]. Available: http://ieeexplore.ieee.org/document/5783382/?arnumber=5783382&tag=1

[15] Wikipedia contributors, "Skin effect," Wikipedia The Free Encyclopedia, 2018, [Online; accessed 22-March-2018]. [Online]. Available: https://en.wikipedia.org/w/index.php?title=Skin_effect&oldid=829612858

[16] All about Circuits, "Skin and proxmity effect of ac current," Online Technical Article, Jun. 2005. [Online]. Available: https://www.allaboutcircuits.com/technical-articles/skin-and-proximity-effects-of-ac-current/

[17] R. Wilcoxon, "Does a 10 °C Increase in Temperature Really Reduce the Life of Electronics by Half?" Online Article, Aug. 2017, [Online; accessed 15-January-2018]. [Online]. Available: https://www.electronics-cooling.com/2017/08/10c-increase-temperature-really-reduce-life-electronics-half/#

[18] D. Bayoumi, "What is the life span of a distribution transformer?" Mar. 2017, [Online; accessed 3-May-2018]. [Online]. Available: http://ask.abb.com/products/___/distribution-transformers/question/What-is-the-life-span-of-a-distribution-transforme/1929

[19] F. P. Incropera, *Foundation of Heat Transfer*, 6th ed. Hoboken, N.J: John Wiley, 2012. [Online]. Available: https://www.amazon.com/Foundations-Heat-Transfer-International-Incropera/dp/B00EKYPFN4/ref=sr_1_sc_1?ie=UTF8&qid=1521806701&sr=8-1-spell&keywords=Faundation+og+heat+transfer

[20] Wikipedia contributors, "Richardson number," Wikipedia The Free Encyclopedia, 2017, [Online; accessed 19-March-2018]. [Online]. Available: https://en.wikipedia.org/w/index.php?title=Richardson_number&oldid=791203399

[21] ——, "Arrhenius equation," Wikipedia The Free Encyclopedia, Dec. 2017, [Online; accessed 15-January-2018]. [Online]. Available: https://en.wikipedia.org/w/index.php?title=Arrhenius_equation&oldid=815353745

[22] C. A. Helfrich and R. W. Carlson, "Using insulation aging to size transformers in high-ambient-temperature secondary-selective applications," *IEEE Transactions on Industry Applications*, vol. 50, no. 2, pp. 1503–1508, March 2014, [Online; accessed 12-February-2018].

[23] Comsol Multiphysics ®, "COMSOL Multiphysics Quick Start and Quick Reference," [Online; accessed 28-May-2018]. [Online]. Available: https://extras.csc.fi/math/comsol/3.4/doc/multiphysics/wwhelp/wwhimpl/js/html/wwhelp.htm?context=multiphysics&file=html_guideintro.5.1.html

[24] R. A. Adams, *Calculus: A Complete Course.* Pearson Education Limited, 2013. [Online]. Available: https:

//www.ebook.de/de/product/30352897/robert_a_adams_calculus_a_complete_course.html

[25] R. van Eck, M. Klep, and J. van Schijndel, "Surface to surface radiation benchmarks," *Eindhoven University of Technology*, 2016, [Online; accessed 21-May-2018]. [Online]. Available: https://www.comsol.com/paper/download/358181/vanschijndel_paper.pdf

[26] Comol Inc., "Navier-Stokes equation," [Online Cyclopedia], 2018, [Online; accessed 8-May-2018]. [Online]. Available: https://www.comsol.com/multiphysics/navier-stokes-equations

[27] Wikipedia contributors, "Electrical resistivity and conductivity," Wikipedia The Free Encyclopedia, 2018, [Online; accessed 27-April-2018]. [Online]. Available: https://en.wikipedia.org/w/index.php?title=Electrical_resistivity_and_conductivity&oldid=837521920

[28] Engineering Toolbox, "Specific heat for metals," [Online], 2003, [Online; accessed 27-April-2018]. [Online]. Available: https://www.engineeringtoolbox.com/thermal-conductivity-metals-d_858.html

[29] ——, "Thermal conductivit of metals," [Online], 2005, [Online; accessed 27-April-2018]. [Online]. Available: https://www.engineeringtoolbox.com/thermal-conductivity-metals-d_858.html

[30] ——, "Densities of solids," [Online], 2009, [Online; accessed 27-April-2018]. [Online]. Available: https://www.engineeringtoolbox.com/thermal-conductivity-metals-d_858.html

[31] S. W. Gao, M. Zhang, X. T. Sun, C. H. Yuan, N. Wang, and X. Li, "The research on calculation of temperature field of winding in dry type transformer," in *2012 Fifth International Conference on Intelligent Networks and Intelligent Systems*, Nov 2012, pp. 185–188, [Online; accessed 12-February-2018].

[32] W. T. Song, C.-H. Lin, and M. S.-A. Chuang, "A life distribution study of resin-coated transformer insulation systems in taiwan," *Journal of Industrial and Production Engineering*, vol. 30, no. 7, pp. 461–466, 2013. [Online]. Available: https://doi.org/10.1080/21681015.2013.864847

[33] S. O. Nyberg, *Statistikk: en bayesiansk tilnærming (Norwegian Edition)*. CreateSpace Independent Publishing Platform, 2014. [Online]. Available: https://www.amazon.com/Statistikk-en-bayesiansk-tiln%C3%A6rming-Norwegian/dp/1494441039?SubscriptionId=0JYN1NVW651KCA56C102&tag=techkie-20&linkCode=xm2&camp=2025&creative=165953&creativeASIN=1494441039

A Number of turns in a transformer

The number of turns in the primary and secondary windings of a transformer can be estimated by deriving Faraday's law for a tightly wound coil of wire with N number of identical turns.

$$V = -N\frac{d\phi}{dt} \qquad (71)$$

where V is the supply voltage of the coil, and ϕ_B is the magnetic flux induced by the coil. It is the product of the flux density in the transformed cross-sectional area of the core. Usually it is the cross-sectional area surrounded by the coil, but it is assumed that the core is the main conductor of magnetic flux. (71) can then be written as

$$V = -NA_{core}\frac{dB}{dt} \qquad (72)$$

The voltage is set as a sinusoidal

$$V = \sqrt{2}V_{RMS}\sin(2\pi f t) \qquad (73)$$

Combining (72) and (73) and integrating both side of the equation gives the following expression

$$NA_{core}B(t) = \frac{\sqrt{2}}{2\pi f}V_{RMS}\cos(2\pi f t) \qquad (74)$$

$B(t)$ is equal to B_{max} when $\cos(2\pi)$ is set equal to 1. (74) can be simplified and rearranged to the following expression

$$V_{RMS} = \frac{2\pi}{\sqrt{2}}NB_{max}A_{core}f \qquad (75)$$

The number of turn of the transformer windings can be estimated by rearranging (75) to

$$N = \frac{\sqrt{2}V_{RMS}}{2\pi B_{max}A_{core}f} \qquad (2)$$

The voltage rating of the distribution transformer studied in this thesis has the frequency 50 Hz. The transformer leg thickness is 0.38 m and model depth 1 m ($A_{core} = 0.38\ m^2$) the number of turns are respectively 44 and 156 for the primary and the secondary windings. Original the model depth should have been 0.38 m because of the size of the transformer. The number of turns of the transformer would then be 118 (primary) and 414 (secondary). This was too computational heavy for the model.

B Derivation of F_{aa} for insulation classes B, H and F

Arrhenius' equation is defined as

$$k_{rate} = A_{Arr}e^{-\frac{E_a}{RT}} \tag{19}$$

Assuming the lifetime of the insulation of a transformer can be defined as an equation proportional to the rate constant k_{rate} in Arrhenius' equation.

$$Lifetime = A_L e^{\frac{B_L}{T}} \tag{76}$$

A_L and B_L are fitting parameters. Equation (76) is proportional to the inverse of (26). The exponent B_L is equal to $\frac{E_a}{R}$. The parameters are estimated by the graphs of the figure in the textbook written by S.J. Chapman page 183 [11]. Table 14 shows the values from insulation class B.

Table 14: Lifetime versus temperature - Insulation class B

Temperature ($°C$)	Lifetime (hours)
150	5900
140	13200
130	22100
128	25000
117	50000
111	75000
107	100000
104	125000
101	150000
99	175000
97	200000
95	225000
94	250000
93	275000
91	300000

The table is written in Excel and with two extra columns. The first one is the estimated lifetime by equation (76) with the parameters best fitted for the the dataset in table 14. The second column is the square error between the values in Table 14 and the approximated equation. The sum of square error were minimized by the solver function in Excel. Figure 54 shows the window of the Excel-solver.
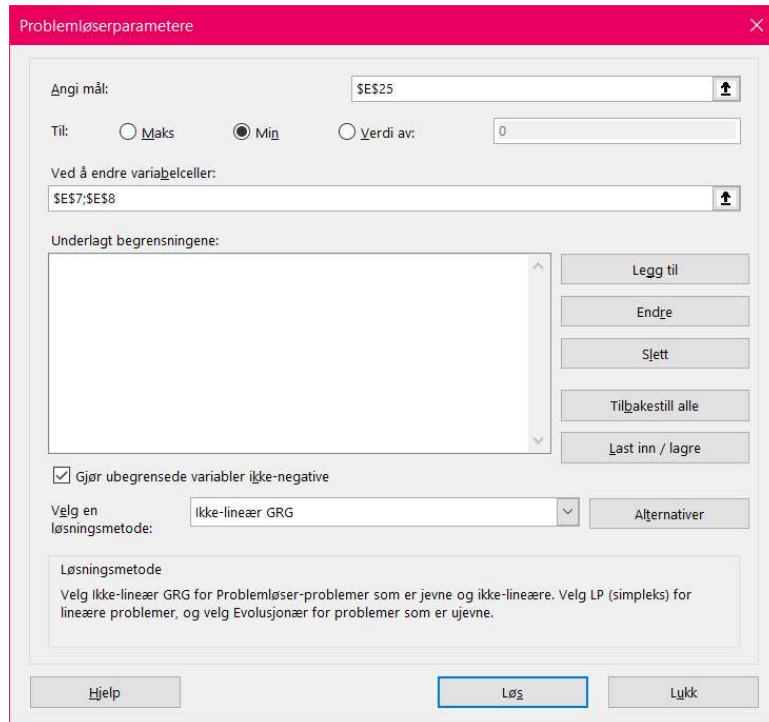
Figure 54: The Excel solver window

The objective function is the sum of the square error. The solver is enable to minimize the objective cell and the variables are the parameters A_L and B_L in the general equation (77). Which cells depend on how the Excel sheet is set up. The constant A_L and exponent B_L are $2.234 \cdot 10^{-6}$ h and -9340 K for insulation class B. Setting these parameters into (76) gives

$$Lifetime_B = 2.124 \cdot 10^{-6} e^{\frac{9340}{T+273}} \tag{61}$$

This results gives F_{aa} for insulation class B.

$$F_{aa:B} = e^{\frac{9340}{403} - \frac{9340}{T+273}} \tag{64}$$

A_L and B_L were fitted for the insulation classes F and H with the same method. Table 15 shows the values from insulation class F.

Table 15: Lifetime versus temperature - Insulation class F

Temperature ($^{\circ}C$)	Lifetime (h)
180	2900
170	7400
160	16200
153	25000
142	50000
137	75000
132	100000
129	125000
126.5	150000
124	175000
122	200000
120	225000
119	250000
117.5	275000
116	300000

Following the same procedure as for insulation class B, give A_L equal to $8.762 \cdot 10^{-8}$ h and B_L equals to -11240 K. The lifetime function is

$$Lifetime_F = 8.762 \cdot 10^{-8} e^{\frac{11240}{T+273}} \tag{62}$$

and F_{aa} for insulation class F is

$$F_{aa:F} = e^{\frac{11240}{428} - \frac{11240}{T+273}} \tag{65}$$

Table 16 shows the values from insulation class H.

Table 16: Lifetime versus temperature - Insulation class H

Temperature (°C)	Lifetime (h)
200	5900
190	10300
180	19100
177	25000
167	50000
161	75000
157	100000
154	125000
151.5	150000
149	175000
147	200000
145.5	225000
144	250000
142.5	275000
141	300000

Following the same procedure as for insulation class B and F, gives the function of the lifetime.

$$Lifetime_H = 1.122 \cdot 10^{-8} e^{\frac{12810}{T+273}} \tag{63}$$

and F_{aa} for insulation class H.

$$F_{aa:F} = e^{\frac{12810}{453} - \frac{12810}{T+273}} \tag{66}$$

Figure 55 shows the plot of the lifetime versus temperature for the datasets in tables 14, 15 and 16, it is indicated by dots and the continuous functions of (64), (65) and (66). T
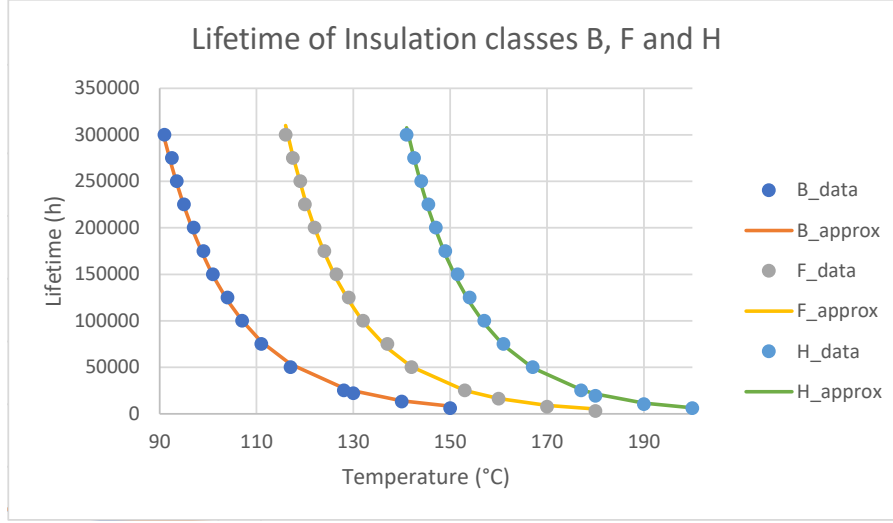
Figure 55: Lifetime of insulation classes B, F and H

The general equation for F_{aa} in (26) is rewritten to

$$F_{aa} = e^{B_{aa}\left(\frac{1}{T_{ref}} - \frac{1}{T}\right)} \tag{77}$$

where B_{aa} is $\frac{E_a}{R}$ from equation (26). Temperature T_{ref} is reference temperature T_{ref} and T is operating temperature

$$T = T_{ref} + \Delta T \tag{78}$$

Equation (78) is set in (77) and gives this expression

$$F_{aa} = e^{B_{aa}\left(\frac{\Delta T}{T_{ref}\left(T_{ref} + \Delta T\right)}\right)} \tag{79}$$

Rearranging (79) gives an expression for the relative temperature tolerance (RTT)

$$RTT = \frac{\Delta T}{T_{ref}} = \frac{\ln(F_{aa})}{\frac{B_{aa}}{T_{ref}} - \ln(F_{aa})} \tag{80}$$

Equitation (80) tells what temperature increase is acceptable at a certain value F_{aa} relative to T_{ref}. Higher operating temperature results in a shorter lifetime of the paper insulation. ABB often designed distribution transformers with lifetime of 25 years [18]. The connection between F_{aa} and the loss of lifetime (L_{Loss}) is

$$F_{aa} = \frac{1}{1 - L_{Loss}} \tag{69}$$

Equation (69) is put in (80)

$$RTT = \frac{\ln\left(\frac{1}{1-L_{Loss}}\right)}{\frac{B}{T_{ref}} - \ln\left(\frac{1}{1-L_{Loss}}\right)} \tag{67}$$

Combining equations (76) and (67) gives

$$RTT = \frac{\ln\left(\frac{1}{1-L_{Loss}}\right)}{\ln\frac{L_{Life}(1-L_{Loss})}{A}} \tag{68}$$

Plots of (67) and (68) are shown in the results in Section 7.2.5 on pages 54 and 54

C   Plots of J^2

Figures 56a and 56b show the plots of $f(x)$ and $g(x)$ in the primary windings on the left side of the transformer core. All the 2D-plots of J^2 are dunction defined by the x-coordinate with the unit m and the y-axis is J^2 with the unit $\frac{A^2}{m^4}$
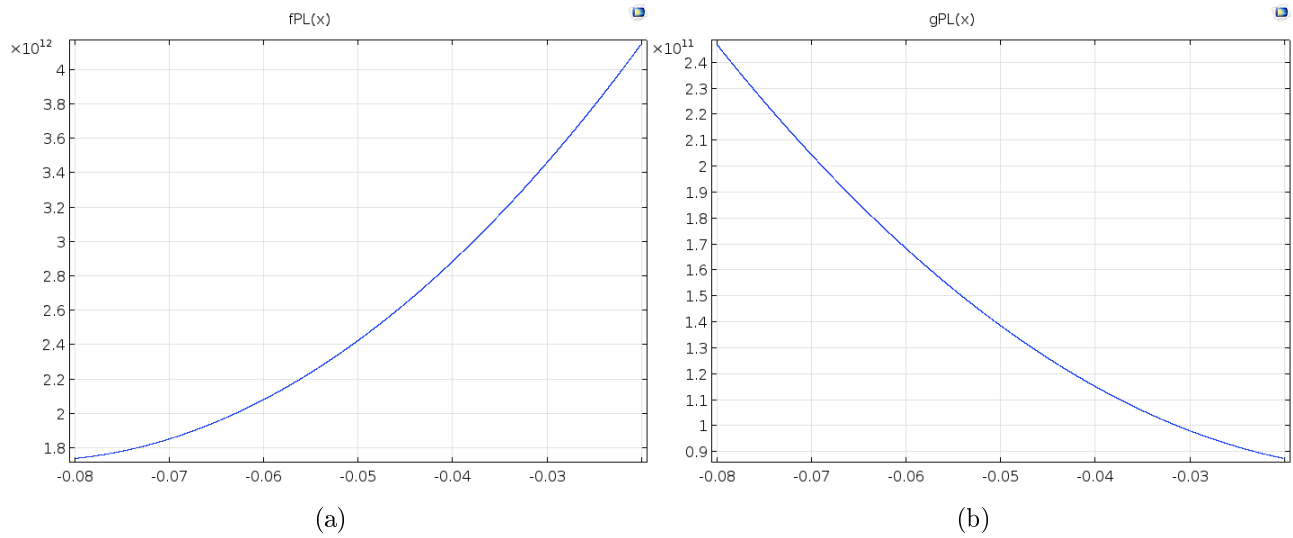

(a)   (b)

Figure 56: $f(x)$ (a) and $g(x)$ (b) in primary windings - Left side

Figures 57a and 57b show the plots of $f(x)$ and $g(x)$ in the primary windings on the right side of the transformer core.

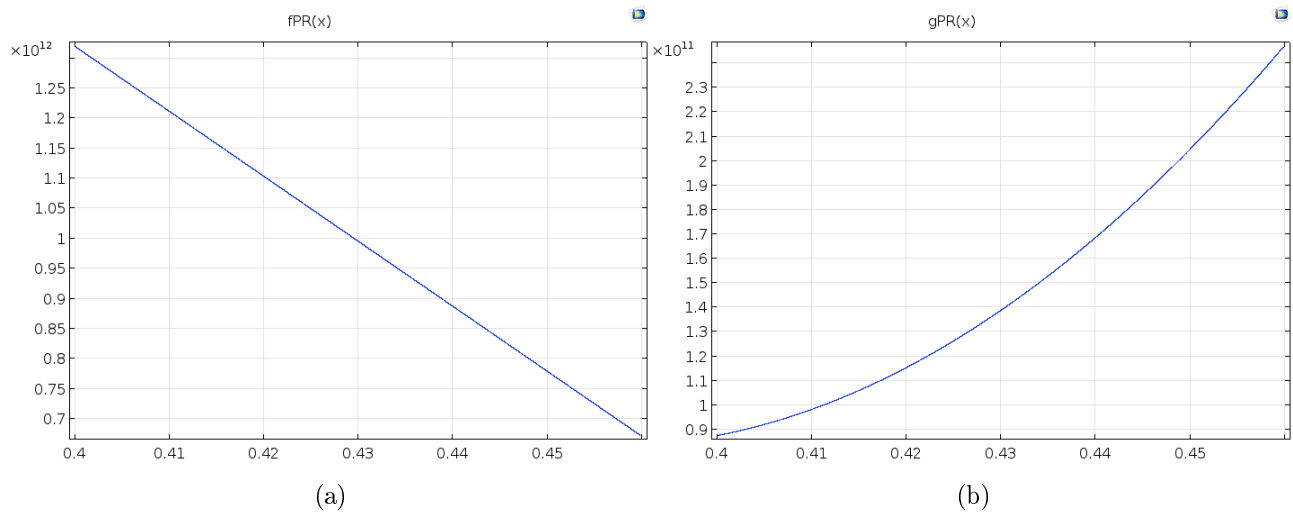(a)   (b)

Figure 57: $f(x)$ (a) and $g(x)$ (b) in primary windings - Right side

Figures 58a and 58b show the plots of $f(x)$ and $g(x)$ in the secondary windings on the left side of the transformer core.
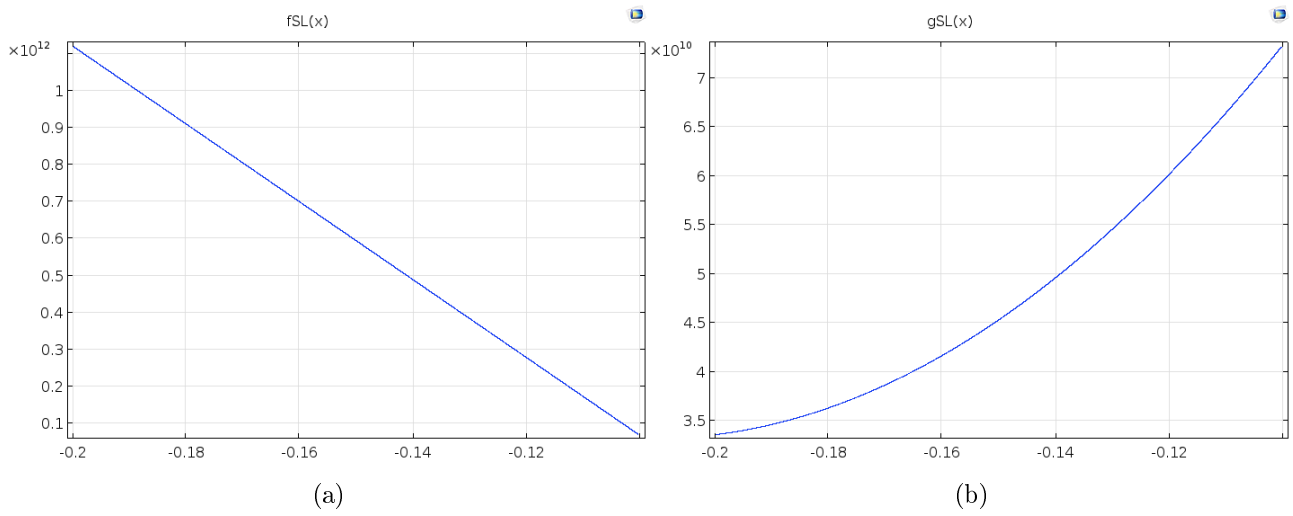

Figure 58: $f(x)$ (a) and $g(x)$ (b) in secondary windings - Left side

Figures 59a and 59b show the plots of $f(x)$ and $g(x)$ in the secondary windings on the right side of the transformer core.
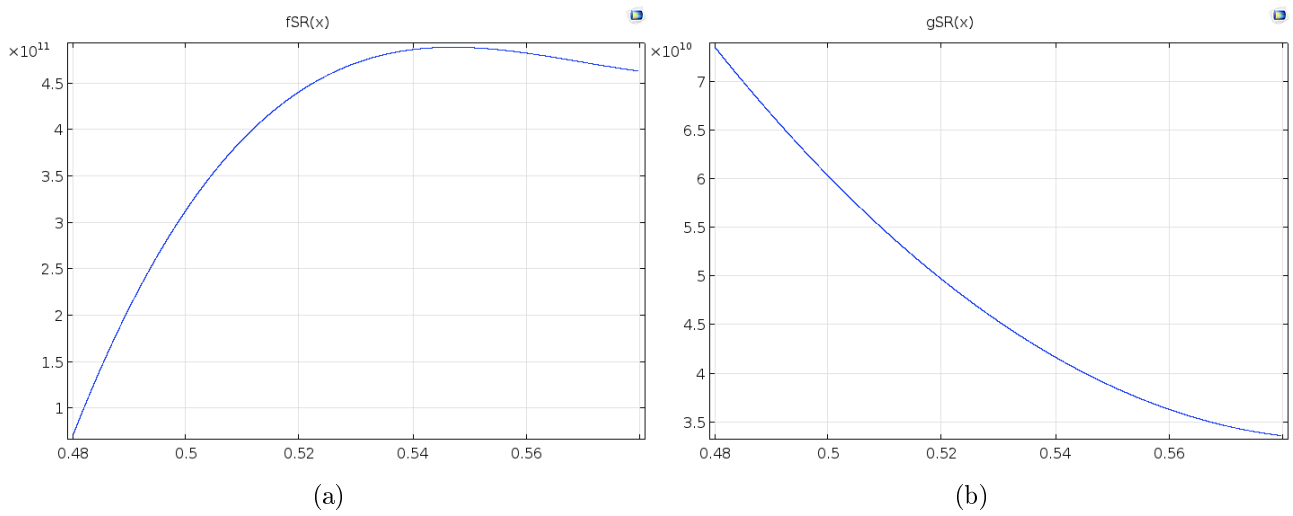

Figure 59: $f(x)$ (a) and $g(x)$ (b) in secondary windings - Right side

Figure 60a and Figure 60b show the plot of $J^2(x,y)$ in the primary windings. The unit on the x- and y-axis is m and the z-axis is $\frac{A^2}{m^4}$. This is also the case for the plots in Figures 61a and Figure 61b.
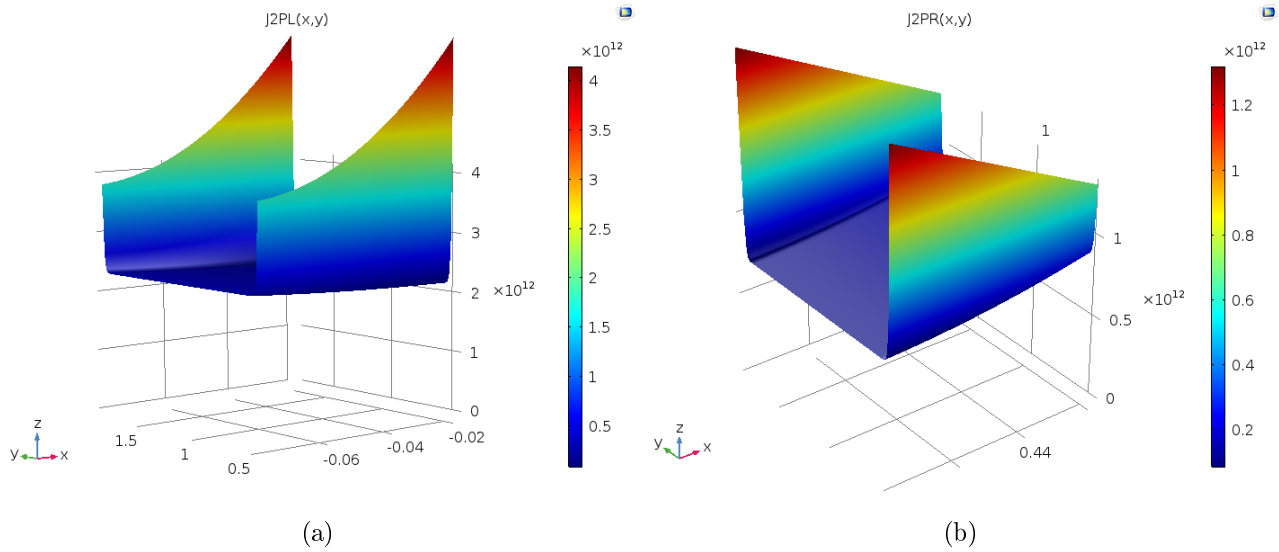

(a)

(b)

Figure 60: J^2 - Primary winding on the left (a) and right (b) side of the core

The intervals on the x-axis are stretched out compared to the y-axis. This make the cross-section of the windings look like a square, but it makes it easier to see the shape of the functions.
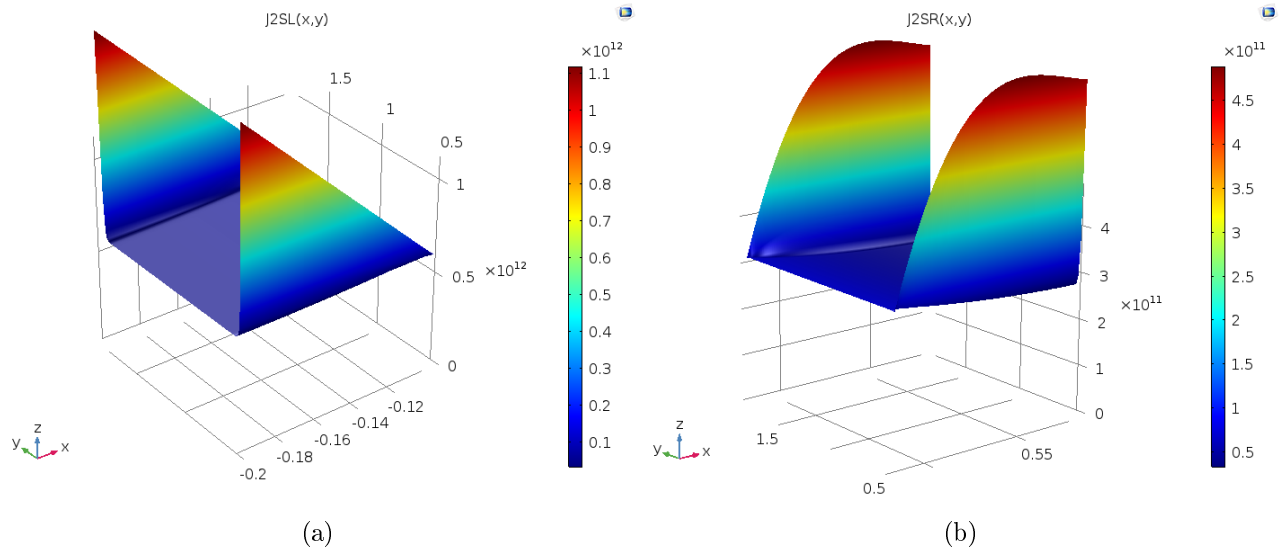

(a)

(b)

Figure 61: J^2 - Secondary winding on the left (a) and right (b) side of the core

D Probability distribution function

The main 2-parameter distribution functions used to describe the lifetime of transformers are Gamma, Weibull and Lognormal [32]. The gamma distribution is described with the parameters α_1 and β_1 [33]

$$Gamma_{(\alpha_1,\beta_1)} = \frac{\left(\frac{x}{\beta_1}\right)^{\alpha_1-1}}{\Gamma(\alpha_1)} \left(\frac{1}{\beta_1}\right) e^{-\left(\frac{x}{\beta_1}\right)} \tag{81}$$

Weibull distribution is described with the parameters α_2 and β_1 in the following equation [33]

$$Weibull_{(\alpha_2,\beta_1)} = \left(\frac{\alpha_2}{\beta_1}\right) \left(\frac{x}{\beta_1}\right)^{\alpha_2-1} e^{-\left(\frac{x}{\beta_1}\right)^{\alpha_2}} \tag{82}$$

Lognormal distribution is described with the parameters μ and σ_{std} in the following equation. [33]

$$lnN_{(\mu,\sigma_{std})} = \frac{1}{\sqrt{2\pi}\sigma_{std}x} e^{-\frac{(-\mu+\ln x)^2}{2\sigma_{std}^2}} \tag{83}$$

All these distributions are all two-parameter distribution functions. They all have a wide range of shapes that can fit the lifetime distribution for different transformers. The three-parameter generalized Gamma function (GG3) is a generalisation of many commonly used life distributions, such as Weibull, Gamma and Lognormal. [32]. It is described with the parameter α_1, α_2 and β_1. [32]

$$GG3_{(\alpha_1,\alpha_2,\beta)} = \frac{1}{\Gamma(\alpha_1)} \left(\frac{\alpha_2}{\beta_1}\right) \left(\frac{x}{\beta_1}\right)^{\alpha_1\alpha_2-1} e^{-\left(\frac{x}{\beta_1}\right)^{\alpha_2}} \tag{84}$$

The link between Gamma, Weibull and GG3 is as follows

$$GG3_{(\alpha_1,1,\beta_1)} = Gamma_{(\alpha_1,\beta_1)} \tag{85}$$

$$GG3_{(1,\alpha_2,\beta_1)} = Weibull_{(\alpha_2,\beta_1)} \tag{86}$$

The link between Lognormal and GG3 is described in [32]. The expected value μ_x and the variance σ_{std}^2 for the different probability functions are listed in Table 17. [33]

Table 17: Expectation μ_x and variance σ_{std}^2 for different distribution functions

Function	μ_x	σ_{std}^2
Gamma	$\alpha_1\beta_1$	$\alpha_1\beta_1^2$
Weibull	$\frac{\beta_1}{\alpha_2}\Gamma\left(\frac{1}{\alpha_2}\right)$	$\beta_1^2\left(\Gamma\left(1+\frac{2}{\alpha_2}\right) - \left(\Gamma\left(1+\frac{1}{\alpha_2}\right)\right)^2\right)$
Lognormal	$e^{\mu+\frac{\sigma_{std}^2}{2}}$	$\left(e^{\sigma_{std}^2}-1\right)e^{2\mu+\sigma_{std}^2}$
GG3	$\beta_1\frac{\Gamma\left(\alpha_1+\frac{1}{\alpha_2}\right)}{\Gamma(\alpha_1)}$	$\beta_1\left(\frac{\Gamma\left(\alpha_1+\frac{2}{\alpha_2}\right)}{\Gamma(\alpha_1)} - \left(\frac{\Gamma\left(\alpha_1+\frac{1}{\alpha_2}\right)}{\Gamma(\alpha_1)}\right)^2\right)$